SKB

Organic materials with the potential for complexation in SFR, the final repository for short-lived radioactive waste

Investigation of new acceptance criteria

Miranda Keith Roach

Pirouz Shahkarami

SVENSK KÄRNBRÄNSLEHANTERING

Organic materials with the potential for complexation in SFR, the final repository for short-lived radioactive waste

Investigation of new acceptance criteria

Miranda Keith Roach, Pirouz Shahkarami

Kemakta Konsult AB

This report is published on www.skb.se

Abstract

Organic complexing agents from cleaning and hygiene products are present in some SFR wastes and may reduce radionuclide sorption. Additionally, polymers in waste materials, cement additives and anti-corrosion paint may undergo alkaline degradation to produce complexing agents *in situ*. This report investigates complexing agents and polymers present in SFR in order to identify maximum acceptable dissolved concentrations that are not expected to reduce radionuclide sorption. The recommended concentration limits are intended to inform the selection of waste acceptance criteria (WAC) for SFR1 waste packages.

The report addresses complexing agents, cellulose, superplasticisers, plasticisers, plastics and rubber, anti-corrosion paint, filter aids, tributyl phosphate (TBP), bitumen and lignin. For each category of organic material, information is given on its origin, structure, solubility, degradation characteristics and reactions, coordination and denticity, presence in SFR, occurrence in future waste, and form following the resaturation of SFR. This is followed by a literature review of the effect of the complexing agent or degradation products on radionuclide speciation and sorption. The literature review is then complemented with PhreeqC thermodynamic speciation calculations where appropriate. The information is used to recommend maximum dissolved concentrations that are not expected to reduce radionuclide sorption. The recommended limits are summarised in a final chapter together with a discussion of the effect of several complexing agents being present in a single waste package, how the existing inventory may affect the new WAC for specific parts of SFR, a comparison of the recommended limits with the existing WAC, and a discussion of the limitations of the study. The corresponding maximum mass of each of the materials in relevant waste types is given in Appendix.

The most important conclusions of this report are:

- Metal hydrolysis and competition from Ca^{2+} limit the effect of aminopolycarboxylate complexing agents on radionuclide speciation under SFR conditions, thus the WAC for aminopolycarboxylate complexing agents can be made less restrictive.

- Metal hydrolysis and competition from Ca^{2+} negate the effect of bi- and tri-dentate carboxylate complexing agents on radionuclide speciation under SFR conditions. Maximum tolerable masses are instead defined on the basis of their impact on cement degradation.

- Interactions with Ni(II), rather than actinides, define the tolerable concentrations of the N-containing complexing agents disposed of in SFR (e.g. EDTA, NTA, iminodisuccinate).

- Strong Ni(II)-amine interactions are important for anti-corrosion paints and Nylon.

- Many of the recommended concentration limits are less restrictive than the existing WAC.

Sammanfattning

Visst SFR-avfall innehåller organiska komplexbildare från rengörings- och hygienprodukter som kan försämra sorptionen av radionuklider. Dessutom kan vissa polymerer i avfallet, cementtillsatsmedel och rostskyddsfärger brytas ner i den basiska miljö som råder i SFR, och nedbrytningsprodukterna kan vara komplexbildande. Föreliggande rapport presenterar en undersökning av komplexbildare och polymerer i SFR i syfte att identifiera de högsta koncentrationer som kan tolereras utan att försämra radionuklidsorptionen. De rekommenderade koncentrationsgränsvärdena är avsedda som underlag för framtagning av motsvarande acceptanskriterier för avfall till SFR1.

Rapporten omfattar organiska komplexbildare, cellulosa, superplasticerare, mjukgörare, plast och gummi, rostskyddsfärg, filterhjälpmedel, tributylfosfat, bitumen och lignin. För varje materialkategori presenteras information om dess ursprung, struktur, löslighet, nedbrytningsegenskaper och -reaktioner, koordinering och denticitet, närvaro i SFR och i framtida avfall, samt form efter förslutning och vattenåtermättnad av förvaret. Därefter följer en genomgång av litteraturen avseende komplexbildning och påverkan på radionukliders speciering och sorption. Som ett komplement till litteraturstudien har för vissa material termodynamiska specieringsberäkningar med mjukvaran PhreeqC utförts. Baserat på resultaten rekommenderas maximala lösta koncentrationer som inte förväntas påverka radionuklidsorptionen. De rekommenderade gränsvärdena sammanfattas i slutet av rapporten tillsammans med en diskussion kring effekten av mer än en typ av komplexbildare i ett kolli, hur redan deponerade komplexbildare i ett förvarsutrymme kan påverka acceptanskriterier för nytt avfall, en jämförelse mellan de nya rekommenderade gränsvärdena och de nu gällande, samt en diskussion kring utredningens begränsningar. Motsvarande maximal massa per kolli för ett antal material och avfallstyper beräknas i appendix.

Rapportens viktigaste slutsatser är:

- Hydrolys samt konkurrens från stabilt Ca^{2+} begränsar radionuklidspecieringens påverkan av fler-karboxylerade aminer under SFR-förhållanden. Därmed medges mindre strikta acceptanskriterier avseende dessa komplexbildare.

- Hydrolys och höga halter stabilt Ca^{2+} under SFR-förhållanden konkurrerar helt ut bi- och tridentata karboxylater avseende påverkan på radionuklidspeciering. Tolererbara mängder av dessa komplex-bildare definieras istället baserat på deras cementnedbrytande potential.

- Interaktioner med Ni(II) snarare än aktinider är gränssättande för tolererbar koncentration av komplexbildare som koordinerar med kväve (t ex EDTA, NTA, iminodisuccinat).

- Starka Ni(II)-amin-interaktioner är en viktig effekt, relevant för rostskyddsfärger och Nylon.

- Många av de rekommenderade gränsvärdena är mindre restriktiva än nuvarande acceptanskriterier.

Concepts and acronyms

Acceptance criteria	Criteria imposed to ensure that a requirement is achieved
An	Chemical symbol used for a non-specified actinide
BMA	Vault for intermediate-level waste
BLA	Vault for low-level waste
BTF	Vault for concrete tanks
CADP	Capryloamphodipropionate
CIDP	Capryliminodipropionate
Cit	Citrate
DBP	Dibutyl phosphate
Dien	Iminobis (2-ethylamine)
DOC	Dissolved organic carbon
DTPA	Diethylenetriamine pentaacetate
En	Ethylenediamine
EDTA	Ethylenediaminetetraacetate
GC-MS	Gas chromatography – mass spectrometry
Glu	Gluconate
Gy	Gray, a unit of dose
HMDA	Hexamethylenediamine
IDS	Iminodisuccinate
ISA	Isosaccharinic acid
ML	Metal-ligand
NAPL	Non-aqueous phase liquid
NTA	Nitrilotriacetate
OPC	Ordinary Portland cement
Ox	Oxalate
PC	Polycarboxylate
PCE	Polycarboxlate ether
PEG	Polyethylene glycol
PET	Polyethylene terephthalate
PMS	Polymelamine sulfonates
PNS	Polynaphthalene sulfonates
PVMA	Polyvinyl maleic acid
NTA	Nitrilotriacetaic acid
PAN	Polyacrylonitrile
PVC	Polyvinyl chloride
SFR	Repository for short-lived low- and intermediate-level waste
TBP	Tributyl phosphate
TDP	Tris(dimethylaminomethyl)phenol
TETA	1,4,7,10-tetraazadecane
Tetren	1,4,7,10,13-pentaazatridecane
TOC	Total organic carbon
Tren	Nitrilotris (2-ethylamine)
Trien	1,4,7,10-tetraazadecane; alternative name for TETA
UV	Ultraviolet
WAC	Waste acceptance criteria

Contents

1 Introduction

1.1 Waste acceptance criteria

Waste acceptance criteria (WAC) are criteria that must be fulfilled for waste packages to be accepted for disposal. WAC are used to ensure that:

- the waste packages can be handled and managed safely from a chemical, physical and radiological perspective during all stages of the operational phase,

- the long-term safety functions of a repository are not jeopardized.

Further benefits of WAC are that they:

- avoid technical problems,

- standardise communication,

- standardise waste package production processes,

- enable transport of the waste packages,

- enable the registration process,

- support waste producers in their choice of waste treatment and conditioning.

The WAC for SFR have been amended and improved successively over time. Formalised WAC for complexing agents in waste packages allocated to the Silo, 1BMA and 1–2BTF were introduced in 2012[1]. These were strengthened in version 3.0 of the WAC in 2018[2] to state that strong complexing agents may not be disposed of in the Silo, BMA and BTF. These strong complexing agents are:

- N-carboxylated triamines (aminopolycarboxylates with three amine groups) e.g. DTPA.

- N-carboxylated diamines (aminopolycarboxylates with two amine groups) e.g. EDTA.

- N-carboxylated amino acids (aminopolycarboxylates with one amine group) e.g. NTA.

- α-hydroxycarboxylates e.g. gluconate.

- Fuel extraction solvents, e.g. tributyl phosphate (TBP).

Esters of strong complexing agents also may not be disposed of.

Maximum molar concentrations were defined as WAC for tricarboxylates, e.g. citrate, and dicarboxylates e.g. oxalate, as well as their esters. This version of the WAC also introduced concentration limits for isosaccharinic acid (ISA), a degradation product of cellulose under alkaline conditions. In the WAC, scientific literature and this report, the name ISA is used to describe the molecule under all pH conditions, even when it is present as isosaccharinate.

1.2 SFR conditions and radionuclides of interest

1.2.1 pH

SFR1 consists of four waste vaults (1BMA, 1–2BTF and 1BLA) and a silo. The pH of the water within the repository, including the waste packages, will be affected strongly by alkaline cement leachate. During the evolution of SFR, the pH of 1BMA, the Silo and 1–2BTF is expected to decrease from ~13 to 12.5 (Table 1-1). 1BLA, on the other hand, contains little structural concrete and the pH

---

[1] **Almkvist L, 2012.** Acceptanskriterier för avfall i SFR. SKBdoc 1336074 ver 1.0, Svensk Kärnbränslehantering AB. (In Swedish.) Internal document.

[2] **Lihnell M, Södergren K, 2018.** Acceptanskriterier för avfall i SFR1. SKBdoc 1336074 ver 3.0, Svensk Kärnbränslehantering AB. (In Swedish.) Internal document.

is expected to decrease to pH 7.5 after 21 000 years. Because of this, and the fact that the total radio-active inventory of the waste is low, 1BLA is not credited with the safety function *Good retention*. Therefore, the focus of this study is on the highly alkaline range of pH 12.5–13.

Table 1-1. Summary of pH regimes for waste vaults. Cells shaded with grey indicate that no further changes are predicted over 100 000 years. Times refer to AD (reproduced from SKB 2015a).

pH	1BMA – cement		1BMA – Bitumen		1BLA	1BTF Ash section	2BTF	Silo	
	Date AD								
	Waste	Wall	Waste	Wall				Waste	Wall
13.0	2000	2000	2000	2000		2000	2000	2000	2000
12.5	7000	6000	7000	8000	2000	4000	7000	26 000	34 000
12.0		22 000		22 000	8000				
11.5		58 000		50 000	9000				
10.5					9200				
9.0					11 000				
7.5					21 000				

1.2.2 Ionic strength and dissolved metal ion concentrations

The ionic strength of the water within the waste packages will vary over time and space due to changes in the ionic strength of the groundwater, cement degradation and dissolution of waste materials.

The brackish groundwater that will infiltrate SFR in the period up to ~1 000 years after closure has an ionic strength in the range 0.05–0.19 M (calculated from data in Table 6-1 of the Main report for SR-PSU (SKB 2015a). The freshwater expected to dominate after this has an ionic strength of ~0.009 M (calculated from the data in Table 3-2 in Höglund 2014). However, the dissolution of port-landite results in an ionic strength of 0.1 M at pH 13 and 0.06 M at pH 12.5 (portlandite dissolution) (Lagerblad and Trägård 1994, Engkvist et al. 1996). The dissolution of waste components, including complexing agents, will increase the ionic strength further.

Ca^{2+} is an important ion in terms of the ionic strength of the water and the chemistry of the system. The brackish groundwater is expected to contain ~15 mM Ca^{2+} (SKB 2015a), and relatively high dissolved concentrations of Ca^{2+} are also associated with portlandite dissolution.

Metallic iron is also present in many wastes, which will corrode over time. The low solubility limits of iron ions restrict the dissolved concentrations in SFR, in the absence of the formation of organic complexes.

1.2.3 Redox potential

As described in SKB (2015a), microbially mediated oxidation of organic matter rapidly depletes oxygen in the repository system after closure. The corrosion of steel-based material present in the repository is expected to maintain reducing conditions for a long time. The redox potential imposed by the anoxic corrosion of steel and hydrogen production is approximately −0.75 V at pH 12.5.

1.2.4 Water saturation

After closure, the engineered structures of SFR will become hydraulically saturated. Total saturation of the Silo will take around 25 years, whereas the other vaults are expected to become saturated in just a few years (Holmén and Stigsson 2001). From a safety assessment perspective, the saturation process is assumed to be instantaneous upon closure (SKB 2015a).

1.2.5 Radionuclides of interest

The extent to which a complexing agent can reduce radionuclide sorption to cement is greatest for radionuclides that sorb strongly to cement in the absence of complexing agents. Radionuclide species that have high sorption coefficients (K_d values) also tend to interact most strongly with complexing agents. In the *high concentrations of complexing agents* less probable scenario of the safety assessment SR-PSU (SKB 2015a), the dose to humans increased mainly as a result of the reduced sorption of ^{59}Ni(II), but the effect of the reduced sorption of ^{239,240}Pu(IV) was also apparent. Therefore, Ni(II) and tetravalent actinides are of particular importance with regard to complexing agents. Trivalent actinides are also considered important in this report.

1.3 Report aims

The aims of this report are to:

1. Introduce the chemistry of complex formation, trends in the strength of complexes and the degradation of polymers to complexing agents.

2. Review the available literature for each type of relevant organic material in turn, to support the selection of concentration limits for each material in the waste packages. PhreeqC calculations are used to complement the available literature.

3. Recommend dissolved concentration limits for each material in the waste packages.

4. Review the recommended concentration limits in light of the existing inventory of each vault. This is necessary as some vaults such as 1BMA and the Silo already contain large amounts of certain complexing agents and organic materials.

5. Compare the recommended concentration limits with the current WAC.

6. Calculate WAC in terms of the mass of chemicals or materials per waste package for relevant waste packages (given in Appendix).

This report was commissioned to inform the selection of WAC 4.0, which will apply to SFR1. However, the results are equally relevant for 2BMA. As previously, the WAC that relate to complexing agents apply to waste that will be deposited in the Silo, 1BMA and 1–2BTF, but not 1BLA.
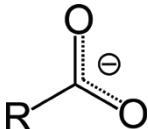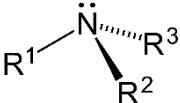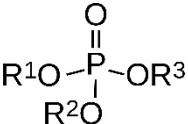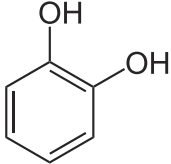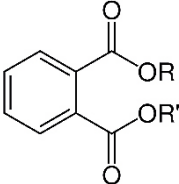
2 Background information and concepts

2.1 Complexing agents and complex formation

2.1.1 Complexing agents

A complexing agent can be defined as an anion or molecule that binds to another atom or ion, typically a metal cation, via a coordination bond. A coordination bond involves electron pair donation from the complexing agent to the central metal ion. Some inorganic species can be complexing agents, for example H_2O, OH^-, Cl^-, NH_3, CN^-. Organic molecules with certain functional groups, for example carboxylates, amines, organophosphates, alcohols, phenols and phthalates can also be complexing agents (see Table 2-1).

Table 2-1. Structures of some organic functional groups that can form complexes with metal ions.

		Comment	Location of donor lone pair
Carboxylate		Delocalised electronic structure shown	Oxygen atoms
Amine		Tertiary amine shown in example	Nitrogen atom
Organophosphate			Double bonded oxygen atom
Alcohols	R-OH		Oxygen atom
Phenols		Catechol, with two phenolic alcohol groups, is shown in the example	Oxygen atom
Phthalic acid (if R = H) or phthalic acid ester if R is an alkyl group		Orthoposition shown in example	Oxygen atom

Coordination chemistry is very important for transition metals (d-block), lanthanides and actinides (f-block). Most d-block metal coordination complexes have a coordination number of 6, thus coordination bonds form at six points around the central metal ion. According to crystal field theory, the complexing agents are arranged to minimize repulsive electrostatic forces between the donated electron pairs. This results in an octahedral complex. However, a coordination number of 4 can also be exhibited by certain elements, such as Ni-group metals. This coordination number gives a tetrahedral or, in a few cases, square planar geometry.

Ions of f-block metals have relatively large ionic radii and their coordinate bonds have a substantially ionic character (Runde 2000). The maximum number of coordination sites is limited by electrostatic and steric effects (Runde 2000). In oxidation state $\leq$ IV, f-block metals exhibit high coordination numbers, for example coordination numbers of 8–10 are common. Actinides in oxidation states V and VI exist as the oxycations $An(V)O_2^+$ and $An(VI)O_2^{2+}$. The oxygen atoms in the oxycations occupy space around the actinide centre and coordination numbers between 2–8 are seen.

2.1.2 Denticity

When a complexing agent has only one lone pair to donate to the metal ion, it is described as monodentate. It "bites", or forms a bond, at one coordination site. This is common for inorganic complexing agents. However, organic molecules that have more than one functional group with a lone pair of electrons can, where sterically possible, form coordinate bonds at more than one of the coordination sites around the metal ion. These complexing agents are described generally as multidentate, with a specific name for each denticity. A summary of common denticities is given in Table 2-2, together with examples of complexing agents that can exhibit these denticities. In most cases, a carboxylate group can only donate one lone pair of electrons as the two oxygens are too close to each other to occupy two coordination sites simultaneously. Therefore, oxalate is bidentate via two carboxylate groups. Steric hindrance is also observed in citrate, as only three of the four potential lone pair donor groups can coordinate to a single metal ion simultaneously. Citrate can be tetradentate in complexes involving > 1 metal centre, but tridentate bonding is of most relevance to this report.

Metal ions exist in solution as aquo complexes, i.e. complexed by water molecules. Replacement of these water molecules with complexing agents is a rapid, reversible reaction (e.g. Equation (2-1)), controlled thermodynamically by the stability constant of the complex formed and the concentration of the complexing agent and metal ion (Equation (2-2)). The concentration of water is constant in dilute solutions and so does not affect the reaction.

$$M(H_2O)_6^{x+} + 6NH_3 \rightleftarrows M(NH_3)_6^{x+} + 6H_2O \tag{2-1}$$

$$\text{Stability constant}, K = \frac{[M(NH_3)_6^{x+}] \cdot [H_2O]^6}{[M(H_2O)_6^{x+}] \cdot [NH_3]^6} = \frac{[M(NH_3)_6^{x+}]}{[M^{x+}] \cdot [NH_3]^6} \tag{2-2}$$

Where [] indicates molar concentration. The definition of the stability constant in Equation (2-2), based on molar concentration rather than activity, is only valid for ideal solutions (see Section 2.2.3).

Complexes involving multidentate complexing agents generally have higher stability constants than those involving monodentate ligands. This empirical observation is explained through the chelate effect, which refers to changes in entropy as a complex forms. A reaction between a metal and six monodentate complexing agents to produce one complex reduces entropy to a greater extent than a reaction between a metal and three bidentate complexing agents.

The stability of a chelate complex, formed by a multidentate complexing agent and metal cation, also depends on the size of the ring formed. In general, chelates that form 5- or 6-membered rings are more stable than chelates that form 4-, 7-, or 8-membered rings (Britannica 2020). The chelate ring in the case of oxalate, for example, involves the metal, one oxygen in each of the two carboxylate groups and two carbon atoms, i.e. 5 members.

Carbonaro et al. (2011) identified that oxalate is a more stable complexing agent than other bidentate dicarboxylates and is the only dicarboxylate to have a 5-membered chelate ring. In citrate, the coordination of the alcohol group in complex formation reduces the size of the chelate rings, adding to the stability of the complexes formed. The interaction of the amine groups in the aminopolycarboxylates NTA, EDTA and DTPA with actinide centres occurs due to the stabilizing effect of chelation. Nitrogen groups alone cannot displace water in the hydration shell of actinide ions (Katz et al. 1986).

Table 2-2. Denticities of example complexing agents.

Denticity	Example	Location of lone pairs	Structure of the protonated, acid form or salt
Monodentate	Acetate	1 carboxylate group	
Bidentate	Oxalate	2 carboxylate groups	
	Ethylenediamine	2 amine groups	
Tridentate	Capryliminodipropionate (CIPD)	1 amine group, 2 carboxylate groups	
Tridentate (due to steric effects)	Citrate	2 carboxylate groups, 1 alcohol	
Tetradentate	Nitrilotriacetate (NTA)	1 amine group, 3 carboxylate groups	
Pentadentate	Iminodisuccinate (IDS)	1 amine group, 4 carboxylate groups	
Hexadentate	Ethylenediaminetetraacetate (EDTA)	2 amine groups, 4 carboxylate groups	
Octadentate	Diethylenetriamine pentaacetate (DTPA)	3 amine groups, 5 carboxylate groups	

Multidentate complexing agents can exhibit hypodentate bonding, in which only some of the lone pair donors are involved in bonding. Blackman (2005) reviewed hypodentate bonding in polyamines. Hypodentate bonding is rare in the diamine ethylenediamine, which forms a 5-membered chelate ring, but becomes increasingly common as the carbon chain between the amine groups increases. Due to this, the Cambridge Structural Database shows 1 473 transition metal complex structures containing chelated ethylenediamine, 194 containing chelated propylenediamine, 17 containing chelated butanediamine and none containing chelated pentanediamine (Blackman 2005). Also, bidentate diamine complexes of the type $[Co(NH_3)_4(NH_2(CH_2)_nNH_2-N,N')]^{3+}$ formed in the polar organic solvent DMSO when n = 2, 3, 4, 12 and 14, but monodentate complexes formed when n = 5, 7, 8, and 10. Finally, in branched tetradentate polyamines, hypodentate bonding is exhibited when the pendant arm would result in a chelate ring of > 6 members (Blackman 2005).

2.1.3 Stability of complexes

The strength of interaction between a complexing agent and metal varies according to the complexing agent, its functional groups and denticity, the metal and the oxidation state of the metal. These factors are described below.

Hard–soft (Lewis) acid/base description

Metal-complexing agent interactions can be described in terms of hard and soft Lewis acids and bases. A Lewis acid (metal) can accept an electron pair from a Lewis base (complexing agent), and the process is most favourable for a metal when the complexing agent has the same type of hard or soft character. Hard acids and bases have a relatively high charge density, thus complexes between hard acids and bases have a strongly ionic character. Soft acids and bases have a low charge density and result in coordination bonds with a more covalent character.

The stability constants for Ni(II), Ca(II) and Th(IV) with some molecules that are representative of important donor groups are shown in Table 2-3. Alcohols are discussed separately below. Table 2-3 shows that organic acids (based on acetate) and sulfate are important for all three metal ions, while amines (based on ammonia) are important for Ni(II). It can also be seen that Th(IV) forms the most stable complexes of the three with all complexing agents except ammonia. In terms of hard–soft acid/base theory, Th(IV) and Ca(II) are harder Lewis acids than Ni(II) and so form more stable complexes with hard bases. They also form less stable complexes than Ni(II) with the soft base ammonia.

According to Van Loon and Hummel (1995), the stabilities of amine complexes with soft metal ions decrease with increasing number of methyl groups. As a general rule, the stability constants show the following trend: ammonia = methylamine > dimethylamine > trimethylamine (Rorabacher and Melendez-Cepeda 1971). This trend is consistent with steric effects (Rorabacher and Melendez-Cepeda 1971).

Many actinides, such as U, Pu and Np are redox-sensitive, and their oxidation state affects their hardness as a Lewis acid and therefore the strength of their interaction with a complexing agent. The order of complex stability with hard complexing agents follows the trend in the effective charge of the central actinide ion (Choppin 1983 cited in Runde 2000):

$$An(IV) > An(VI)O_2^{2+} \geq An(III) > An(V)O_2^+$$
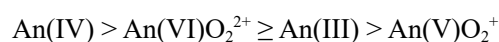
Table 2-3. Comparison of the logarithms of the stability constants of 1:1 complexes of Ca(II); Ni(II) and Th(IV) with selected ligands, from the Thermochimie_v10a database.

	Ca(II)	Ni(II)	Th(IV)
Acetate	1.12	1.34	5.24
Ammonia	−0.1	2.6	–
Nitrate	0.6*	0.5	1.3
Sulfate	2.31	2.35	6.17

* Taken from Thermochimie_V9b as no value is given in Thermochimie_v10a

The strength of complexing agents that contain -OH groups, such as carboxylic acids, phenols and alcohols, increases with the acidity of the -OH group (e.g. Carbonaro et al. 2011). Phenols are more acidic than aliphatic alcohols due to stabilization of the negative charge after deprotonation, with the charge delocalized in the resonance structures of the phenoxide anion. The alcohol group in citrate also has a higher acidity than typical alcohol groups due to the proximity of the electron-withdrawing carboxylic acid group.

Stability of carboxylate and aminocarboxylate complexes

Carbonaro et al. (2011) examined the stability of complexes with 5- or 6-membered chelate rings formed via bidentate complexing agents with negatively charged oxygen donor atoms (dicarboxylic acids, carboxyphenols, *ortho*-diphenols, *ortho*-hydroxybenzaldehydes, α-hydroxycarboxylics acids and α-ketocarboxylic acids). There was a clear relationship between the predicted stability based on the sum of the stability constants of the equivalent monodentate donor groups (with a few outliers such as oxalate) and the actual stability constants for the complexes. The results showed the additional stability given by the chelate effect.

Allard et al. (2002) summarized the stability constants from Martell et al. (1997) for Ni(II), Eu(III) and Th(IV) for a range of organic complexing agents. The data are presented in Table 2-4 together with a description of the denticity and size of the chelate ring. The log stability constants for the bidentate ligands, which are all dicarboxylates, are presented in Figure 2-1 as a function of the chelate ring size. The higher stability of chelate rings with 5 or 6 members is clear in Figure 2-1, and the 5-membered chelate ring (oxalate) has the highest stability, as noted for previously by Carbonaro et al. (2011). Once the chelate ring has 7 members, no additional influence of the change in the chelate ring size can be seen.
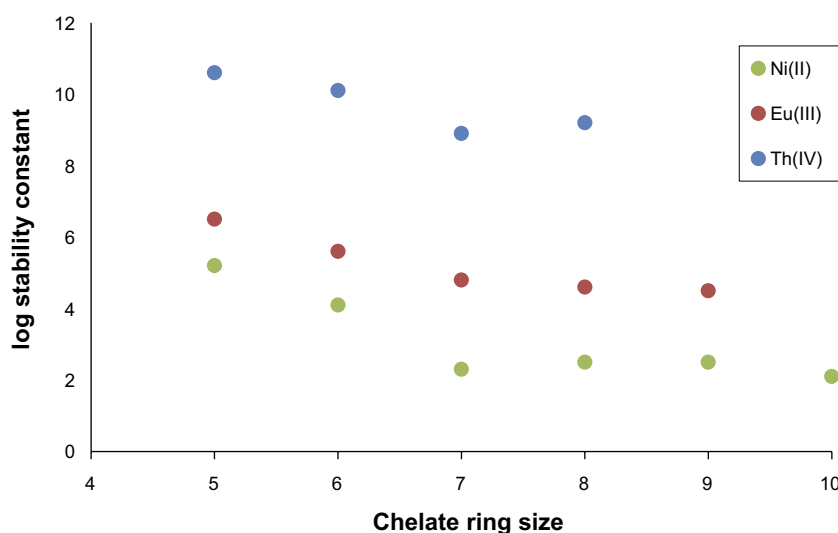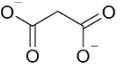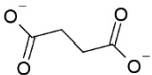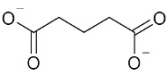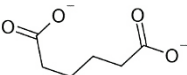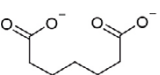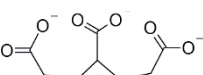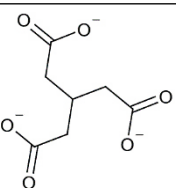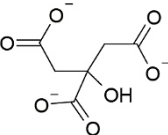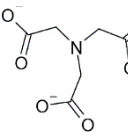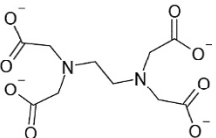
Figure 2-1. *The logarithms of the stability constants for Ni(II), Eu(II) and Th(IV) with dicarboxylate ligands as a function of the chelate ring size. Based on the data given in Allard et al. (2002).*

Table 2-4. The structure, denticity, chelate ring size, pKa, and log stability constants of selected 1:1 metal complexes (Allard et al. 2002).

Complexing agent	Structure	Denticity	Chelate ring size	pK_a	logK$_{MA}$ Ca(II)	Ni(II)	Eu(III)	Th(IV)
Formate	HCOO⁻	Mono	–	3.75	1.4	1.3	2.1	4.3
Acetate	CH$_3$COO⁻	Mono	–	4.76	1.2	1.4	2.8	5.1
Oxalate		Bi	5	4.27	3.2	5.2	6.5	10.6
Malonate		Bi	6	5.70	2.4	4.1	5.6	10.1
Succinate		Bi	7	5.64	2.0	2.3	4.8[a]	8.9
Glutarate		Bi	8	5.42	2.0	2.5	4.6[a]	9.2
Adipate		Bi	9	5.42	2.2	2.5	4.5[a]	–
Pimelate		Bi	10	5.43	–	2.1	–	–
Carboxypimelate		Tri	8	–	3.0	3.3[b]	–	–
3-(carboxymethyl) pentandicarboxylate		Tri	8	5.77	–	3.8	–	–
Citrate		Tri	5 and 6	6.40	4.9	6.9	9.5	14.3
NTA		Tetra	5	10.5	7.9	12.8	13.3	15.1
EDTA		Hexa	5	10.95	12.4	20.2	19.9	26.8

[a] Value for Sm(III).

[b] Value for Mn(II).

The stability of the radionuclide complexes in Table 2-4 can also be seen to have a linear relationship with the stability of the equivalent Ca^{2+} complexes (Figure 2-2).
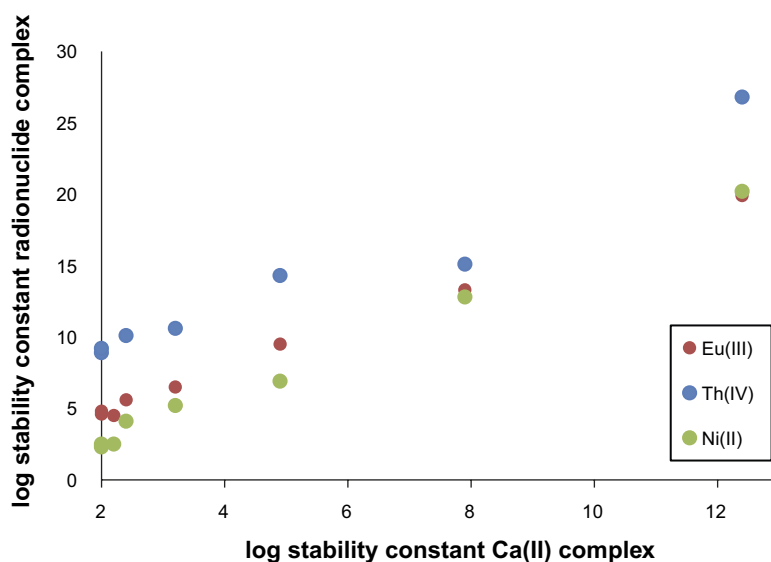
Figure 2-2. *Relationship between the 1:1 stability constants for radionuclide complexes and Ca²⁺ complexes based on the data in Table 2-4.*

Stability of Ni(II) amine complexes

Amines can form strong complexes with Cu(II), Ni(II) and other relatively soft metal ions. As Ni(II) is of particular relevance to SFR, stability constants compiled by Tanaka and Tabata (2009) for Ni(II) with ammonia and multidentate amines that form 5-membered chelate rings are shown in Table 2-5. The stability constants of the Ni(II)-multidentate amine complexes are high. When the data are compared with the data in Table 2-4, it can be seen that the stability constant for Ni(II)en²⁺ is greater than for NiOx thus Ni(II) forms more stable 1:1 complexes with amines than carboxylic acids. The stability constants for tetradentate Ni(II)trien²⁺ and Ni(II)tren²⁺ complexes are higher than for tetradentate Ni(II)NTA⁻. However, this trend is no longer seen with the hexadentate aminocarboxylate EDTA and hexadentate amine penten.

Influence of higher coordination numbers

In addition to 1:1 metal:ligand complexes, 1:2 (bis) and 1:3 (tris) complexes can form between metals and complexing agents such as oxalate, citrate and ethylenediamine. Table 2-6 shows stability constants for Ni(II) and Th(IV) with these example complexing agents. It is clear that the additional stability inferred by coordination of the second complexing agent in Ni(II)L₂ is much greater for en than for the two carboxylates. En ligands are uncharged, which reduces electronic repulsion effects. Coordination of the third en also is associated with a great deal of additional stability, while NiOx₃⁴⁻ is not reported. The stability of a second carboxylate ligand for Th(IV) is greater than for Ni(II), which is consistent with the greater positive charge and the larger ionic radius of the Th(IV) metal centre.

The relative concentration of the 1:1, 1:2 and 1:3 complexes in solution depends on both the difference between the stability constants of the species and the complexing agent concentration (Equation (1-2)). The concentration of the 1:1 complex is affected linearly by the complexing agent concentration. However, the concentration of the 1:2 and 1:3 complexes depends on the square and cube of the complexing agent concentration, respectively. Therefore 1:2 and 1:3 complexes form to a greater extent as the complexing agent concentration increases.

Table 2-5. Stability constants of 1:1 Ni(II) polyamines (Tanaka and Tabata 2009).
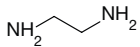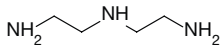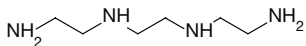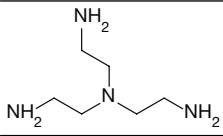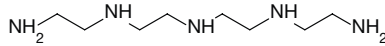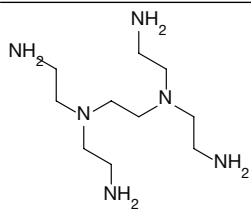
Complexing agent	Structure	Denticity	$\log K_1$
Ammonia	NH_3	Mono	2.73
en (ethylenediamine, 1,2 diaminoethane)	$NH_2CH_2CH_2NH_2$	Bi	7.51
dien (iminobis (2-ethylamine)	(structure)	Tri	10.7
trien (1,4,7,10-tetraazadecane	(structure)	Tetra	14.0
tren (nitrilotris (2-ethylamine)	(structure)	Tetra	14.8
tetren (1,4,7,10, 13-pentaazatridecane)	(structure)	Penta	17.1
Penten (ethylenedinitrilotetrakis (2-ethylamine))	(structure)	Hexa	19.3

Table 2-6. Comparison of metal–ligand (ML) ML^{x-}, ML_2^{x-}, ML_3^{x-} stability constants for Ni(II) and Th(IV) with oxalate and citrate (Thermochimie) and Ni(II) with en (Paoletti 1984). Note that only ML complexes with deprotonated carboxylic acids are included, as this study focusses on alkaline conditions.

Radionuclide	Complexing agent	ML^{x-}	ML_2^{x-}	ML_3^{x-}
Ni	Oxalate	5.19	7.64	
	Citrate	6.76	8.50	
	en	7.52	13.84	18.33
Th	Oxalate	9.70	16.00	22.2
	Citrate	16.80	25.80	

2.2 Influence of local conditions on radionuclide complexation

2.2.1 Overview

Complex formation occurs when it is thermodynamically favourable in the context of all reaction equilibria in the system. It is therefore highly sensitive to the chemical environment. The pH, redox potential (E_h), ionic strength and concentrations of other species control the balance of thermodynamically favourable reactions. In essence:

- Precipitation or dissolution of metal hydroxides can occur as the pH and OH^- concentration increase, depending on the solubility of metal-hydroxo complexes.

- The prevalence of oxidized or reduced species of redox-sensitive elements changes with pH and E_h (as illustrated for example in Pourbaix diagrams).

- Ionic strength affects the formation of complexes, e.g. at low ionic strengths, an increase in ionic strength reduces the formation of metal ion – charged complexing agent complexes.

- The temperature affects complex formation reactions.

- The presence of other metals may reduce or limit the complexation of another, due to preferential complexation.

- The presence of one complexing agent may reduce or limit the influence of another.

- Some complexing agents have a low solubility product with certain dissolved metal ions, e.g. CaOx(s) precipitates at low oxalate concentrations in a cementitious environment.

- Some complexing agents sorb to solid materials such as cement, which reduces their solution-phase concentrations.

The extent to which a complexing agent sorbs to cementitious materials or precipitates is affected by the concentrations of cations present. The typical concentrations of dissolved cationic radionuclides ($\sim 10^{-8}$ M) are much lower than the complexing agent concentrations generally of interest ($\sim 10^{-4}$ M). Therefore, the radionuclides are assumed to have a negligible influence on the overall sorption or precipitation of complexing agents.

2.2.2 Competition with hydroxide species

The influence of hydroxide species on the formation of organic complexes is illustrated below for 1:1 Ni, Am and Th species with NTA using the approach presented in Allard et al. (2002).

The logarithm of the equilibrium constants for the formation of the aqueous hydroxo species $Ni(OH)_3^-$, $Eu(OH)_4$ and $Th(OH)_4(aq)$ that are dominant at pH 12.5 are as follows, according to the Thermochime_v10a database (Themochimie_PhreeqC_SIT_oxygen_v10a.dat):

$$Ni^{2+} - 3\,H^+ + 3H_2O \rightleftarrows Ni(OH)_3^- \qquad \log K = -29.4$$

$$Eu^{3+} - 4\,H^+ + 4\,H_2O \rightleftarrows Eu(OH)_4^- \qquad \log K = -40.7$$

$$Th^{4+} - 4\,H^+ + 4\,H_2O \rightleftarrows Th(OH)_4 \qquad \log K = -17.4$$
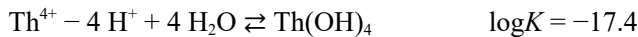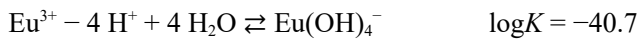
The equations and log equilibrium constants given above include the dissociation of water reaction.

$$H_2O \rightleftarrows H^+ + OH^- \qquad \log K = -14.0$$

To define $\log K$ values based on the radionuclide and OH^- concentrations only, the contribution from this reaction can be removed as follows:

$$\log K_{Ni(OH)3^-} = -29.4 - 3(-14) = 12.6$$

$$\log K_{Eu(OH)4^-} = -40.7 - 4(-14) = 15.3$$

$$\log K_{Th(OH)4} = -17.4 - 4(-14) = 38.6$$

The log stability constants agree well with those reported in Allard et al. (2002) for $Ni(OH)_3^-$ and $Th(OH)_4(aq)$ of 12 and ~ 40, but the value for $Eu(OH)_4^-$ is lower than that reported in Allard et al. (2002), of ~ 21.

For the reaction:

$$M(OH)_x^y + NTA^{3-} \rightleftarrows M(NTA)^{y+x-3} + xOH^-$$
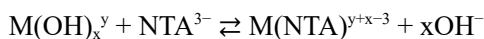
K_{NTA} can be defined where:

$$K_{NTA} = K_{M(NTA}^{y+x-3}{}_)\,/\,K_{M(OH)x}^y$$

Thus:

$$[M(NTA)^{y+x-3}]\,/\,[M(OH)_x^y] = [NTA] \times K_{NTA}\,/\,[OH^-]^x$$

When $[NTA] = [OH^-]^x\,/\,K_{NTA}$, then $[M(NTA)^{y+x-3}]\,/\,[M(OH)_x^y]$ is equal to 1, and so the species are present at equal concentrations.

The OH^- concentration of pure water at pH 12.5 (0.032 M) was used in this calculation and the results are presented in Table 2-7 for both the Thermochimie data and the data presented in Allard et al. (2002). This method is simple and only addresses a single complex under ideal solution conditions (very low ionic strength). However, it demonstrates that the Ni(II)NTA$^-$ species is expected

to form at low NTA concentrations, while impossibly high concentrations of NTA are required for ThNTA$^+$ to form at pH 12.5. The dominant Th-NTA species at high pH is a mixed hydroxide complex (Th^{4+} + 2OH$^-$ + NTA^{3-} ⇄ Th(OH)$_2$NTA$^-$ log$K$ = 35.2), which can compete with Th(OH)$_4$ formation to a greater extent than ThNTA$^+$. The stability of Th(OH)$_4^-$ is however an important factor for understanding Th(IV) complex formation at high pH.

Table 2-7. The logarithm of the stability constants for OH and NTA, and the resulting concentrations of NTA required for 1:1 MNTA species to form at pH 12.5 for Ni(II), Eu(III) and Th(IV).

	Ni(II)	Eu(III)	Th(IV)
log$K_{M(OH)x}$ (Thermochimie)	12.6	15.3	38.6
log$K_{M(OH)x}$ (Baes and Mesmer 1976, in Allard et al. 2002)	12	21	40
log$K_{M(NTA)z}$ (1:1) (Thermochimie)	12.75	13*	17.15
log$K_{M(NTA)z}$ (Allard et al. 2002)	12.8	13.3	15.1
log($K_{M(NTA)z}/K_{M(OH)x}$) (Thermochimie)	0.15	−2.3	−21.5
log($K_{M(NTA)z}/K_{M(OH)x}$) (Allard et al. 2002)	0.80	−7.7	−24.9
K_{NTA}/OH^x (Thermomochimie)	4.3 × 10^4	4.8 × 10^3	3.4 × 10^{-16}
K_{NTA}/OH^x (Allard et al. 2002)	1.9 × 10^5	1.9 × 10^{-2}	1.2 × 10^{-19}
[NTA] (Thermomochimie)	2.3 × 10^{-5}	2.1 × 10^{-4}	3.0 × 10^{15}
[NTA] (Allard et al. 2002)	5.2 × 10^{-6}	5.3 × 10^1	8.3 × 10^{18}

* Based on Am data, which has the same hydrolysis constant as Eu.

Due to the range of different reactions and factors that affect radionuclide and stable element speciation at high pH, and the number of different species that can form, this calculation is only indicative. Speciation calculation programmes, such as PhreeqC (Parkhurst and Appelo 1999) are needed to predict the persistence of a species under the high pH conditions of SFR.

2.2.3 Ionic strength

The ionic strength of a solution affects speciation. The concentrations of Th(IV) and Ni(II) species in solutions containing Th(IV) and NTA or Ni(II) and oxalate at pH 12.5 as a function of ionic strength are shown in Figure 2-3. Figure 2-3 was calculated using PhreeqC (Parkhurst and Appelo 1999) Version 3 and the Thermochimie_v10a database (Thermochimie_PhreeqC_SIT_oxygen_v10a.dat). Although stability constants have been largely discussed so far in terms of concentrations, they are in fact a function of thermodynamic activities rather than concentrations. Since all but very dilute solutions deviate from ideal behaviour, the thermodynamic activity of each species is affected by the ionic strength of the solution. Ni(II) oxalate complexes are less sensitive to the ionic strength than Th(IV)-NTA complexes (Figure 2-3).

2.2.4 Challenges associated with speciation modelling

Despite the clear advantages of using a speciation calculation programme, there are also some important challenges. To successfully predict speciation, in principle every individual interaction between the components of the system needs to be quantified. Table 2-7 showed a large difference in the stability constants for Eu(OH)$_4^-$ in Thermochimie and Allard et al. (2002), and the effect that has on the predicted impact on EuNTA$^-$ formation. Questions have also been raised about the dominant Ni(II) hydroxide aqueous species at pH 12.5 following recent experiments (Bruno et al. 2018). The Thermochimie database predicts that Ni(OH)$_3^-$ is the major solution species at pH 12.5 and that the solubility of Ni(II) increases as the pH increases from pH 10.5 to 13 as a result of the increasing dominance of this species. However, the experimental results showed that Ni(II) solubility is quite constant from pH 10–13. Bruno et al. (2018) therefore concluded that the dominant solution species at high pH is Ni(OH)$_2$(aq). The lack of an increase in solubility in this pH range has also been observed in other solubility studies, for example at elevated temperature (250 and 350 °C) in Palmer et al. (2004), and was supported by data from a laboratory transport experiment (Felipe-Sotelo et al. 2016).
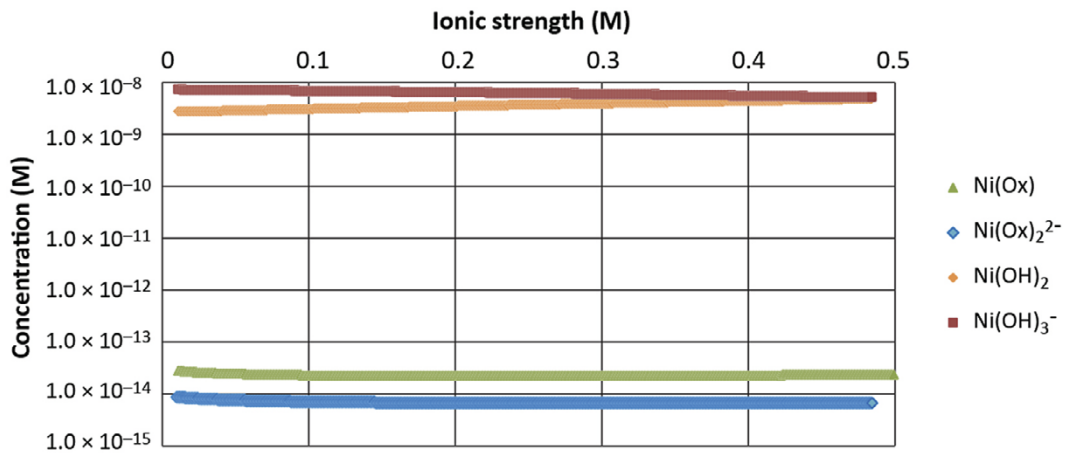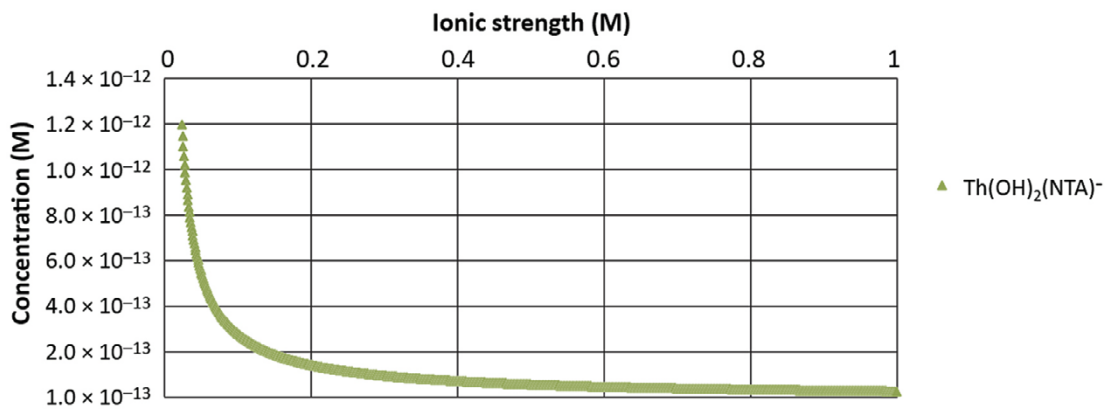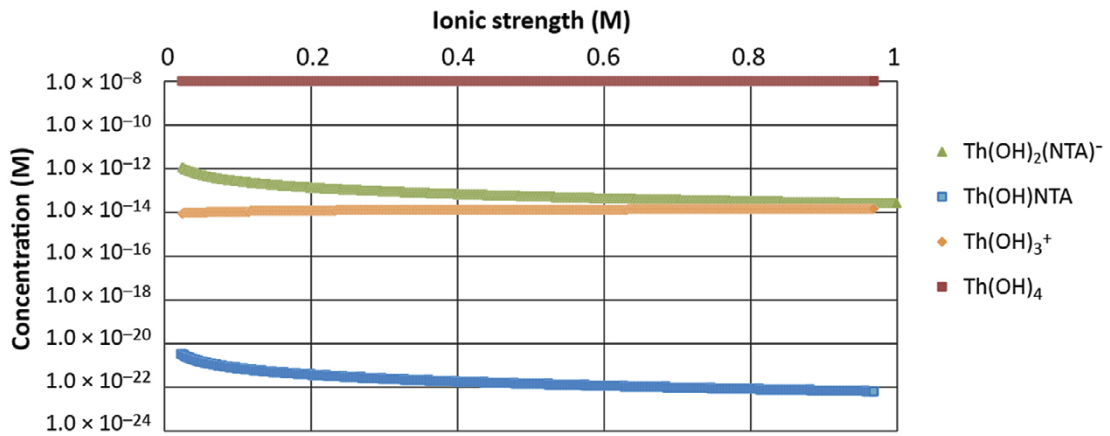
Figure 2-3. *The effect of ionic strength on the concentrations of Th(IV) and Ni(II) species in solutions of a) 10^{-8} M Th(IV) and 10^{-3} M NTA, with the Th(OH)$_2$NTA$^-$ concentration shown on a normal scale in b), and c) 10^{-8} M Ni(II) and 10^{-3} M oxalate, at pH 12.5.*

The stability constant for $Ni(OH)_2(aq)$ was redefined by Bruno et al. (2018):

$$Ni^{2+} + 2\,H_2O \rightleftarrows Ni(OH)_2(aq) + 2\,H^+ \qquad \log K = -19.7$$
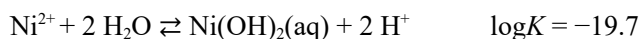
This can be converted into the form of the Thermochimie stability constants by removing the contribution from the formation of OH^-:

$$Ni^{2+} + 2OH^- \rightleftarrows Ni(OH)_{2(aq)} \qquad \log K_{Ni(OH)2}(aq) = -19.7 - 2(-14) = +8.3$$

Using Equation (2-2) and the OH^- concentration of 0.032 M at pH 12.5, the ratios of the Ni-hydroxide species to Ni^{2+} concentrations are as follows:

$[Ni(OH)_2(aq)]/[Ni^{2+}(aq)]$: $10^{8.3} \times 0.032^2 = 2.0 \times 10^5$ (from Bruno et al. 2018)

$[Ni(OH)_3^-(aq)]/[Ni^{2+}(aq)]$: $10^{12.7} \times 0.032^3 = 1.6 \times 10^8$ (from Thermochimie)

Applying the data from Bruno et al. (2018) would therefore reduce competition from hydroxide formation at pH 12.5 by a factor of $\sim 1\,000$ under these simplified conditions and for simple 1:1 complexes. This introduces large uncertainties in the predicted impact of complexing agents. It is not always easy to take the new data into account. For example, when stability constants for radionuclide-organic complexes are derived from experimental data, thermodynamic data describing the inorganic speciation of the radionuclide are included in the derivation. Therefore, if the data describing inorganic speciation change, the stability constants for organic complexes of the metal need to be re-evaluated. In the case of Ni-NTA, the stability constants of a number of species in the Thermochimie database, e.g. $NiNTA^-$, $NiNTA_2^{4-}$ and $Ni(OH)(NTA)^{2-}$ have been defined in the context of the Ni hydroxide data selected. Therefore, changing the Ni(II)-hydroxide data alone would remove the internal consistency of the database, and falls outside the scope of this report. However, it is important to be aware of these uncertainties, especially when using stability constants from the literature.

2.3   Polymers

Polymers are organic macromolecular structures built from repeat units of the reactants. They can be natural or man-made, and polymers of relevance for this report include cellulose, superplasticisers, plastics, rubber, filter aids, anti-corrosion paints and lignin.
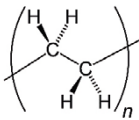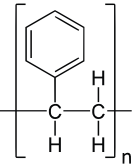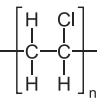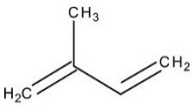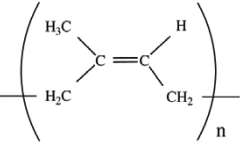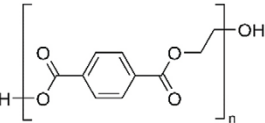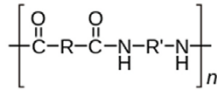
Some natural polymers, such as lignin, show variable composition, both within the structure of a single polymer and between polymer chains. However, most of the polymers of interest consist of chains of a single repeat unit formula. Anthropogenic polymers are designed for purpose, but their exact structures are sometimes proprietary information.

Some common plastic and rubber polymers are described in Table 2-8 and these are used in the following general description of polymers. Specific information regarding cellulose, superplasticisers, plastics, rubber, filter aids, anti-corrosion paints and lignin is given in the relevant sub-sections of Chapter 4.

In general, polymers can be divided into two categories according to the polymerisation reaction used in their production, see Table 2-8 for the structures discussed:

1. Addition polymers, such as polyethylene $((C_2H_4)_n)$, polystyrene $((C_8H_8)_n)$, polyvinyl chloride (PVC) $((C_2H_3Cl)_n)$ and rubber $((C_5H_8)_n)$.
2. Condensation polymers, such as polyesters and polyamides.

Table 2-8. Chemical structures of some common plastic polymers and rubber.

Polymer	Chemical formula	Reactant(s)	Structure of repeat unit[a]	Comment
Polyethylene (polyethene)	$(C_2H_4)_n$	$H_2C=CH_2$		Addition polymer
Polystyrene	$(C_8H_8)_n$			Addition polymer
Polyvinyl chloride	$(C_2H_3Cl)_n$	$H_2C=CHCl$		Addition polymer
Rubber	$(C_5H_8)_n$			Addition polymer[b]
Polyester	Variable	Dicarboxylic acid and diol		Condensation polymer. Example shows polyethylene terephthalate (PET)
Polyamide	Variable			Condensation polymer, generic example[c]

[a] Reproduced with permission from wikipedia.com where not otherwise stated.

[b] Reproduced from Surya et al. (2017) with permission under Creative Commons Attribution 3.0 Licence (https://creativecommons.org/licenses/by/3.0).

[c] Reproduced from Lumen Learning (2020) with permission under Creative Commons Attribution-ShareAlike 4.0 International License (https://creativecommons.org/licenses/by-sa/4.0).

Catalysts are used to drive the formation of addition polymers, with the cleavage of the C–C double bond to produce a radical that can propagate the polymerisation reaction. As a result, and as can be seen in Table 2-8, addition polymers generally contain only C atoms in the backbone of the polymeric chain (Van Loon and Hummel 1995). The C–C backbone of addition polymers is generally very stable and insensitive to alkaline degradation.

The formation of condensation polymers, on the other hand, involves the copolymerisation reaction of two different chemicals or functional groups, both of which contribute to the polymer chain. The condensation reaction produces a small molecule such as water as well as the polymer (Figure 2-4). As can be seen in Table 2-8, condensation polymers contain functional groups in their polymeric chains. In polyesters, there are ester groups, and in polyamides, amide groups. These functional groups generally provide a point of chemical attack, introducing the possibility of hydrolysis of the polymeric chain (Van Loon and Hummel 1995). Both ester and amide groups are prone to alkaline hydrolysis, which is essentially the reverse of the condensation reaction used to form the polymer. Therefore, hydrolysis of polyamides is expected to produce dicarboxylic acids and diamines, while alkaline degradation of polyesters produces dicarboxylic acids and diols. Polyamides and polyesters can also be homopolymers synthesised from a single type of monomer that contains one of each of the reactive groups. Examples include amino acids or molecules with a carboxylic acid group and an alcohol group, such as lactic or glycolic acid. These monomers are also the hydrolysis products of homopolymeric polyamides and polyesters.

Alkaline degradation of condensation polymers can therefore lead to the formation of complexing agents.
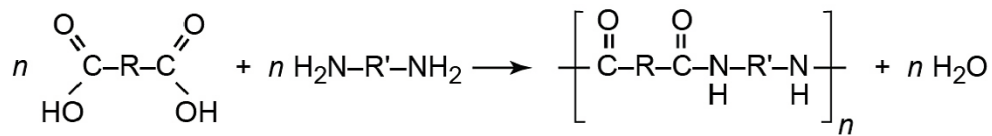
Figure 2-4. Polymerisation of a generic polyamide. Adapted from Lumen Learning (2020) with permission under Creative Commons Attribution-ShareAlike 4.0 International License (https://creativecommons.org/ licenses/by-sa/4.0).

2.4 Effect of complexing agents on cement degradation

Hard complexing agents form complexes with Ca^{2+} and some form low solubility Ca^{2+} salts. Complexation and precipitation of Ca^{2+}-complexing agent salts will affect the equilibrium between the dissolved Ca^{2+} concentration and solid phase portlandite, which is a major component of cement. It can therefore result in dissolution of portlandite and degradation of cement (De Windt et al. 2015). Additionally, reactions associated with the alkaline hydrolysis of organic condensation polymers consume hydroxide. Therefore, both Ca^{2+} complexation and polymer degradation reactions can theoretically affect the integrity of cement.

The extent to which these processes can affect cement in a waste package was evaluated in Keith-Roach et al. (2021) in the context of cellulose degradation. In the worst case waste type (F.23 in steel packaging), i.e. the waste type with the highest ratio of cellulose:cement, ~11 % of the cement could degrade theoretically due to consumption of OH^- during alkaline degradation of cellulose, and ~20 % due to Ca^{2+} complexation. Therefore, accelerated cement degradation in SFR waste packages could be significant.

Cement degradation can have negative effect on two key safety functions of SFR, *good retention* and *limited advective transport*. Therefore, the influence of complexing agents and organic waste disposed of in SFR needs to be considered in this regard, as well as the direct effect on radionuclide sorption through radionuclide complexation.

3 PhreeqC calculations

The thermodynamic software PhreeqC (Parkhurst and Appelo 1999) Version 3 and the Thermochimie_v10a database (Thermochimie_PhreeqC_SIT_oxygen_v10a.dat) were used to calculate aqueous radionuclide speciation in the presence of complexing agents in this report. Calculations were carried out when appropriate experimental sorption data were not available. Three main approaches were used:

1. pH titrations of a solution containing the radionuclide and complexing agent at defined concentrations.

2. Titration of the complexing agent into a solution of a radionuclide in equilibrium with excess portlandite, which is representative of the conditions in SFR. Solid portlandite was therefore present in every step of the titration.

3. Titration of the complexing agent into a radionuclide solution representative of the experimental conditions used to examine the effect of ISA on Ni(II) sorption to cement (Bruno et al. 2018).

The conditions used in these calculations are summarised in Table 3-1. The temperature in SFR is likely to be closer to 12 °C than experimental temperatures, which tend to be ~25 °C. However, the dissolution equilibrium of portlandite temperature dependent and 25 °C results in a pH of 12.5. Therefore, all calculations were carried out at 25 °C. The only equilibrium phase was portlandite. Precipitation of other phases was not included in these calculations to maintain focus on the solution phase speciation.

Table 3-1. Summary of the conditions used in the PhreeqC calculations.

	pH titration	Titration of complexing agent into a solution representative of SFR	Titration of complexing agent under the experimental conditions of Bruno et al. (2018)
Temperature	25	25	25
Initial pH	6.0	8.0	6.0
Na [M] – charge balance	Variable	Variable	0.5
Cl [M]	Variable	Variable	0.5
Radionuclide [M]	10^{-8}	10^{-8}	2.83×10^{-10}
Initial portlandite [M]	0	1*	0.0525

* Based on Keith-Roach et al. (2021).

The most relevant ionic strength for this report is the ionic strength of the waste packages, which will vary over time and space (see Section 1.2.2). The ionic strength of concrete porewater is also influenced by the equilibrium with portlandite and the concentration of complexing agent added. Bruno et al. (2018) controlled the ionic strength of their experiments by adding NaCl (0.5 M), and so this was included in the relevant calculations. In the other calculations, the ionic strength was kept above 0.1 M so as to reduce the sensitivity of the results to the ionic strength. This is also a reasonable minimum ionic strength expected in the repository, especially when complexing agents are present at a concentration that affects the ionic strength.

Although the conditions used in the calculations of speciation in a) concrete porewater and b) under the experimental conditions of Bruno et al. (2018) are different, the results of the calculations are similar. The pH and the concentration of free, dissolved Ca^{2+} are controlled by portlandite dissolution. While solid-phase portlandite remains in the calculations, the concentration of portlandite does not affect the results. Additionally, as the complexing-agent and dissolved Ca^{2+} concentrations, in equilibrium with portlandite, are always in large excess of the radionuclide concentration, the relative proportion of radionuclide complexed is not dependent on the total radionuclide concentration (2.83×10^{-10} or 10^{-8} M).

Complexation of a radionuclide by a complexing agent occurs over a concentration range of the complexing agent. When speciation is calculated, the percent radionuclide present as an organic complex needs to be translated into an effect on radionuclide sorption for this report. Broadly speaking, if 1 % of the radionuclide in the solution phase is complexed, it will increase the solution phase concentration by 1 %, due to the equilibrium between the radionuclide in the sorbed and solution phase readjusting. The effect on sorption increases as the percentage of the radionuclide that is complexed increases. When organic complexes comprise 50 % of the radionuclide solution species (with excess complexing agent as considered here), the sorption equilibria would readjust to double the concentration of radionuclide in solution. With 90 % complexation, the sorption reduction would be very large. The model of Bruno et al. (2018) suggested that over 20 % of Ni(II) was complexed by ISA when a small sorption reduction effect was observed, and over 50 % when a sorption reduction effect of between 3–6 times was observed.

Metallic iron is a major component of SFR waste. Corrosion to Fe(II)/Fe(III) with subsequent complexation of the Fe(II, III) ions may be expected to reduce the interactions of complexing agents with radionuclides. However, since many relevant waste packages only contain iron in the packaging material, these interactions are not considered in the PhreeqC calculations or in this report in general. It can also be noted that defining Fe chemistry in SFR is complex and associated with a large degree of uncertainty.

4 Complexing agents and organic materials in SFR

This chapter introduces the organic materials considered in this report. For each material, the following are discussed in turn:

- Origin.

- Structure.

- Degradation characteristics and reactions.

- Solubility and sorption.

- Coordination and denticity of relevant complexing agents.

- Presence in SFR (per waste type and vault, and on the inside or outside of the packages and/or in packaging material).

- Occurrence in future waste (according to the assessment in Chapter 4).

- Form following the resaturation of SFR (dissolved, low solubility salt, polymer, etc).

- Literature review of effect on radionuclide speciation and sorption.

- PhreeqC calculations.

- Recommended concentration limits for WAC 4.0.

In this chapter, the impact of complexing agents on Th(IV), as a well-studied, redox insensitive analogue of Pu(IV), and Ni(II) are generally the focus when assessing the risks associated with complexing agents and organic materials. However, trivalent actinides are also considered. Complexing agents may affect trivalent actinides to a greater extent than tetravalent actinides at pH 12.5. The softer character of Ni(II) means that it is the focus of the assessment of the effect of polyamines.

PhreeqC calculations are used to complement the available literature, especially where they can aid our understanding of the effect of a complexing agent on radionuclide speciation at alkaline pH.

Esters undergo alkaline hydrolysis to produce a carboxylic acid and an alcohol. Esters are not discussed explicitly in this report, but the WAC recommended in this report are equally relevant for complexing agents in their ester form as in their corresponding carboxylic acid form.

4.1 Cellulose

4.1.1 Origin

Cellulose is a major component of cloth, paper products, some tissues and wood waste materials.

4.1.2 Structure

Cellulose is a linear polysaccharide (Figure 4-1). Individual polymeric chains interact with each other via hydrogen bonding between hydroxyl groups and oxygen atoms, resulting in a 3D structure. The 3D structures can be crystalline or amorphous, and macroscopic cellulose typically contains regions of both. The main degradation product of cellulose under repository conditions is ISA, and its structure is shown in Figure 4-2.
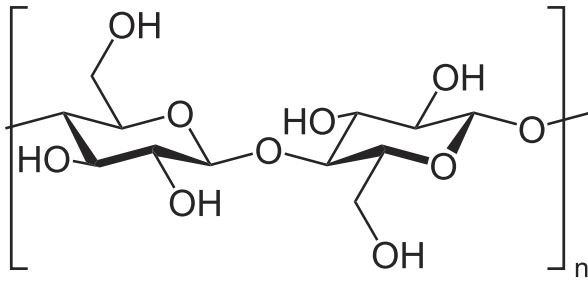
Figure 4-1. *Chemical structure of cellulose.*
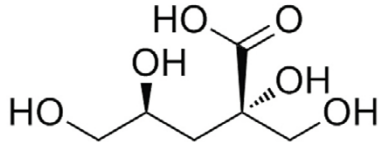
Figure 4-2. *Chemical structure of isosaccharinic acid, ISA.*

4.1.3 Degradation characteristics and reactions

Amorphous regions of the cellulose structure degrade via the "peeling off" reaction under alkaline conditions. In this reaction, reducing end groups of the cellulose polysaccharide chain isomerise into reactive intermediates that are then eliminated from the chain (Van Loon and Glaus 1998). The reaction produces new reducing end groups for further reaction, leading to step-wise elimination of glucose units and depolymerisation of the chain. The reaction sequence stops when the reactive intermediate is converted to a stable meta-saccharinic end group on the polysaccharide chain, or a crystalline (inaccessible) region of the chain is reached. These two stopping reactions are termed the chemical stopping reaction and the physical stopping reaction, respectively. Once all end groups are stable or inaccessible, the peeling off reaction depends on the formation, or increased accessibility, of reducing end groups. The possible reaction mechanisms for this are termed "mid-chain scission", which involves alkaline hydrolysis of glycosidic bonds in the polymeric chain, and "decelerated peeling", which involves a dynamic equilibrium between crystalline and amorphous structures of cellulose (Glaus and Van Loon 2008).

The products of alkaline cellulose degradation depend on the composition of the surrounding solution (Bradbury and Van Loon 1997, Van Loon and Glaus 1997). In the presence of Ca^{2+}, as found in cement pore waters, the formation of ISA is favoured with a typical yield of $\sim 80~\%$ (Bradbury and Van Loon 1997, Van Loon and Glaus 1997, Pavasars et al. 2003, Glaus and Van Loon 2008). The α- and β-diastereoisomers of ISA are formed in approximately equal proportions (Van Loon et al. 1999a). α-ISA exhibits particularly strong complexing properties and therefore is of concern in terms of its potential to enhance radionuclide mobility (Pavasars 1999, Glaus et al. 1999, Van Loon et al. 1999b). The β-ISA-Eu(III) complex is about 100 times less stable than the equivalent α-ISA complex (Van Loon and Glaus 1998). Minor degradation products comprise short chain aliphatic carboxylates such as formate, acetate and lactate (Glaus et al. 1999, Van Loon et al. 1999a).

The overall chemical formula of cellulose is $(C_6O_5H_{10})_n$, although the reactive end group has the formula $C_6O_6H_{11}R$. The equation for the production of ISA in each step of the peeling off process is as follows:

$$C_6O_6H_{11}R + OH^- \rightarrow C_6O_6H_{12} + OR^- \tag{4-1}$$

Since hydroxide ions that attack cellulose are incorporated into the ISA molecules formed, 162 g of the original cellulose degrades in each step. Therefore, 162 g of cellulose is degraded per mole of ISA produced.

The rate of cellulose degradation under cementitious conditions depends on the type of cellulose in question, due to the availability of reducing end groups (Glaus and Van Loon 2008). In the safety assessment SR-PSU(PSAR), the ISA concentration was calculated after 5 000 years of Tela tissue cellulose degradation, when ~99 % of the cellulose was judged to have degraded.

Gamma irradiation has been seen to increase the rate of alkaline cellulose degradation (Baston et al. 2002). The maximum absorbed dose in the experiments was ~230 kGy. The leachates from the experiments were found to increase the solubility of plutonium as a function of absorbed dose. The results indicated that irradiation increases the accessibility of the crystalline regions of cellulose, and therefore enhances alkaline degradation (Baston et al. 2002, Filby et al. 2016).

4.1.4 Solubility and sorption

Cellulose is a solid, but its degradation products are soluble in water. The solubility of the degradation product α-ISA is however limited to about 20 mM by precipitation of the calcium salt in water in equilibrium with portlandite (0.02 M Ca^{2+}; 0.05 M ionic strength) (Van Loon and Glaus 1998). The β-diastereoisomer forms much more soluble calcium salts (Van Loon and Glaus 1998).

ISA also sorbs to cement according to Equation (4-2) (Van Loon and Glaus 1998).

$$[ISA]_{sorbed} = \frac{K_1 \cdot q_1 \cdot (ISA)_{eq}}{1 + K_1 \cdot (ISA)_{eq}} + \frac{K_2 \cdot q_2 \cdot (ISA)_{eq}}{1 + K_2 \cdot (ISA)_{eq}} \tag{4-2}$$

where

K_1 = adsorption-affinity constant of site 1 = 1 730 L mol^{-1}

q_1 = adsorption capacity of site 1 = 0.1 mol kg^{-1}

K_2 = adsorption-affinity constant of site 2 = 12 L mol^{-1}

q_2 = adsorption capacity of site 2 = 0.17 mol kg^{-1}

Rosdahl (2020) used this equation and the current WAC ISA concentration limit of 10^{-4} M, to estimate that 5 g cellulose can be tolerated in the waste per kg of dry cement (Appendix A in Rosdahl 2020). The estimate also included the assumption that the maximum ISA concentration would be reached when 85 % of the cellulose has degraded, due to outward transport of ISA. The limit is equivalent to 3.6 g cellulose per kg of hydrated cement.

4.1.5 Coordination and denticity

ISA is an α-hydroxycarboxylate with multiple alcohol groups. The term α-hydroxycarboxylate refers to the presence of an alcohol group on the carbon adjacent to the carboxylate group. As seen with citrate, this position leads to a higher acidity than usually seen in an alcohol group. ISA can therefore coordinate to metal ions as a bidentate complexing agent via the α-hydroxycarboxylate group, with the formation of a 5 membered chelate ring. The hydroxyl oxygen may or may not be deprotonated in this arrangement. Tasi (2018) suggested that metal coordination enhances deprotonation. Based on analogy with gluconate (see Section 4.2.5), tridentate bonding can take place involving the hydroxyl group two carbons along from the α-carbon in addition to the groups involved in bidentate bonding. Tetradentate bonding may also occur. EXAFS data has provided evidence that Th(IV) is bound via depronotated alcohol groups, not the carboxylate, and the number of groups involved was tentatively suggested to be two, i.e. bidentate binding (Colàs 2014).

4.1.6 Presence in SFR

Cellulose is present within the waste packages. It is also used as an additive in the Silo grout, but the grout is used outside the waste packages and it is not subject to WAC.

4.1.7 Occurrence in future waste

The Swedish nuclear facilities have in recent years replaced cellulose with other materials where possible, in order to conform to the existing WAC.

4.1.8 Form following the resaturation of SFR

Cellulose will be present as a solid. ISA will be present as dissolved isosaccharinate, but it will also sorb according to its isotherm to available hydrated cement and precipitate as a calcium salt if the solubility product is exceeded (Section 4.1.4).

4.1.9 Literature review of effect on radionuclide speciation and sorption

The effect of ISA on radionuclide sorption to hydrated cement has been studied widely (e.g. Van Loon and Glaus 1998, Wieland et al. 1998, 2002, Dario et al. 2004, Tasi 2018, Bruno et al. 2018).

Sorption of ISA onto hydrated cement affects its ability to enhance radionuclide solubility, thus experimental results are influenced by the solid:solution ratio of the experiment, as well as the solid phase and pH used. Therefore, comparability between experimental results is only expected if the same solid:solution ratio was applied or the concentration of ISA remaining in the solution phase was reported. Van Loon and Glaus (1998) used feldspar specifically to avoid the complications of ISA sorption to the experimental solid phase, since feldspar sorbs radionuclide cations but not ISA. Furthermore, whether enantiomerically mixed ISA or pure α-ISA is used may affect the impact on radionuclide sorption. The conditions used in the experiments discussed in this section are summarised in Table 4-1.

Since α-ISA comprises approximately half of the total ISA, the potential variations in the aqueous phase concentration of α-ISA due to the experimental setup and sorption are greater than the effect due to the presence of β-ISA. Therefore, the discussion below does not specify whether ISA or α-ISA was used in each experiment. It is also worth noting that different experimental approaches, such as the order in which the ligand and metal are added and the times between these, may affect short term results due to kinetics. This was observed, for example, by Tasi (2018) in sorption experiments with ISA.

The effect of ISA on Eu(III) sorption has been investigated in a number of studies. Van Loon and Glaus (1998) found that ISA concentrations $> 1 \times 10^{-4}$ M affected Eu(III) sorption to feldspar in artificial cement porewater. Dario et al. (2004) found that short term (24 hours) Eu(III) sorption to hydrated cement was reduced when ISA was added at concentrations of 10^{-3} and 10^{-2} M. Changes over 400 days were investigated using $10^{-2.5}$ M ISA and although Eu(III) sorption increased during the first 50 days, this ISA concentration reduced the sorption of Eu(III) at equilibrium by over an order of magnitude. Wieland et al. (1998) found that ISA had a negligible effect on Eu(III) sorption to hydrated cement until the ISA concentration exceeded 10^{-2} M.

ISA was found to reduce Th(IV) sorption to hardened cement paste by over four orders of magnitude as the ISA equilibrium concentrations increased from 10^{-4}–10^{-2} M, but it had no influence at concentrations $\leq 10^{-4}$ M (Wieland et al. 1998, 2002). Van Loon and Glaus (1998) found that ISA concentrations in the range 10^{-4}–10^{-3} M reduced Th(IV) sorption to feldspar. Experiments by Pavasars (1999) showed that the addition of a high concentration of ISA (3×10^{-2} M) resulted in a persistent reduction of radionuclide sorption; after 3 months Th(IV) sorption was reduced at least 50 times. However, lower concentrations ($3 \times 10^{-3} - 5 \times 10^{-3}$ M ISA) only reduced sorption of ^{234}Th(IV) significantly for 1 month (Pavasars 1999).

More recently, Tasi (2018) examined the effect of ISA on Pu(IV) sorption to cement. In the most relevant experiments for this report, ISA was present at a total concentration of 10 mM, the initial Pu concentration was 4×10^{-9} M and the S:L ratio was 2–4 g/L. Two sets of experiments were carried out. The first set involved equilibrating the hydrated cement phase, Pu and redox buffer in the porewater solution, with subsequent addition of ISA, while the second set involved equilibrating Pu and ISA in the redox-buffered porewater solution, with subsequent addition of fresh cement powder. Sorption of Pu(IV) was reduced by a factor of 1 000 when Pu was pre-equilibrated with the cement, and a factor of 32 000 when Pu was pre-equilibrated with ISA. Tasi (2018) judged that the first set of experiments were most representative of equilibrium conditions.

ISA has also been found to reduce Ni(II) sorption to feldspar, but significant effects were only seen at ISA concentrations higher than 10^{-2} M (Van Loon and Glaus 1998). The degradation products of cellulosic materials (tissues, cotton and paper) were more effective than ISA at solubilising Ni(II), but these have not been fully characterised or studied to the same extent as ISA (Van Loon and Glaus 1998, Van Loon et al. 1999b). Recently, Bruno et al. (2018) examined the effect of ISA on Ni(II) sorption to cement and observed a reduction in Ni(II) sorption at an ISA concentration of 4×10^{-3} M, of between 1.2 and 2.4 times. With a 2×10^{-2} M ISA concentration, sorption was reduced by a factor of 3–6.

Table 4-1. Experimental conditions in ISA sorption experiments described. "Total" indicates the racemic mixture of ISA diastereoisomers.

Radionuclide	Type of ISA	Radionuclide concentration [M]	HCP [g/L]	pH	Reference
Eu(III)	α-ISA	6.7×10^{-10}	0.67 (Feldspar)	13.3	Van Loon and Glaus (1998)
Eu(III)	Total	10^{-8}	1	12.3–12.7 (initial pH)	Dario et al. (2004)
Eu(III)	Total	$\leq 5 \times 10^{-10}$	10^{-5}	13.3	Wieland et al. (1998)
Th(IV)	α-ISA	6.7×10^{-9}	0.67 (Feldspar)	13.3	Van Loon and Glaus (1998)
Th(IV)	α-ISA	$\leq 10^{-10}$	0.1 and 5	13.3	Wieland et al. (2002)
Th(IV)	Total	$\leq 5 \times 10^{-10}$	10^{-4}	13.3	Wieland et al. (1998)
Th(IV)	Total				Pasavars (1999)
Pu(IV)	α-ISA	4×10^{-9}	2–4	12.6	Tasi (2018)
Ni(II)	α-ISA	3×10^{-10}	16 (Feldspar)	13.3	Van Loon and Glaus 1998
Ni(II)	Total	2.83×10^{-10}	25	12.5	Bruno et al. (2018)

There have also been a number of studies that have investigated the speciation of radionuclide-ISA complexes and derived stability constants. Bruno et al. (2018) re-evaluated the species and stability constants relevant to the formation of Ni(II)-hydroxide and -ISA complexes at high pH. The most stable Ni(II)-ISA species under cementitious conditions was identified as $Ni(OH)_2ISA^-$. The Ni hydroxide and Ni-ISA species selected and applied in Bruno et al. (2018), and their stability constants, differ from those in the Thermochimie database (Table 4-2). The solution phase speciation resulting from calculations using the defined stability constants is shown in Figure 4-3.

Table 4-2. Log stability constants for Ni(II) hydroxide and ISA species in the Thermochimie database and those derived by Bruno et al. (2018).

	log$K$ Themochimie	log$K$ (Bruno et al. 2018)
$Ni(OH)_2$(aq)	−18.0	−19.7 ± 0.4
$Ni(OH)_3^-$	−29.38	
NiOHISA(aq)		−6.5 ± 0.3
$Ni(OH)_2ISA^-$		−17.6 ± 0.5
$Ni(OH)_3ISA^{2-}$	−26.5	−31.0 ± 0.7
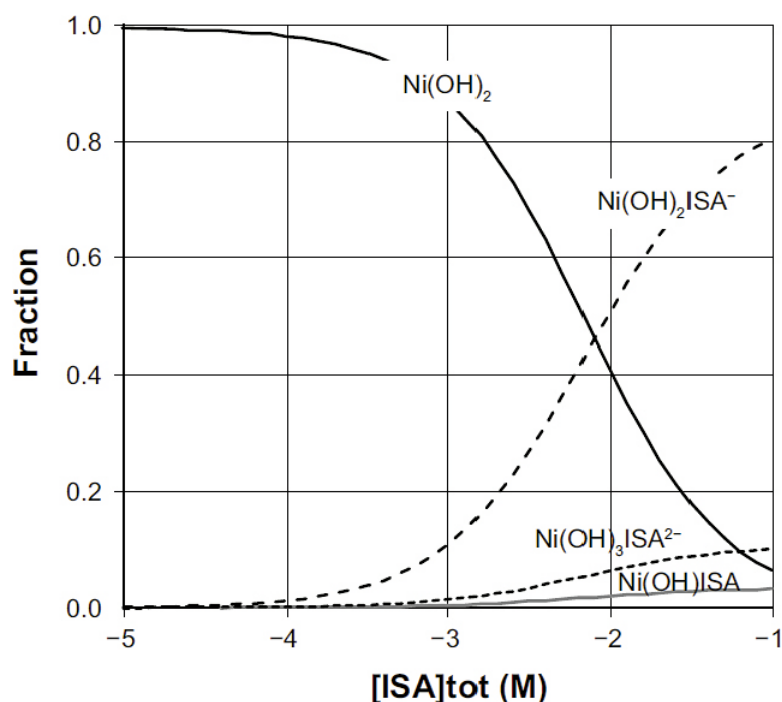
Figure 4-3. *Solution phase speciation calculated in Bruno et al. (2018).*

Rai and Kitamura (2017) reviewed the isosaccharinate binding constants for Ca, Fe(III), Th, U(IV), U(VI), Np(IV), Pu(IV), and Am(III). According to the Thermochimie database, the most stable Th-ISA species under cementitious conditions is $CaTh(OH)_4HISA^+$. However, Rai and Kitamura (2017) judged that the data behind the formation of this species is unreliable and they did not recommend data for this species. The Th(IV)-ISA species and stability constants recommended in Rai and Kitamura (2017) show significant differences from those in Thermochimie database (Table 4-3). This shows that despite the relatively abundant data, there remains a significant uncertainty in the thermodynamic description of radionuclide-ISA complexes.

Thermochimie data have been used to predict Am(III) speciation, as an analogue of Eu(III), under the conditions of Dario et al.'s (2004) experiments with ISA (Keith-Roach et al. 2021). The results of the calculations were generally consistent with the observed effects on sorption.

Table 4-3. Stability constants for Th(IV) and Pu(IV) in the Thermochimie_v10a database and those recommended by Rai and Kitamura (2017).

Radionuclide	Th stability constants (Thermochimie)	Th stability constants (Rai and Kitamura 2017)	Pu stability constants (Thermochimie)	Pu stability constants (Rai and Kitamura 2017)
$An(OH)_3$	−11			
$An(OH)_4$	−17.4		−8.5	
$An(OH)ISA^{2+}$		3.2		
$An(OH)_3HIsa$	−5.65			
$An(OH)_3(HISa)_2^-$	−4.9	−4.9		
$An(OH)_4HIsa^-$	−13.2		−3.6	−0.69
$An(OH)_4(HISa)_2^{2-}$	−10.4	−12.5	0.7	3.15
$CaAn(OH)_4HISa^+$	−9			

4.1.10 PhreeqC calculations

The abundant experimental data available for the effect of ISA on radionuclide sorption means that additional speciation calculations are not required.

4.1.11 Recommendations for WAC 4.0

The recommended maximum tolerable concentration for ISA is 10^{-4} M in the aqueous phase, based on experimental results for Th(IV) and Eu(III).

Cellulose degradation should be assumed to generate ISA as 80 % of the mass of the original cellulose (Section 4.1.3). For consistency with the safety assessment SR-PSU(PSAR), the ISA concentration should be calculated after 5 000 years of cellulose degradation when ~99 % has degraded (based on Tela tissue degradation). A molar mass of 162 g/mol should be used for ISA in the calculations to account for the inclusion of OH$^-$ in every step of the degradation reaction. Sorption to available cement should be taken into account using the sorption isotherm and the parameter values given in Section 4.1.4.

4.2 Complexing agents used at the nuclear facilities

This section discusses complexing agents that are used at the nuclear facilities and can therefore be present in SFR wastes. The masses of the following complexing agents have been estimated in SFR: EDTA, NTA, citrate, oxalate, gluconate, methylglycine diacetic acid (MGDA), capryliminodipropionate (CIDP) and an unidentified carboxylate amine that may be or relate to CIDP (Keith-Roach et al. 2021). CIDP has been referred to previously as NKP (e.g. Keith-Roach et al. 2021), reflecting the Swedish name for the sodium salt (natrium kapryliminodipropionat).

EDTA, NTA, gluconate, MGDA and CIDP are considered strong complexing agents according to WAC 3.0 (Section 1.1) and are currently not allowed in wastes destined for the Silo, BMA and BTF. Maximum concentrations of citrate and oxalate were specified in WAC 3.0.

A recent survey by SKB[3] identified that aminocarboxylates, di- and tricarboxylic acids (often citric acid), amine-polyols (often triethanolamine), and α-hydroxycarboxylic acids (lactic acid) are present in cleaning and hygiene products currently used in active areas of the nuclear facilities, and are expected to be present in waste packages. The survey also noted that the aminopolycarboxylates, which are of most interest for radionuclide sorption, comprise MGDA, iminodisuccinate (IDS), glutamate, CIDP (also named 2-ethylhexyliminodipropionate) and caprloamphodipropionate (CADP).

4.2.1 Origin

Organic complexing agents are present in many detergents, cleaning products and personal hygiene products used at nuclear facilities. Their purpose is to reduce the concentration of free Ca^{2+} and Mg^{2+} ions in solution since these ions lower the activity of surfactants. When these products are used in the active areas of the facilities, the wastewater treatment process can result in their accumulation in waste packages destined for SFR. Examples of these processes include evaporation of the wastewater or treatment of the wastewater using exchange resin. In these cases, the complexing agents are placed in waste packages with the evaporate or spent resin for disposal in SFR. Personal hygiene products such as soap are more minor sources of complexing agents in the waste. These have not generally been accounted for in the complexing agent inventory but have been considered where relevant in the recent survey by SKB[3].

---

[3] Inventering av produkter med komplexbildare hos avfallsproducenter. SKBdoc 1904743 ver 1.0, Svensk Kärnbränslehantering AB. (In Swedish.) Internal document.

4.2.2 Structures

The structures of EDTA, NTA, IDS, CIDP, citrate and oxalate were given in Table 2-2, while the structures of gluconate (shown as gluconic acid), MGDA, glutamate, CADP, lactate and triethanolamine are shown in Figure 4-4. MGDA is shown next to NTA to highlight the similarity of their structures.

4.2.3 Degradation characteristics and reactions

CADP contains an amide group, which can be hydrolysed to form a primary amine and carboxylic acid under alkaline conditions. There is no evidence to the authors' knowledge that the other complexing agents named above degrade under anoxic, alkaline conditions. It is therefore assumed that they persist throughout the safety assessment.

4.2.4 Solubility and sorption

The solubility of the complexing agents is high in pure water, as required by their intended function in their products. However, the solubility products of oxalate and citrate with Ca^{2+} are low, thus their dissolved concentrations will be limited by precipitation. The dissolved oxalate concentration will be limited to 10^{-5} M under the portlandite stage of cement degradation (Van Loon and Hummel 1995). The citrate concentration is also limited to about 10^{-3} M due to precipitation of calcium citrate (Keith-Roach et al. 2021). This means that their effect on radionuclide speciation will be limited.

Gluconate sorbs strongly to cement, which reduces its aqueous phase concentration in cementitious systems, such as SFR. The sorption isotherm has been investigated by Glaus et al. (2006) and was found to be described by the same equation as ISA, see Equation (3-1), but with the following parameters:

K_1 = adsorption-affinity constant of site 1 = $(2 \pm 1) \times 10^6$ L mol^{-1}

q_1 = adsorption capacity of site 1 = 0.04 ± 0.02 mol kg^{-1}

K_2 = adsorption-affinity constant of site 2 = $(2.6 \pm 1.1) \times 10^3$ L mol^{-1}

q_2 = adsorption capacity of site 2 = 0.7 ± 0.3 mol kg^{-1}

Gluconate and ISA (see Sections 4.1.3 and 4.1.4) can be expected to sorb to the same cement sorption sites, thus the presence of one may affect the sorption of the other. However, based on information in Keith-Roach et al. (2021), none of the current cementitious SFR waste types contains both gluconate and cellulose.

Gluconic acid

NTA and MGDA

NTA   MGDA
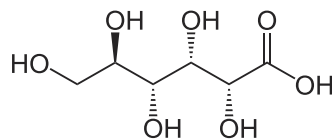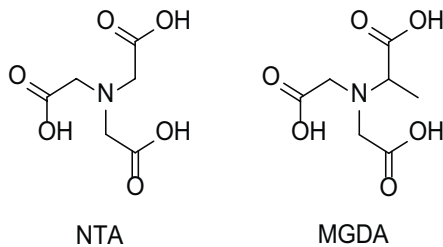
Glutamate

CADP

Lactate

Triethanolamine
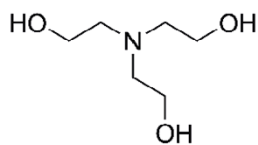
Figure 4-4. *Chemical structures of gluconic acid, NTA and MGDA, glutamate, CADP, lactate and triethanolamine.*

4.2.5 Coordination and denticity

The structures and maximum denticities of EDTA, NTA, iminodisuccinate, capryliminodipropionate, citrate and oxalate were given in Table 2-2. EDTA and NTA coordinate to metal ions via their carboxylate and amino groups, while tri- and dicarboxylic acids bind via their carboxylate groups (Table 2-2). Citrate is a tricarboxylate but uses two carboxylate groups and the oxygen in the alcohol group on the α-carbon, the carbon adjacent to a carboxylic acid group, to achieve tridentate bonding (Figure 4-5). It is not sterically possible for all four electron pair donor groups in citrate to interact with a single metal cation simultaneously. Alcohol groups on an α-carbon have a higher acidity than typical alcohol groups, due to the proximity of the electron-withdrawing carboxylic acid group. The involvement of this oxygen in chelation reduces the size of the chelate rings formed to 5 and 6 members, and thus is the most energetically favourable arrangement (see Section 2.1).

The additional complexing agents known to have been disposed of in SFR in significant quantities are MGDA and gluconate (Figure 4-4). MGDA is tetradentate via the 3 carboxylate groups and tertiary amine, and the chelate rings that form with a central metal ion have 5 members. Gluconate (Figure 4-4) can bind as a monodentate complexing agent via the carboxylate group. However, the presence of the alcohol group on the α-carbon makes bidentate bonding common, with the formation of a 5-membered chelate ring (Allscher et al. 2008). The hydroxyl oxygen may or may not be deprotonated in this arrangement, but deprotonation is expected at the pH of SFR. Tridentate bonding can take place involving the hydroxyl group two carbons along from the α-carbon in addition to the groups involved in bidentate bonding. This group becomes deprotonated at pH 8 (Allscher et al. 2008). Tetradentate bonding has also been observed and, at alkaline pH, this involves the four deprotonated hydroxyl groups furthest from the carboxylate group.

Colàs (2014) identified that gluconate coordinated to Th(IV) via deprotonated alcohol groups at pH 12, and suggested tentatively that two alcohols were involved, i.e. bidentate bonding. The position of the alcohols creates stable 5-membered chelate rings.

Glutamate is expected to be a bidentate complexing agent that coordinates via the glycine-like part of the molecule. Coordination of the second carboxylate group would involve a large chelate ring and is therefore not expected. The alkaline hydrolysis product of CADP is expected to be tridentate with coordination via the two amine groups and the nearby carboxylate. The two amine groups are separated by an ethane unit, as also seen in ethylenediamine.

Lactate is a weak bidentate complexing agent (e.g. Carbonaro et al. 2011), coordinating via the carboxylate group and alcohol group on the α-carbon. Triethanolamine is expected to be monodentate, coordinating via the nitrogen atom. Lactate and triethanolamine are therefore not considered further.
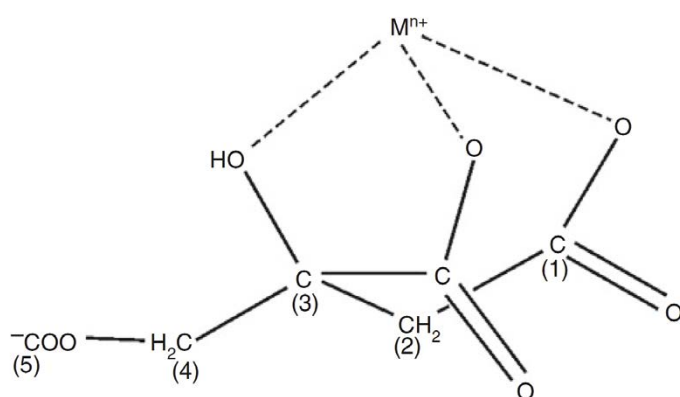
Figure 4-5. *Coordination of citrate to a metal cation. Reproduced from Wyrzykowski and Chmurzyński (2010) with permission under Creative Commons Attribution Noncommercial License (https://creativecommons.org/licenses/by-nc/2.0).*

4.2.6 Presence in SFR

Complexing agents are present within waste packages that are disposed of in the Silo (B.04, C.02, O.02, R.16), 1BMA (F.17, R.10, R.15), 2BMA (S.09), 1–2BTF (B.07, O.07).

The amounts judged to be present in the 2020 complexing agent assessment for SFR (Keith-Roach et al. 2021) are summarised in Table 4-4.

Table 4-4. Mass [kg] of complexing agents in the 1BMA compartments, 1–2BMA, the Silo and 1–2BTF (Keith-Roach et al. 2021).

	EDTA	NTA and MGDA	Citrate	Sodium caprylimino-dipropionate	Oxalate	Sodium gluconate
1BMA compartment						
1						
2						
3		122	53		3.0	5.4
4	0.3	107				11
5		24	10		0.6	1.1
6	1.3	220	95		5.3	9.8
7						
8	0.1	31				3.1
9	0.1	41				4.2
10	0.8	98	42		2.4	4.4
11	0.1	26	2.6		0.1	2.3
12	0.2	31	14		0.8	1.4
13		0				
14	0.1	12	5.1		0.3	0.5
15	0.02	2.5	1.1		0.1	0.1
Total 1BMA	3.1	715	222		13	43
Total 2BMA	5.2	5.9				0.17
Total Silo	1.9	1 271			90	126
Total 1 BTF	0.5	78	86	52		
Total 2BTF	4.5	3 320	3 370	15		0.59

4.2.7 Occurrence in future waste

It is likely that the accumulated mass of complexing agents disposed of in SFR will increase to an extent over time, depending on the new WAC and the early identification of complexing agents in new products. Since new complexing agents can require consideration in the context of the WAC, broad complexing agent categories are considered in the recommendations as well as named complexing agents.

4.2.8 Form following the resaturation of SFR

The form of each complexing agent in SFR is assumed to be as follows:

- EDTA, NTA, MGDA, iminodisuccinate, capryliminodipropionate, glutamate and the alkaline hydrolysis product of CADP: dissolved species

- Citrate is present as a dissolved species up to a maximum concentration of ~1 mM, due to precipitation with Ca^{2+} as $Ca_3Cit_2(s)$.

- Oxalate is assumed to be present as a dissolved species up to a maximum concentration of ~0.01 mM, due to precipitation with Ca^{2+} as $CaOx(s)$ (Van Loon and Hummel 1995).

- Gluconate sorbs to cement and the concentration remaining in solution is calculated using the sorption isotherm given in Equation (4-2).

All carboxylic acid groups will be deprotonated as well as the more acidic alcohol groups such as α-hydroxy groups. Deprotonation is discussed specifically where relevant.

There is experimental evidence that EDTA sorbs with a K_d of ~0.015 m³/kg to degraded cement with a porewater pH of 11.9, but not to fresh cement (Pointeau et al. 2006). The assumption that EDTA is present entirely as dissolved species may therefore be somewhat conservative.

4.2.9 Literature review of effect on radionuclide speciation and sorption

Solution phase speciation

Rochford (2014) investigated the interactions of Th(IV) and U(IV) with the complexing agents shown in Figure 4-6 over a large pH range. The results showed that the triol, H₃thme, and the aminotriol, H₃tea, did not affect actinide(IV) speciation at any pH. H₃bic, H₃heidi, H₃NTA, H₂ADA and H₃cit, however, formed complexes with Th(IV) and U(IV). For example, H₃heidi formed 1:2 complexes with Th(IV) at pH < 11, and tridentate bonding was observed via two carboxylates and the amine. Despite these interactions, none of the complexing agents prevented Th(IV) or U(IV) precipitation at pH > 12. Rochford (2014) therefore provides experimental evidence that many polyols and aminocarboxylates, including NTA, do not affect actinide(IV) speciation at pH > 12.
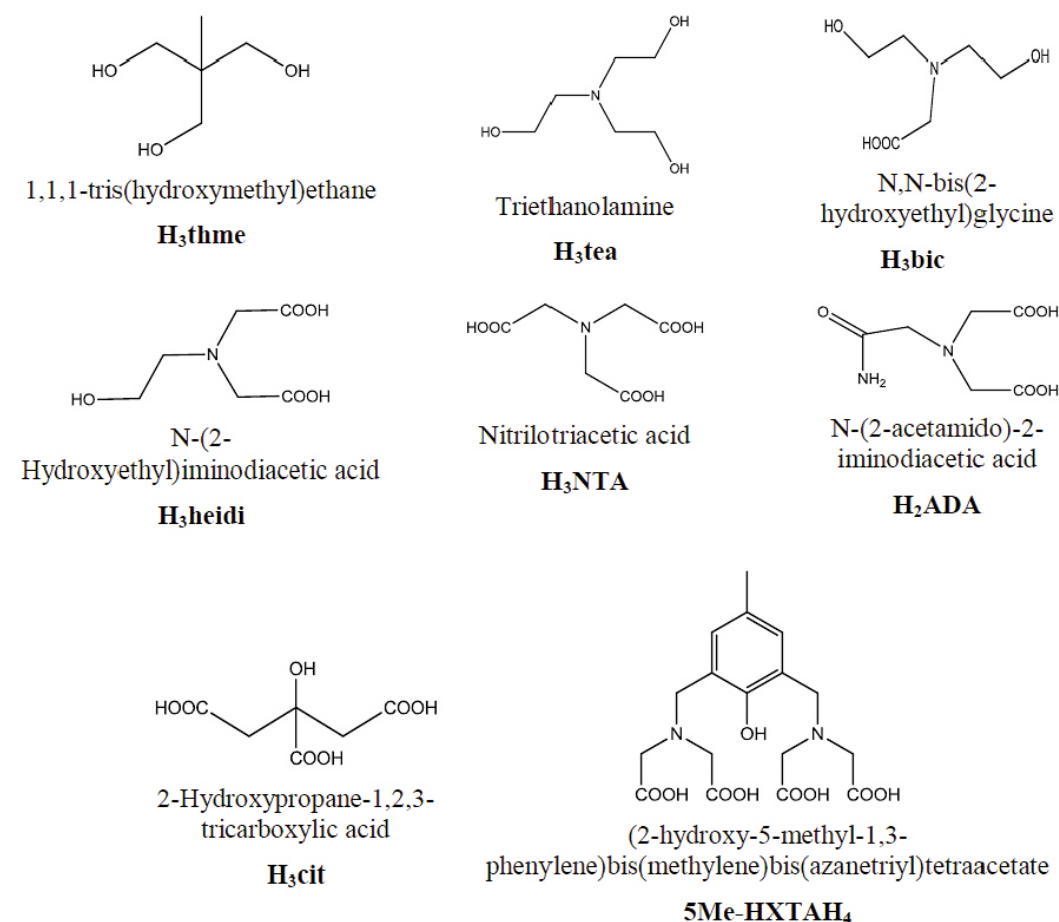
Figure 4-6. Complexing agents investigated by Rochford (2014) with Th(IV) and U(IV). Reproduced with permission from Rochford (2014).

Cartwright et al. (2007) used electrospray ionisation-mass spectrometry to examine the speciation of Th-EDTA and Th-NTA complexes. Th-EDTA complexes were identified at all pH values investigated, between pH 2.5–10.8, but Th-NTA species were not identified at pH 10.0 or 10.8.

Colàs (2014) found that EDTA affected Th(IV) solubility at pH 12, but the effect was smaller than that of gluconate. Some of the experimental systems included Ca^{2+}, to examine the possible formation of Ca-Th-EDTA complexes. Ca^{2+}, however, did not affect the observed dissolution of Th(IV) under these conditions. As the EDTA concentration was always in excess of the Ca^{2+} concentration, the data did not provide information on the competitive effect of Ca-EDTA species formation on Th(IV) speciation and solubility.

Colàs (2014) derived stability constants to explain the observed effects of EDTA on Th(IV) solubility in the experiments described above. The stability constants were then corrected to $I = 0$ M using Specific Interaction Theory (SIT) to give:

$Th^{4+} + 2H_2O + EDTA^{4-} \rightleftarrows Th(OH)_2(EDTA)^{2-} + 2H^+$ $\qquad \log K = 13.4 \pm 0.7$

The stability of the $Th(OH)_2(EDTA)^{2-}$ complex described by Colàs (2014) ($\log K = 13.4$) can be compared with that of the only Th-hydroxo-EDTA species in the Thermochimie database, $Th(OH)(EDTA)^-$ ($\log K = 19.5$), by subtracting the contribution of hydroxide formation:

$H_2O \rightleftarrows H^+ + OH^-$ $\qquad \log K = -14$

Therefore:

Colàs (2014): $Th^{4+} + 2OH^- + EDTA \rightleftarrows Th(OH)_2EDTA^{2-}$ $\log K = 13.4 - (2 \times -14) = 41.4$

Thermochimie: $Th^{4+} + OH^- + EDTA \rightleftarrows Th(OH)EDTA^-$ $\log K = 19.5 - (-14) = 33.5$
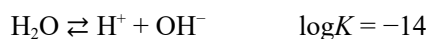
At pH 12.5, with a 0.032 M OH^- concentration, the difference is sufficiently large for the complex proposed by Colàs (2014) to form more readily than the complex in Thermochimie by many orders of magnitude.

Stability constants were experimentally derived for a range of 1:1 cyclic polycarboxylates and aminopolycarboxlyate complexes (Figure 4-7) with Am(III), Eu(III) and Cm(III) (Thakur et al. 2011). H_3heidi was included (named HIDA in the article) and the complex had a log stability constant of between 9.69 and 10.3 (Thakur et al. 2011). Both 1:1 and 1:2 complexes were detected and tetravalent bonding was observed in both, with lone pair donation from the alcohol group. The stability constants for 1:1 complexes of the complexing agents investigated by Thakur et al. (2011) are given in Table 4-5.

A log stability constant of 8.13 (25 °C, $I = 0.1$ M) is given for the 1:1 complex of H_3heidi/HIDA with Ni(II) in Tanaka and Tabata (2009).
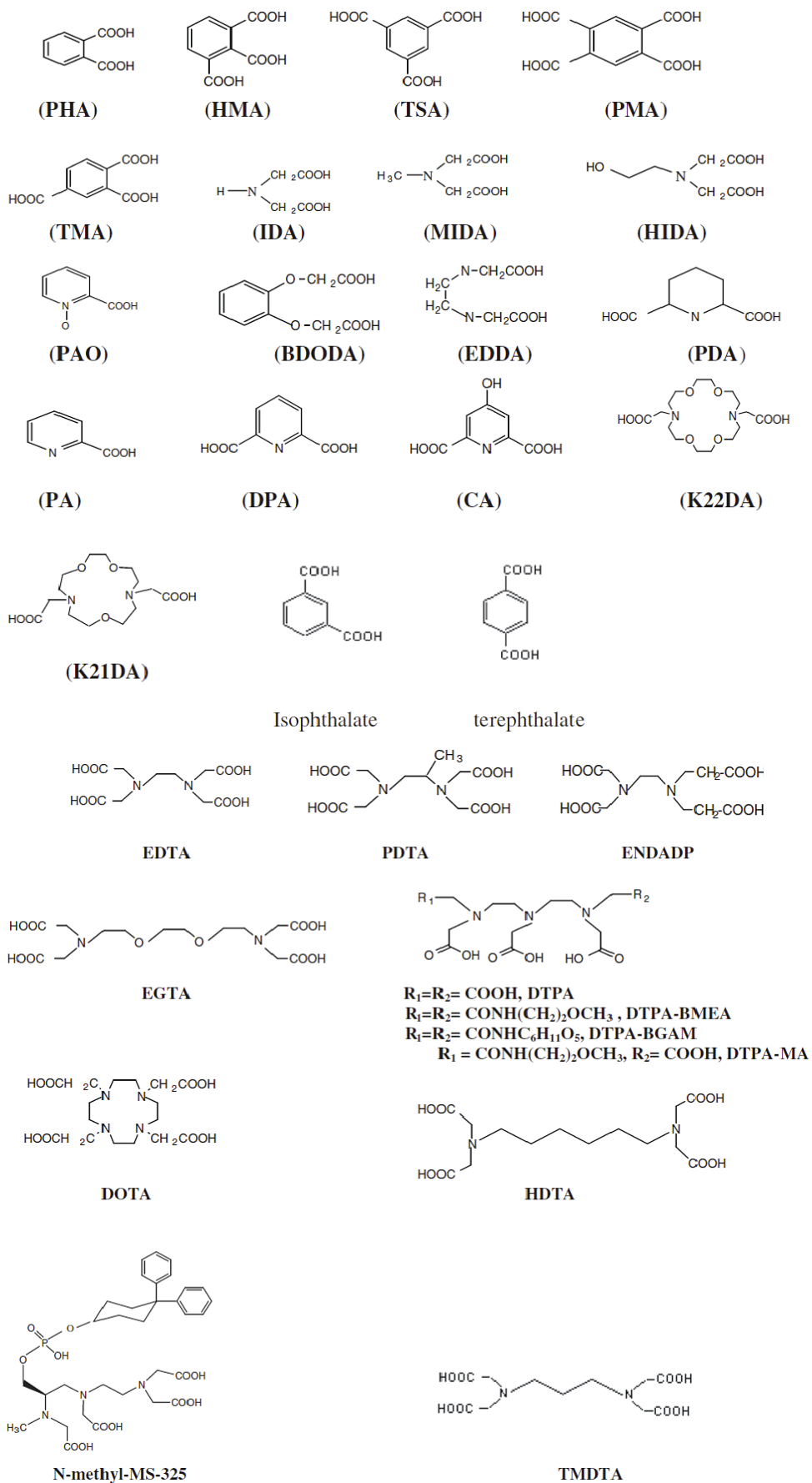
Figure 4-7. *Complexing agents included in Thakur et al. (2011). Reprinted by permission of Taylor & Francis Ltd. from Journal of Coordination Chemistry https://www.tandfonline.com/gcoo20 14 Sep 2011.*

Table 4-5. Log stability constants of Am(III), Cm(III), and Eu(III) with linear and cyclic carboxylates and polyaminocarboxylates. I = 0.1 M (NaClO$_4$), T = 25 °C.

Ligand	Method	Am(III)	Cm(III)	Eu(III)	Ref.
PHA	sx	3.75 ± 0.03	3.84 ± 0.04	3.70 ± 0.03	Thakur et al. (2011)
	lif	-	-	3.45 ± 0.02	Wang et al. (1999)
TMA	sx	4.55 ± 0.06	4.48 ± 0.05	4.32 ± 0.04	Thakur et al. (2011)
	lif	-	-	4.19 ± 0.10	Wang et al. (1999)
PMA	sx	5.42 ± 0.05	5.35 ± 0.03	4.98 ± 0.03	Thakur et al. (2011)
	lif	-	-	5.81 ± 0.04	Wang et al. (1999)
HMA	sx	5.68 ± 0.05	5.64 ± 0.04	5.08 ± 0.03	Thakur et al. (2011)
	lif	-	-	5.25 ± 0.01	Wang et al. (1999)
TSA	sx	3.76 ± 0.03	3.62 ± 0.04	3.70 ± 0.03	Thakur et al. (2011)
	lif	-	-	3.56 ± 0.10	Wang et al. (1999)
BDODA	sx	5.24 ± 0.05	5.10 ± 0.04	5.02 ± 0.03	Thakur et al. (2011)
MIDA	sx	7.52 ± 0.06	7.69 ± 0.04	7.45 ± 0.05	Thakur et al. (2011)
				6.92	Martell et al. (2003)
HIDA	sx	10.30 ± 0.06	9.98 ± 0.07	9.69 ± 0.05	Thakur et al. (2011)
		9.14	9.14	9.10	Martell et al. (2003)
IDA		6.90	-	6.73	Martell et al. (2003)
EDDA		-	-	8.38	Martell et al. (2003)
DPA	Pot*	8.52 ± 0.04	8.32 ± 0.05	8.15 ± 0.05	Thakur et al. (2011)
		15.05 ± 0.05	15.15 ± 0.04	14.98 ± 0.04	
CA	Pot*	7.85 ± 0.03	7.62 ± 0.03	7.52 ± 0.03	Thakur et al. (2011)
		13.95 ± 0.05	14.15 ± 0.05	14.56 ± 0.05	
K21DA	sx	12.06 ± 0.06	11.98 ± 0.05	11.62 ± 0.06	Thakur et al. (2011)
	pot	12.86 ± 0.03**	-	11.85	Manchanda and Mohapatra (2003)
K22DA	sx	13.60 ± 0.05	13.47 ± 0.06	12.76 ± 0.05	Thakur et al. (2011)
		13.33 ± 0.11**	-	12.02	Manchanda and Mohapatra (2003)
ENDADP	sx	13.84 ± 0.06	14.01 ± 0.07	13.77 ± 0.05	Thakur et al. (2011)
PDTA	sx	17.85 ± 0.06	17.92 ± 0.05	17.75 ± 0.07	Thakur et al. (2011)
HDTA	sx	10.09 ± 0.04	10.12 ± 0.05	9.36 ± 0.04	Thakur et al. (2011)
EGTA		17.980 ± 0.09	17.940 ± 0.09	17.65 ± 0.08	Thakur et al. (2011)
DOTA	sx	23.95 ± 0.09	24.02 ± 0.11	23.95 ± 0.10	Thakur et al. (2011)
		-	-	23.5	Chang et al. (1998)
DTPA-BMEA	sx	16.30 ± 0.06	16.58 ± 0.04	16.35 ± 0.05	Thakur et al. (2011)
		-	-	16.48	Schaab (1998)
DTPA-BGAM	sx	15.9 ± 0.05	15.78 ± 0.06	16.02 ± 0.05	Thakur et al. (2011)
		-	-	16.0	Schaab (1998)
DTPA-MA	sx	18.48 ± 0.06	18.56 ± 0.05	18.95 ± 0.06	Thakur et al. (2011)
N-MS-325	sx	20.12 ± 0.08	20.08 ± 0.06	20.17 ± 0.07	Thakur et al. (2011)

Pot = potentiometry; sx = solvent extraction; lif = laser-induced fluorimetry.
* = log β_{102}; ** = sx.

Gluconate (Glu) is relatively well studied and has been seen to form stable complexes with, for example, Ni(II) (Warwick et al. 2003), U(IV) (Warwick et al. 2004), Th(IV) (Colàs 2014), U(VI) (Colàs 2014) and Np(IV) (Rojo et al. 2013) under alkaline conditions. Colàs (2014) found that gluconate interacts slightly more strongly than ISA with Th(IV), but the difference was small. The stability constant derived for the Np(OH)$_4$Glu$^-$ complex indicated that gluconate would dominate Np(IV) speciation when the free dissolved gluconate concentration exceeds 10^{-6} M (Rojo et al. 2013). The stability constant was consistent with the linear free energy relationship between analogous Th(IV)-, U(IV)- and Pu(IV)-gluconate aqueous complexes (Rojo et al. 2013). The relationship between the stability of An(IV)(OH)$_4$Glu$^-$ and An(IV)(OH)$_4$(aq) complexes was constant for the actinides investigated, indicating that gluconate will have an equal effect on these tetravalent actinides. The An(IV)(OH)$_4$Glu$^-$ species are approximately 5 orders of magnitude more stable than the An(IV)(OH)$_4$(aq) complexes.

Stability constants for divalent metals ions (Cd(II), Cu(II), Pb(II) and Zn(II)) with iminodisuccinate were reported to be ~4 orders of magnitude lower than their respective stability constants with EDTA (Kołodyńska 2013).

Altun and Köseoğlu (2005) determined stability constants of Ni(II) glycine complexes at 25 °C and $I = 0.1$ M KCl via potentiometry. The log stability constants of the 1:1, 1:2 and 1:3 complexes were found to be 5.8, 10.5 and 14.1, respectively. These results are relevant for glutamate complex formation, since glutamate contains a glycine-like structure.

Sorption experiments

Radionuclide sorption experiments involving complexing agents used in detergents are surprisingly few. An important sorption study was conducted by Dario et al. (2004), which examined the effect of many of the complexing agents disposed of in SFR on trivalent actinide sorption to titanium dioxide and cement under a defined set of experimental conditions. Allard et al. (2002) presented Dario's data to show the difference between complexing agents on Eu(III) sorption to titanium dioxide in the absence and presence of Ca^{2+} (Figure 4-8). It is clear that in the absence of Ca^{2+}, EDTA influences Eu(III) sorption at by far the lowest concentrations of the complexing agents studied, followed by NTA. The difference between the effect of EDTA and NTA was reduced when Ca^{2+} was present. It can also be noted that 10^{-2} M oxalate did not affect Eu(III) sorption significantly.

In addition to the data shown in (Figure 4-8), Dario et al. (2004) found that very low concentrations of dissolved gluconate reduced Am(III) sorption to cement and titanium dioxide. In the case of TiO_2, the addition of Ca^{2+} (0.002 M) increased the effect of gluconate. For cement, Am(III) sorption was reduced in the short-term (24 hours) from an added concentration of $\sim 10^{-5}$ M gluconate. Data in the appendices of the report suggest that when 10^{-5} M gluconate was added, most of the gluconate sorbed to the cement within 24 hours. Therefore, the dissolved gluconate concentration was much lower than 10^{-5} M. Long term Eu(III) sorption experiments with 3.1×10^{-5} M added gluconate showed that the sorption reduction effect observed in the 24 hour experiments decreased quite rapidly.

When 10^{-4} M gluconate was added to the experiments containing cement, half of the gluconate remained in solution and Eu(III) sorption was reduced by ~4 orders of magnitude after 24 hours. The long-term trends were not determined for this gluconate concentration, thus sorption reduction may decrease over time. However, the experiments suggest that the interaction between Eu(III) and gluconate is strong.

The observations that NTA affected Eu(III) sorption (Dario et al. 2004) but did not affect Th(IV) solubility (Rochford 2014) are consistent with the discussion of complexation formation at high pH in Section 2.2. The high stability of the $Th(OH)_4(aq)$ complex requires extremely high stability constants for Th-organic complexes to form at pH 12.5, to out-compete the formation of hydrolysis products. The effect of Ca^{2+} observed in Dario et al. (2004) described above, also needs to be considered. Allard et al. (2002) concluded that even strong ligands will not have an effect on Eu(III) at concentrations $\leq 10^{-4}$ M due to Ca^{2+}.
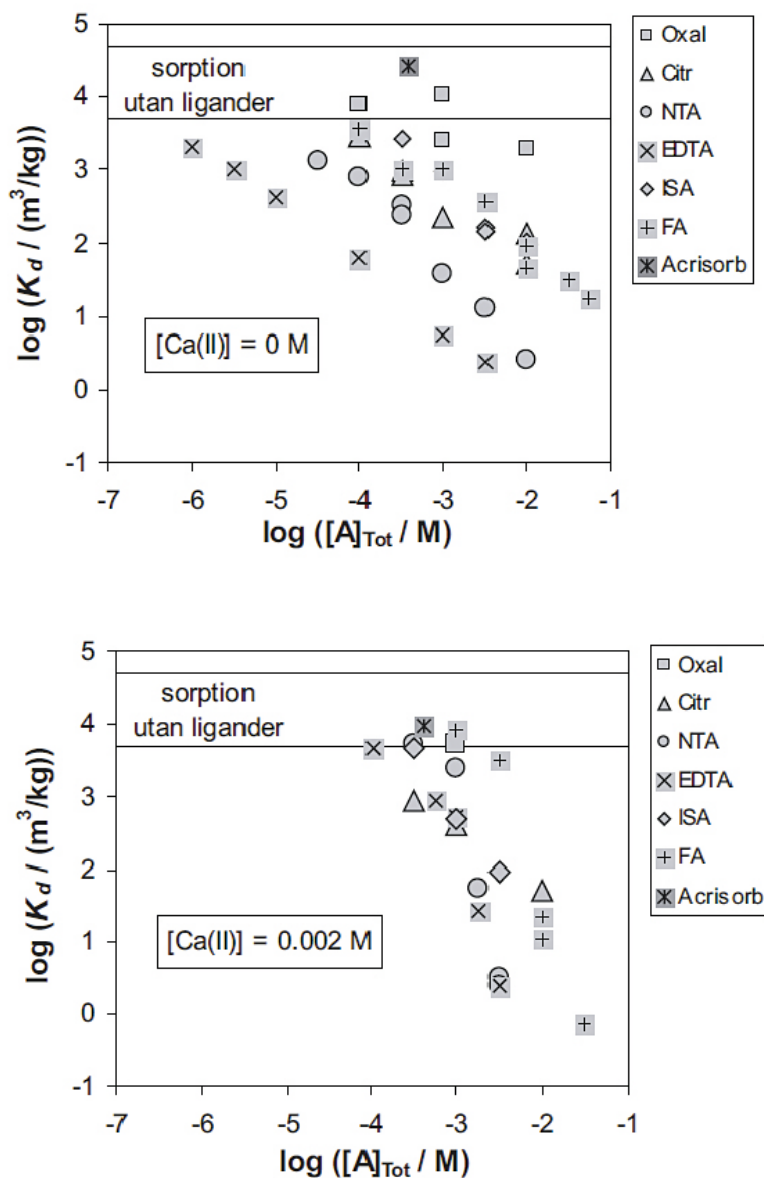
Figure 4-8. Summary of the results of Dario et al. (2004) as given in Allard et al. (2002).

Speciation calculations

Keith-Roach et al. (2021) complemented Dario's studies by first calculating the speciation of Am(III), as a trivalent actinide, in the experiments using PhreeqC together with the Thermochimie_v9 database and then extending the calculations to a system with a representative concentration of portlandite (1 mol/L $Ca(OH)_2$). This combination of experiment and modelling was useful in explaining the trends seen in the experiments and identifying whether similar effects would be expected in SFR. Further calculations were also carried out with Th(IV) to examine whether complexes would persist when portlandite ($Ca(OH)_2$) is present at a concentration representative of SFR.

The PhreeqC calculations suggested that Am(III)-citrate complex formation is sensitive to pH in the pH range above pH~ 11. Even a slight reduction in the experimental pH below pH 12.5, as seen in the experiments of Dario et al. (2004) due to the addition of citric acid, was calculated to increase the formation of complexes. When the portlandite concentration was representative of SFR, negligible concentrations of the Am(III)-citrate and Am(III)-NTA complexes were predicted to form. For citrate, the pH was the dominant factor, with the preferential formation of Am(III) hydroxide species. For NTA, Am(III)-NTA complexes did not form due to the preferential formation of Ca-NTA complexes when abundant portlandite was present.

When Th(IV) was included in the calculations with up to 10^{-2} M citrate, Th-citrate complexes were not found to persist significantly. NTA was predicted to control Th(IV) speciation in the presence of a representative concentration of portlandite. However, the database used, Thermochimie_v9, contained large errors in the stability constants for the Th(OH)(NTA) and Th(OH)$_2$NTA$^-$ species, which were too large by 14 and 28 orders of magnitude, respectively (Campos et al. 2018). Therefore, the apparent persistence of these species at high pH was due to this error. Recalculation of this case with Thermochimie_v10a predicts that 10^{-6} % of Th(IV) is complexed by 0.01 M NTA at pH 12.5.

Rochford (2014) used ^{1}H NMR and potentiometric titrations to obtain stability constants for Th-NTA species (Table 4-6). These values were used to predict Th speciation over a pH range and the results are shown in Figure 4-9. The results for a 1:2 ratio of Th:NTA are in agreement with those of Cartwright et al. (2007), who detected Th(NTA)$^+$ as the major species at pH 2.5 and 3.6, Th(NTA)$_2^{2-}$ at pH 6.0, 7.2 and 8.3, and did not identify Th-NTA species at pH 10.0 or 10.8.

Table 4-6. Th-NTA species identified and log stability constants derived (*I* = 0.5 M*) in Rochford (2014).

Species	Log stability constant
Th(NTA)$^+$,	15.88
Th(NTA)$_2^{2-}$	25.15
Th(OH)(NTA)	11.9
Th(OH)$_2$(NTA)$^-$	
Th(OH)(NTA)$_2^{3-}$	15.2
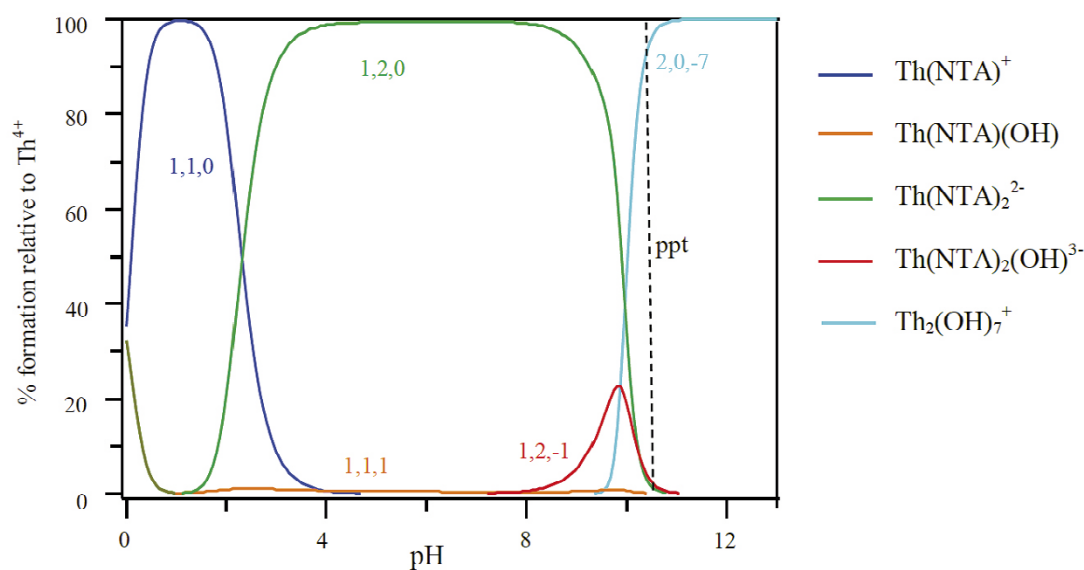
Figure 4-9. *Speciation diagram for Th(IV) in a 1:2 Th(IV):NTA ratio in aqueous solution. T = 25 °C; I = 0.5 M (NaNO$_3$), 10 mM NTA, 5 mM Th. The ratio of Th(IV):NTA:OH$^-$ is denoted as 1,1,−1 etc. Note that Th(NTA)(OH) is incorrectly labelled as 1,1,1. The dashed line marked "ppt" shows the pH at which precipitation was observed in the experiments. Reproduced with permission from Figure 4-28 in Rochford (2014).*

4.2.10 PhreeqC calculations

The experimental data available for trivalent actinides (Eu(III)) and Th(IV) with NTA, together with the modelling in Keith-Roach et al. (2021) and the recalculation described above of the Th and NTA case using Thermochimie_v10, suggest that actinide-NTA complexes will not form under SFR conditions. For Th(IV) this is due to the high stability of Th-hydroxide species while competition from Ca^{2+} is also an important factor for trivalent actinides. Complexing agents that form weaker complexes than NTA are therefore not expected to form complexes with actinides under SFR conditions and, where available, the experimental evidence supports this. However, the relationship between actinides and EDTA needs to be investigated further.

The evidence available for the effect of complexing agents on Ni(II) sorption is limited. Therefore, PhreeqC calculations have been carried out to understand the ability of Ni(II) to form complexes a) at the high OH^- concentration of SFR and b) with the high Ca^{2+} concentration of SFR. The complexing agents included in the calculations are oxalate, citrate and NTA, and the data are extrapolated to other dicarboxylates, tricarboxylates and aminopolycarboxylates. The recent reinterpretation of $Ni(OH)_3^-$, and $Ni(OH)_2(aq)$ formation in Bruno et al. (2018) cannot be included here without also re-evaluating the Ni(II)-organic complexing agent stability constants, which falls outside the scope of this report. The Thermochimie_v10a database was therefore used without modification.

Th(IV) and EDTA

EDTA was titrated into a solution in equilibrium with a representative concentration of portlandite for SFR. The initial NaCl concentration ($[NaCl_{init.}]$) was 0.1 M. Due to uncertainties in the thermodynamic data for Th-EDTA species, the calculations first used the Thermochimie_v10a database and then included the $Th(OH)_2EDTA^{2-}$ species proposed by Colàs (2014) with its corresponding stability constant (Section 4.2.9). With 0.01 M EDTA added ($I = 0.2$ M), the Thermochimie data predicted that 10^{-22} M Th(IV) of the total 10^{-8} M Th(IV) would be present as an EDTA complex, while the inclusion of Colàs' species increased this to 10^{-15} M. This indicates that, despite the inclusion of a stability constant for a species observed at pH 12 (Colàs 2014), EDTA is predicted to have a minimal impact on Th(IV) speciation under conditions controlled by portlandite (high Ca^{2+} concentration, pH 12.5).

Am(III) and EDTA

A pH titration of 10^{-8} M Am(III) and 10^{-3} M EDTA ($[NaCl_{init.}] = 0.2$ M; $I = 0.2–0.3$ M) was carried out using the thermodynamic data in Thermochimie_v10a. The calculations predicted that $AmEDTA^-$ will dominate Am(III) speciation over the pH range calculated (pH 6.0–13.2), with 100 % complexed at pH 12.5. However, when EDTA was titrated into a solution containing 10^{-8} M Am(III) ($[NaCl_{init.}] = 0.2$ M) and a representative concentration of portlandite for SFR, $\sim 2.5 \times 10^{-13}$ M Am(III) was found to be present as an EDTA complex when 10^{-2} M EDTA had been added (pH 12.5, $I = 0.3$ M). A similar effect from Ca^{2+} was seen for Am(III) and NTA in Keith-Roach et al. (2021). The result is consistent with the experimental observation of Dario et al. (2004), that the EDTA concentration must exceed the Ca^{2+} concentration to affect Eu(III) sorption. The difference here is that there is a larger source of Ca^{2+} in the portlandite than used in the experiments.

Ni(II) with dicarboxylates

A pH titration was calculated with 10^{-8} M Ni(II) and 0.1 M oxalate ($[NaCl_{init.}] = 0$ M) to examine the predicted formation of Ni(II)-oxalate complexes as a function of pH. The calculations did not allow precipitation even though NiOx has a low solubility, e.g. $NiOx.2H_2O$ has a solubility of 6×10^{-5} M (American Elements 2020) and the solubility of calcium oxalate under cementitious conditions was exceeded in this calculation. The calculation was, however, designed so that the results can be extrapolated to other dicarboxylates, which may not form such insoluble salts. Figure 4-10 shows that Ni(II)-oxalate complexes comprise > 95 % of Ni aqueous species up to pH 10.5 but Ni(II) hydroxide species become increasingly important as the pH increases further. At pH 12.5, 0.4 % of Ni(II) is present as Ni(II) oxalate species. The dominance of $NiOx_2^{2-}$ reflects the high concentration of the oxalate as the log stability constants of NiOx and $NiOx_2^{2-}$ are 5.19 and 7.64 respectively. The calculations therefore predict that Ni(II)-dicarboxylate complexes will not form significantly at pH 12.5, even when the dicarboxylate is present at a concentration of 0.1 M and if precipitation were not relevant.
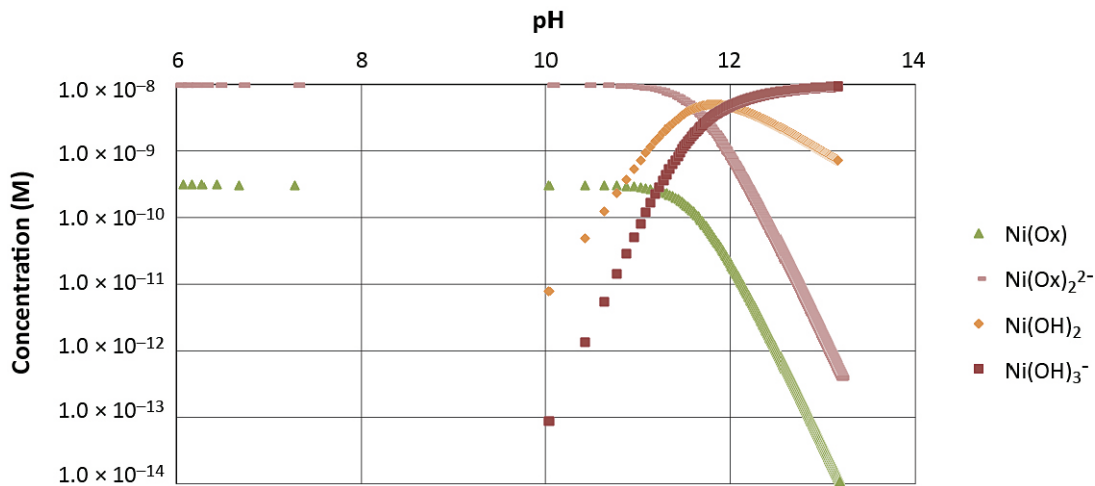
Figure 4-10. *pH titration of 10^{-8} M Ni(II) and 10^{-1} M oxalate, 25 °C, I = 0.2–0.3 M.*

Ni(II) with citrate (tricarboxylate)

A pH titration into a solution containing 10^{-8} M Ni(II) and 0.1 M citrate ($[NaCl_{init.}]$ = 0.05 M) was calculated. The high initial ionic strength of 0.58 M was largely due to the high citrate concentration and increased to 0.73 M during the titration. The results in Figure 4-11 suggest that Ni-hydroxide species formation is energetically preferential compared to Ni(II)-citrate complex formation at highly alkaline pH values. The citrate concentration included in the calculations is two orders of magnitude higher than its expected solubility in SFR.

The titration of citrate into a solution containing 10^{-8} M Ni(II) ($[NaCl_{init.}]$ = 0.2 M) in equilibrium with a representative concentration of portlandite for SFR shows that competition from Ca^{2+} reduces the concentration of Ni(II)-citrate species further (Figure 4-12). Calcium-citrate complexes form preferentially. With 0.1 M citrate added, only 10^{-13} M of the 10^{-8} M Ni(II) was predicted to be present as a citrate complex.
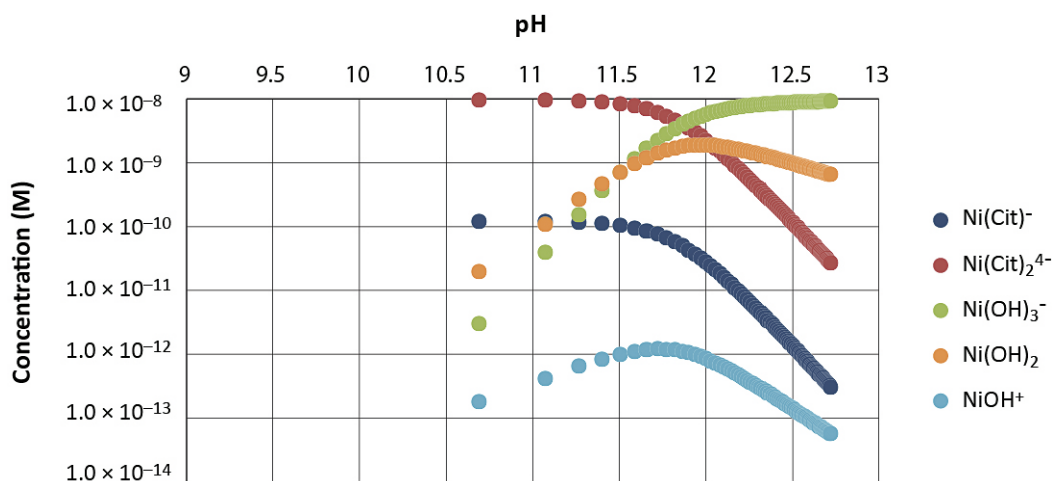
Figure 4-11. *pH titration of 10^{-8} M Ni(II) and 10^{-1} M citrate (I = 0.58–0.73 M).*
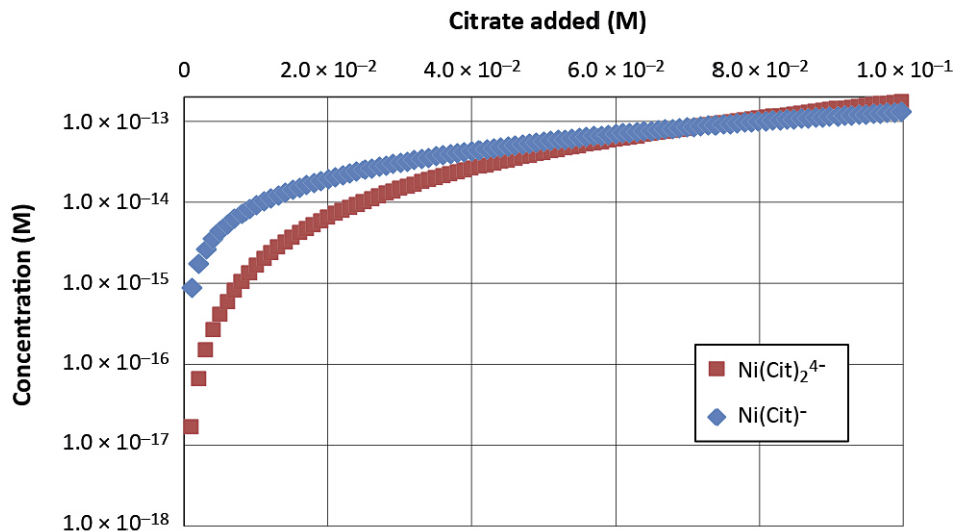
Figure 4-12. *Titration of citrate into a solution containing 10^{-8} M Ni(II) in equilibrium with a representative concentration of portlandite for SFR (I = 0.27–0.40 M).*

Ni(II) with NTA

A pH titration of a solution containing 10^{-8} M Ni(II) and 10^{-3} M NTA ([NaCl$_{init.}$] = 0 M) (Figure 4-13) predicts that NTA species dominate Ni(II) speciation across the pH range investigated, although the distribution of Ni(II)-NTA species changes with pH. The formation of Ni(II)-NTA complexes in a solution in equilibrium with a representative concentration of portlandite for SFR was then calculated (Figure 4-14). This predicted that competition from Ca^{2+} limits the effect of NTA. Only 4 % of the Ni(II) was complexed by 10^{-2} M NTA under these conditions. The formation of Ca-NTA complexes can also be seen to reduce the relative importance of the $NiNTA_2^{4-}$ species, so it is not seen on the scale used in Figure 4-14.
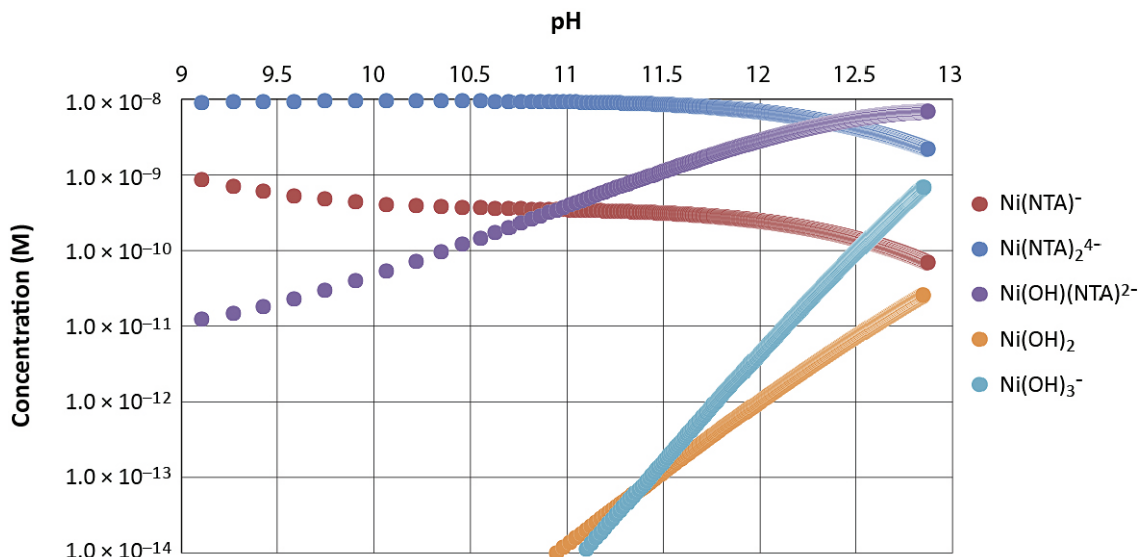
Figure 4-13. *pH titration of 10^{-8} M Ni(II) and 10^{-3} M NTA (I = 0.1–0.2 M).*
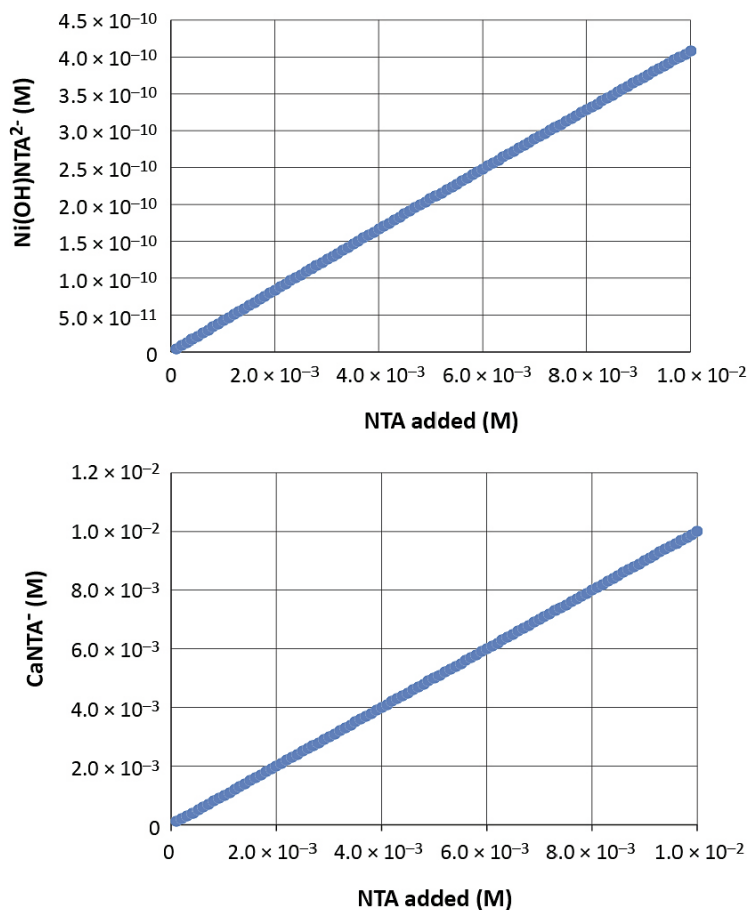
Figure 4-14. *Titration of NTA into water in equilibrium with a representative concentration of portlandite containing 10^{-8} M Ni(II) (25 °C). The calculated pH was 12.5 and I = 0.16–0.17 M. Ni(OH)NTA^{2-} and CaNTA$^-$ are the only species visible on the scale used.*

Ni(II) and EDTA

A pH titration into a solution containing 10^{-8} M Ni(II) and 10^{-3} M EDTA ($[NaCl_{init.}] = 0.1$ M; $I = 0.1$–0.2 M) predicted that NiEDTA^{2-} would be the dominant (> 99.7 %) Ni(II) species in the pH range calculated, from pH 6.0 to 13.2. An EDTA titration into a solution containing 10^{-8} M Ni(II) ($[NaCl_{init.}] = 0.1$ M) in equilibrium with a representative concentration of portlandite for SFR was then calculated. In this case, 43 % of the Ni(II) was predicted to be complexed by 0.01 M EDTA (pH 12.5, $I = 0.2$ M). The log stability constant of NiEDTA^{2-} (20.54) is sufficiently high to allow some degree of complex formation at high Ca^{2+}.

4.2.11 Recommendations for WAC 4.0

Complexing agents known to be present in SFR wastes due to the use of detergents at the nuclear facilities are carboxylates, aminocarboxylates and α-hydroxycarboxylates. Concentration limits for known complexing agents present in the waste are given below, together with recommendations for similar types of complexing agents that could be present in products in the future. The concentrations are converted into mass per waste package later in this report (Appendix).

α-hydroxycarboxylates

Experimental data have shown that gluconate forms stable species with Ni(II) and tri-and tetravalent actinides at high pH and in the presence of Ca^{2+}. Gluconate complexes of tetravalent actinides have been shown to be five orders of magnitude more stable than their hydrolysis species (Rojo et al. 2013), thus will form at low gluconate concentrations in concrete porewater. Dario et al. (2004) showed that

low concentrations of gluconate reduced Eu(III) sorption to concrete and TiO$_2$ and that the addition of Ca^{2+} reduced sorption to TiO$_2$ further. Gluconate is therefore a notably strong complexing agent under SFR conditions.

The structure of gluconate is similar to that of the cellulose degradation product ISA, which has been demonstrated to reduce radionuclide sorption to cement at aqueous phase concentrations > 10^{-4} M (see Section 4.1.9). Colàs (2014) found that gluconate interacts with Th(IV) slightly more strongly than ISA, but the difference is small. Therefore, the maximum tolerable concentration of gluconate in the aqueous phase of SFR is judged to be lower than for ISA: 10^{-5} M. The total mass allowed in each waste package (Appendix) was calculated using the 10^{-5} M limit and the sorption isotherm given in Equation (4-2). This recommendation differs from WAC 3.0 (Section 1.1) but is consistent with the handling of cellulose and ISA.

The same concentration limit should also be applied to all α-hydroxycarboxylates that have multiple hydroxide groups for multidentate bonding. However, small α-hydroxycarboxylates such as lactate have lower stability constants. These are not expected to affect radionuclide sorption in SFR as they are weaker complexing agents than oxalate (e.g. Carbonaro et al. 2011).

Hexadentate aminocarboxylates

The experimental and the thermodynamic data available suggest that EDTA would have to be present at a reasonably high concentration to affect radionuclide speciation. Of the three radionuclides considered here, the speciation of Ni(II) was calculated to be affected to greatest extent by EDTA when portlandite is present at a representative concentration for SFR. Approximately 40 % of Ni(II) was calculated to be present as an EDTA complex when the EDTA concentration was 10^{-2} M, compared to ~0.002 % of Am. EDTA has also been seen to affect Th(IV) solubility (Colàs 2014), and so forms sufficiently strong complexes to compete with Th(IV) hydrolysis at pH 12. However, the concentration of Ca^{2+} was an order of magnitude lower than the EDTA concentration in these experiments. The modelling results suggest that Ca^{2+} will strongly reduce the effect of EDTA in SFR.

In light of the evidence that gluconate forms complexes more readily with radionuclides under SFR conditions than EDTA (Colàs 2014), it seems appropriate and consistent to introduce a concentration limit for EDTA, rather than exclude it completely. Due to the uncertainties in the experimental and thermodynamic data, a limit of 10^{-4} M EDTA can be proposed to be consistent with ISA. The evidence suggests that this is a cautious limit.

The same limit is recommended for other hexadentate aminopolycarboxylates, since variants of EDTA, such as PDTA (Thakur et al. 2011), also have high stability constants with trivalent actinides (Table 4-5). This general limit is, however, expected to be highly conservative for many hexadentate aminopolycarboxylates. For example, Thakur derived stability constants for ENDADP, which contains an extra CH$_2$ link in two of the aminocarboxylate chains compared to EDTA, with trivalent actinides. The stability constants were 4 log units lower than the stability constants for PDTA. Where the hexadentate aminopolycarboxylates had long chains between some electron donor groups, such as HDTA, the stability constants were even lower (Thakur et al. 2011).

Pentadentate aminocarboxylates

The stability constants of iminodisuccinate and similar pentadentate aminocarboxylates that form 5- or 6-membered rings are expected to be intermediate between NTA and EDTA. Transition metal(II) ions tend to form iminodisuccinate complexes that are ~4 orders of magnitude less stable than their EDTA complexes (Kołodyńska 2013). Based on this, the Ni(II)-iminodisuccinate complex would have a log stability constant of around 16. This is consistent with the complex being more stable than NiNTA$^-$, which has a log$K$ of 12.75.

A concentration limit of 10^{-3} M is recommended to reflect the lower stability constant of Ni(II) with iminodisuccinate compared to EDTA. This limit is the same as for NTA (see below) but, as the limit for NTA is conservative, is reasonable.

Tetradentate aminocarboxylates

The experimental data described in Section 4.2.9 indicate that Th(IV)-NTA complexes do not form significantly at pH 12.5 (Rochford 2014, Cartwright et al. 2007) and Am(III)-NTA species start to form when the NTA concentration exceeds the Ca^{2+} concentration (Dario et al. 2004). Keith-Roach et al. (2021) predicted that the effect of Ca^{2+} would limit the formation of Am-NTA species under SFR conditions, using PhreeqC calculations. The PhreeqC calculations in Section 4.2.10 indicate that Ni(II)-NTA species form to a limited extent (4 % of Ni(II) species with 0.01 M NTA) in concrete porewater. The available information therefore suggests that the main concern relating to NTA is with respect to Ni(II). A limit of 10^{-3} M NTA is suggested. This limit is highly conservative on the basis of the calculations but allows for uncertainty in the thermodynamic data used.

This limit is judged to also be acceptable for other tetradentate aminocarboxylates that contain one amino group and form 5- and 6-membered chelate rings. An increase in the number of amino groups can enhance the interaction of the complexing agent with Ni(II) (see for example Sections 4.5.9 and 4.5.10). Essentially, the stability of the Ni(II) complex can increase while the stability of the Ca(II) complex decreases. Therefore, tetradentate aminocarboxylates containing a higher number of amine groups should be assessed individually if found relevant for SFR.

Tricarboxylates

Citrate has been seen to have an effect on Am(III) sorption to HCP but, as discussed in Keith-Roach et al. (2021), the observed experimental effect of citrate on Eu(III) sorption to HCP occurred together with a small decrease in pH. The pH buffering in SFR and the influence of Ca^{2+} ions, in solution and due to Ca-citrate precipitation, led Keith-Roach et al. (2021) to conclude that trivalent actinide-citrate complexes will not form under SFR conditions. The PhreeqC calculations in this report suggest that the formation of Ni(II)-citrate complexes will be very minor at pH 12.5. Th(IV) hydrolysis is so strong that Th-citrate complexes are not expected at these concentrations.

As discussed in Section 4.2.2, citrate is a tridentate tricarboxylate due to the α-alcohol group which is involved in complexation and creates stable 6-membered chelate rings. Allard et al. (2002) presented log stability constants for two tricarboxylates that would form 8-membered chelate rings with Ni(II). The log stability constants were 3.3 and 3.8 compared to the 6.9 for Ni(II)-citrate. Given that citrate is not judged to influence radionuclide speciation significantly at pH 12.5, even when excluding the influence of Ca_3Cit_2 precipitation, other tricarboxylates are not of concern in SFR in terms of radionuclide sorption.

Tridentate aminodicarboxylates

Stability constants for CIDP complexes have not been identified by the authors of this report. However, CIDP has a similar structure to H_3heidi/HIDA (two carboxylates, one amino group, 5- or 6-membered chelate ring) that was investigated by Rochford (2014) and Thakur et al. (2011). Rochford found that H_3heidi/HIDA only formed Th(IV) complexes below pH 11. Thakur derived stability constants for trivalent actinide-H_3heidi/HIDA complexes that were probably more stable than the 1:1 citrate complexes. Since neither citrate nor NTA were calculated to be able to form complexes with trivalent actinides under SFR-relevant conditions (Keith-Roach et al. 2021), CIDP is not expected to be able to do so either. For Ni(II), the log stability constant of 8.13 given in Tanaka and Tabata (2009) suggests that H_3heidi/HIDA forms 1:1 complexes with Ni(II) that are of intermediate stability between citrate and NTA (NiCit⁻, $\log K = 6.76$; NiNTA⁻, $\log K = 12.75$, Thermochimie_v10a). Since 0.01 M NTA has been calculated to form complexes with only a small percentage of solution phase Ni(II) under repository conditions, it is unlikely that CIDP will be able to form complexes with a significant proportion of Ni(II) except at very high concentrations. Therefore, a limit of 10^{-2} M is recommended for CIDP and other tridentate aminodicarboxylates with five- or six-membered chelate rings.

Tridentate carboxylate diamines

CADP was identified in SKB's recent survey of complexing agents currently used at the nuclear facilities that can be disposed of in SFR wastes[4]. The alkaline hydrolysis product of CADP (CADP$_{hydrol}$) is expected to form more stable Ni(II) complexes than CIDP as amine groups form more stable complexes with Ni(II) than carboxylates (e.g. Table 2-3). As discussed in Section 4.5.10, the bidentate en molecule forms the bis Ni(en)$_2^{2+}$ complex with a log$K$ of 13.84 (Paoletti 1984). Tridentate coordination expected with the alkaline hydrolysis product of CADP would increase the stability further, assuming bis complexes still form. Later in this report, the Ni(en)$_3^{2+}$ complex was calculated to dominate Ni(II) speciation in portlandite-equilibrated water from an en concentration of 3×10^{-4} M (see Section 4.5.10). Excluding Ni(en)$_3^{2+}$ from the calculation, so that only the Ni(en)$^{2+}$ and Ni(en)$_2^{2+}$ species are included increases this concentration slightly to $\sim 5 \times 10^{-4}$ M. Ni(CADP$_{hydrol}$)$_2$ may be expected to dominate Ni(II) speciation from a lower concentration than this, so a concentration limit of 10^{-4} M is therefore recommended. This can also be applied to other tridentate carboxylate diamines. The comparison with ethylenediamine is not perfect as the interaction of the alkaline hydrolysis product of CADP with Ca^{2+} is expected to be greater. It is however, a reasonable and conservative approach.

Dicarboxylates

Oxalate is the only dicarboxylate capable of forming a 5-membered chelate ring. 6-membered rings are formed by malonate ($^-$OOC$_3$H$_2$OO$^-$) and molecules containing this structure (with an R-group in place of a H on the central carbon atom) but malonate forms less stable complexes with Ni(II), Eu(III) and Th(IV) than oxalate (Allard et al. 2002).

Oxalate does not appear to be able to compete with the hydrolysis of Ni(II) even at a concentration of 0.1 M, based on the calculations above. Experimental evidence shows that oxalate has a minimal influence on Eu(III) sorption (Dario et al. 2004), who investigated concentrations up to 0.01 M. Th(IV) hydrolysis is so strong that Th-oxalate complexes are also not expected at these concentrations.

The dissolved concentration of oxalate in SFR will be limited to 10^{-5} M by precipitation of CaOx (Van Loon and Hummel 1995). Dicarboxylates in general are therefore of little concern in terms of radionuclide speciation and sorption to cement in SFR.

Bidentate amino acids

The amino acid glutamate was identified in the survey of complexing agents currently used at the nuclear facilities that can be disposed of in SFR wastes. Glutamate contains a glycine functional group, and the 1:1 Ni(II)-glycine complex has a log stability constant of 5.8 (Altun and Köseoğlu 2005). The equivalent Ni(II)-glutamate complex is therefore expected to have a similar stability constant, ~ 2 log units lower than that of Ni(en)$^{2+}$. As discussed above and in Section 4.5.10, ethylenediamine was calculated to dominate Ni(II) speciation in portlandite-equilibrated water from an en concentration of 3×10^{-4} M. Therefore, a concentration limit of 10^{-2} M is recommended for amino acids such as glutamate that have a glycine group. The comparison with ethylenediamine is not perfect as the interaction of amino acids with Ca^{2+} is expected to be greater. It is however, a reasonable and conservative approach.

Amino acids with a longer chain between the amine and carboxylic acid groups are discussed in Section 4.5.11 (subsection Nylon 6,6 and Nylon 6), and these are expected to be only weak complexing agents.

---

[4] Inventering av produkter med komplexbildare hos avfallsproducenter. SKBdoc 1904743 ver 1.0, Svensk Kärnbränslehantering AB. (In Swedish.) Internal document.

4.3 Superplasticisers in cement

4.3.1 Origin

Superplasticisers are polymeric cement additives that are used to optimise the workability of cement and/or allow cementitious materials to be produced at relatively low water:cement ratios (Winnefeld et al. 2007). A low water:cement ratio generally results in a final product of greater strength and lower porosity.

Superplasticisers in the construction concrete of SFR are outside the scope of this report.

4.3.2 Structure

Superplasticisers have been developed and improved over time. To aid the reader, some of the chemical building blocks of the polymers are given in Table 4-7 and some chemical structures of superplasticisers are given in Table 4-8.

First-generation superplasticisers were based on modified lignosulfonates (LS). The next generation of superplasticisers included vinyl maleic acid copolymers (polyvinyl maleic acids PVMA), sulfonated melamine-formaldehyde condensates (polymelamine sulfonates; PMS) and sulfonated naphthalene-formaldehyde condensates (polynaphthalene sulfonates; PNS) (Winnefeld et al. 2007). In the 1990s, polycarboxylate (PC) superplasticisers were introduced. The most common PC superplasticisers are polycarboxylate ethers (PCE), which are polyacrylic or polymaleic acid polymers with long poly-ethylene glycol (PEG) (also referred to as polyoxyethylene and polyethylene oxide) sidechains.

SKB has identified that PNS, PCE and PVMA superplasticisers are used in waste stabilisation matrices in SFR waste packages. A minor amount of lignosulfonate is also present in one of the products used (0.05 % of the cement).

Table 4-7. Chemical building blocks of superplasticisers (Keith-Roach and Höglund 2018).
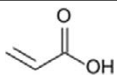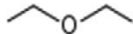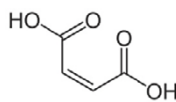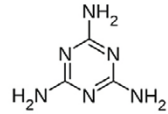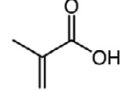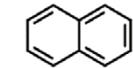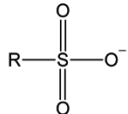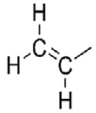
Acrylic acid (prop-2-enoic acid)	
Ether (ethoxyethane)	
Formaldehyde (methanol)	
Maleic acid ((2Z)-But-2-enedioic acid)	
Melamine (1,3,5-Triazine-2,4,6-triamine)	
Methacrylic acid (2-Methylprop-2-enoic acid)	
Naphthalene	
Sulfonate functional group (attached to an organic "R" group)	
Vinyl functional group	

Table 4-8. Chemical structures of selected superplasticisers.

Lignosulfonate (LS, Giraudeau et al. 2009)
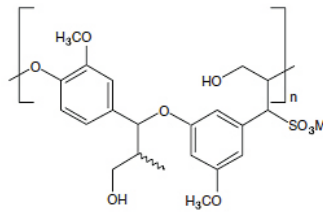
Vinyl copolymers (Giraudeau et al. 2009)
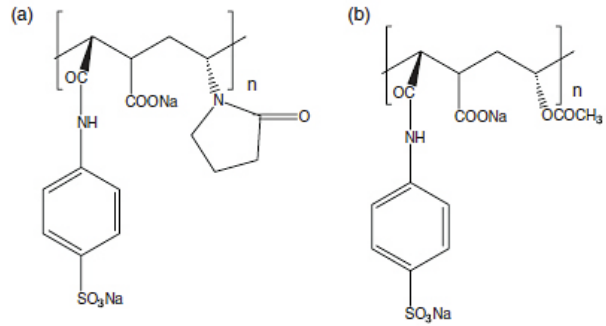
Polyvinylmaleic acid (PVMA, simplest form)
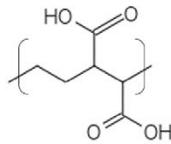
Sulfonated melamine-formaldehyde condensate (PMS)
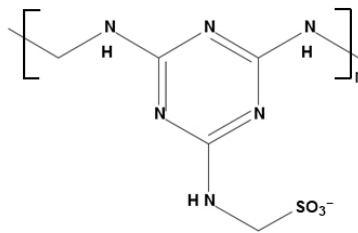
Sulfonated naphthalene-formaldehyde condensate (PNS)
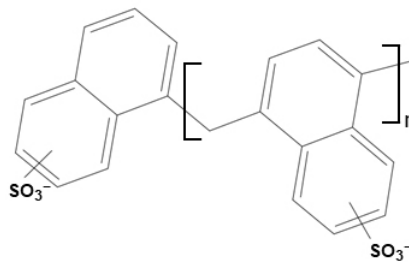
Sodium salt of a polycarboxylate ether (PCE) with a methylacrylate backbone (NDA 2015)
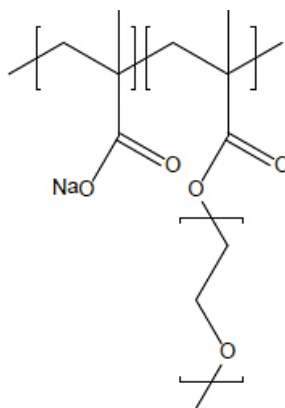
4.3.3 Degradation characteristics and reactions

PNS and PCE superplasticiser degradation was recently reviewed for Posiva Oy's spent fuel repository in Finland by Keith-Roach and Höglund (2018). The review identified the difficulty of differentiating alkaline degradation products from the unreacted reagents, monomers and oligomers present in the product. Smaller molecules have a greater tendency to remain in solution during cement hydration than polymers, and the superplasticiser polymers bind strongly to the cement particles. Alkaline hydrolysis of the labile ester groups that bind the polyethylene glycol side chains to the polymeric backbone of PCE has been observed (e.g. Herterich et al. 2003). However, degradation of the polymeric backbone of cement-bound superplasticisers is not sufficiently fast nor extensive to be observed over the background concentration of molecules that do not initially bind to cement, over experimental timescales.

Yamamoto et al. (2008) characterised the organic substances in solution after leaching concrete prepared with superplasticisers for 56 days using gel permeation chromatography. Ordinary Portland cement (OPC) was prepared with PMS, while low pH cement was prepared with PNS and PCE superplasticisers. The main component of leached organic material came from cement grinding agents, however, species arising from the superplasticiser were also observed in each case. PMS was not detected in the leachate from OPC prepared with PMS, although PMS-related substances such as methylol amine (aminomethanol) or a homologue of methylol amine (H_2N-CH_2-OH) were. Dimers of naphthalene sulfonate leached from low pH cement with PNS, while the methacrylic acid M-PEG monomer (MAA-M-PEG) of the PCE was detected. The same species were detected in the leachate from fresh cement paste (56 day leach) and cement powder that had been hardened and then ground (38 week leach). As noted above, these molecules may have remained in the porewater during cement hydration or been leached from the cement.

Herterich et al. (2003) detected PEG in the leachate from a cement prepared with PCE, and chemically altered naphthalene sulfonates in the leachate from a cement prepared with PNS. PEG arises from the alkaline hydrolysis of the labile ester bonds linking the PEG sidechains to the molecule.

Similar results have been observed in field studies. Ruckstuhl et al. (2002) found that monomers and dimers of PNS leached from grout into groundwater to the greatest extent, while oligomers consisting of more than four repeat units were not detected at all. This was considered to reflect the different binding properties of the molecules. Acrylate, methacrylate and 2-hydroxyethyl methacrylate from a polyacrylate-based grouting agent have been seen to leach quickly during the construction of a tunnel in Norway (Sverdrup et al. 2000). The highest concentrations of these chemicals in the drainage water (4–5 mg/L) occurred during the injection of the materials, and then the concentrations dropped rapidly to < 0.3 mg/L.

Glaus et al. (2006) prepared OPC with LS and PNS superplasticisers and allowed the cement to age for ~20 months. The superplasticisers were extracted from the crushed material using 1 M Na_2CO_3 and it was found that the UV/Vis spectra had not altered with respect to the original superplasticiser solution. The UV/Vis spectra of superplasticisers in the porewater showed changes from 4 to 20 months, suggesting that the compounds in the porewater are more prone to change than those that are sorbed. This is consistent with the smaller molecules in the superplasticiser mix that tend to sorb to a lesser extent being more prone to chemical degradation than the polymers.

Degradation of cement-bound superplasticiser is expected to be slow, which may result in a slow release into the porewater over a long time. Since the polymers become tightly bound or even intercalated in the cement during hydration, degradation of cement may also be an important consideration in terms of the rate at which degradation products leach (Onofrei et al. 1992).

4.3.4 Solubility and sorption

Superplasticisers interact strongly with cement particles when the superplasticiser is added to the cement mix. In the first instance, this is driven by electrostatic attraction between negatively charged functional groups on the superplasticiser and cement minerals with a positive zeta potential. There is a limit to the amount of superplasticiser that can sorb to cement, and as this limit is approached, superplasticiser components remain increasingly in the aqueous phase (Keith-Roach and Höglund 2018).

The interaction of superplasticisers with cement depends on the type of superplasticiser. PNS-type superplasticisers interact to a greater degree than PCE, since the sulfonate groups in PNS compete effectively with sulfate in the cement minerals. The interaction of PCE superplasticisers with cement minerals also varies according to the superplasticiser's properties. A higher charge density results in a greater electrostatic attraction to the tricalcium aluminate clinker minerals. These minerals have a positive zeta potential and are thought to be the most important phase for binding superplasticisers (e.g. Plank and Hirsch 2007, Alonso and Puertas 2015, Ng et al. 2013, Winnefeld et al. 2007). Winnefeld et al. (2007) found that 100 % of polymethacrylic acid sorbed to the cement, which may suggest that PVMA superplasticisers, which have structural similarities to PCE superplasticisers but without ether side chains, will associate more strongly with the cement phase than PCE superplasticisers.

Polymers sorb strongly to cement, thus the compounds remaining in the porewater consist primarily of reactants used in the polymerisation, monomers and small oligomers. The solubility of relevant carboxylate monomers in water is high and naphthalene sulfonate is water soluble (NCBI 2008). Melamine is not water soluble, but the sulfonate group of melamine sulfonate increases hydrophilic interactions. Solubility limits are not assumed to be relevant here.

4.3.5   Coordination and denticity

Superplasticiser polymers and oligomers have the possibility of multidentate bonding via their functional groups. However, the molecules most likely to be present in the porewater over time are those that do not bind to cement and polymer degradation products. These molecules are therefore of interest in terms of radionuclide complexation. It is difficult to identify degradation products with confidence in the absence of a clear degradation pathway. Therefore, the denticity of molecules that have been observed to remain in the porewater of cementitious materials are discussed below.

PMS

Melamine transmutation substances such as methylol amine (aminomethanol) or a homologue of methylol amine (H_2N-CH_2-OH) were observed by Yamamoto et al. (2008). Aminomethanol is too small to form stable chelate rings, as the rings would involve four members. Additionally, the alcohol group is a weak complexing agent and the amine does not form complexes with actinides. It is not therefore expected to be of concern. PMS is not currently used in SFR waste stabilisation matrices.

PNS

Naphthalene sulfonate monomers and dimers were observed by Yamamoto et al. (2008) and Ruckstuhl et al. (2002). NS trimers were also observed by Ruckstuhl et al. (2002) as a relatively small proportion of the total PNS components that leached into groundwater (0.25 µg/L of 233 µg/L). NS dimers and trimers are theoretically able to act as bi- and tridentate complexing agents, via the sulfonate groups (Hedström 2019a). The stability will clearly be affected by the position of the sulfonate groups, and the resultant size of the chelate ring formed.

PCE

PEG sidechains have been observed in solution by Herterich et al. (2003), while Yamamoto et al. (2008) detected the methacrylic acid M-PEG monomer (MAA-M-PEG). Sverdrup et al. (2000) determined acrylate, methacrylate and 2-hydroxyethyl methacrylate. PEG sidechains have no capacity to form complexes with radionuclides (Keith-Roach and Höglund 2018). Acrylate and methacrylate have monodentate capability (see Table 4-7) and 2-hydroxyethyl methacrylate is an ester that, after alkaline hydrolysis, will also have monodentate capability via one carboxylate group. The PEG monomer (MAA-M-PEG) has bidentate capability after alkaline hydrolysis of the ester group, but the chelate ring would be 8-membered, and so be relatively unstable. The use of maleic acid in PCE would introduce a bidentate complexing agent in the product mix but again, the chelate ring would involve 7 members.

PVMA

Although PVMA has not been included in a study examining the molecules remaining in the porewater of cement, similarities can be drawn from PCE. Unreacted maleic acid would be expected to be present in the product and therefore may be present in the porewater. However, 100 % of polymethacrylic acid sorbed to cement in the experiments of Winnefeld et al. (2007), suggesting a strong interaction with the cement phase.

4.3.6 Presence in SFR

Superplasticisers are present in the SFR waste forms due to their use in grout and cement stabilisation matrices. They are also present in concrete waste within the packaging material and structural concrete and grout/backfill used outside the waste packages in SFR. Superplasticisers are only considered within the context of the stabilisation/grouting matrices of the waste packages in this report.

4.3.7 Occurrence in future waste

Superplasticisers are expected to be present in future wastes due to their on-going use. The decommissioning waste planned for the extended SFR3 includes significant amounts of radioactive construction concrete, which may contain superplasticisers. However, this report focusses on SFR1.

4.3.8 Form following the resaturation of SFR

Polymeric superplasticiser molecules are expected to be strongly associated with the cement phases. Smaller molecules present in the product may remain in the bleed water and cement porewater (Section 4.3.3 and 4.3.9). Sulfonate and carboxylate groups will be deprotonated under SFR conditions.

4.3.9 Literature review of effect on radionuclide speciation and sorption

This review focuses on PNS and PCE superplasticisers as the most common superplasticisers currently used in SFR waste stabilization matrices. It is based to a large extent on Keith-Roach and Höglund (2018).

There is no doubt that superplasticisers in the solution phase can increase the solubility of radionuclides. Different types of superplasticisers have been shown to increase the solubility of Ni(II), Tc(IV), U(IV), Pu(IV), Am(III) (Keith-Roach and Höglund 2018).

Several experiments investigating the impact of superplasticisers on radionuclide sorption have been carried out by adding superplasticisers and radionuclides to a solution containing previously hardened cement paste (HCP). With this experimental set-up, superplasticisers have often been seen to have a clear effect on radionuclide sorption. For example, seven superplasticisers used by SKB were found to reduce the sorption of Eu(III) to Portland cement at very low concentrations (Dario et al. 2004). An effect was seen when they were added at 0.001–0.01 % of the solution phase (Dario et al. 2004). The PVMA superplasticiser Sikament 10 was also found to prevent measurable Pu sorption to grout at a PVMA solution phase concentration of 0.5 or 1 % (Boult et al. 1998).

Glaus et al. (2003) carried out this type of experiment with Ni(II), Eu(III) and Th(IV), and eight superplasticisers at concentrations of 2 and 0.2 g/L. Although the effect observed was product-specific, a sorption-reduction effect was often seen with 0.2 g/L (0.02 % of the solution phase) superplasticiser. Wieland et al. (2014), on the other hand, found that neither a polycarboxylate ether (PCE) nor a polynaphthalene sulfonate (PNS) superplasticiser had a significant effect on Ni(II), Eu(III) or Th(IV) sorption to HCP. The maximum concentrations of superplasticiser added to the solution phase in the Eu(III) experiments were around 0.2 g/L (0.02 %), which was slightly higher than the lowest concentrations that had an effect in Dario et al. (2004). However, it appears that Wieland et al. (2014) carried out their experiments very close to the lower limit where an effect has been observed.

The data obtained from this type of experiment are difficult to relate to repository conditions since superplasticisers are added to cement during casting, rather than present in the solution phase, and this strongly affects the composition of the dissolved materials (see Section 4.3.3). The components

of the superplasticiser product that remain in solution during cement hydration differ from the polymeric superplasticiser, and comprise unreacted reagents, monomers and oligomers (Section 4.3.3). Over time, the superplasticiser compounds that leach from cement, if any, will be degradation products, which may be similar to the initial material in the porewater. However, both are rather different from the superplasticiser polymer that dominates the organic material in the product used.

The NDA (2015) carried out a variety of experiments to examine the effect of superplasticisers on radionuclide immobilisation in grout and the main observations are summarised in Table 4-9. As seen before, superplasticisers enhanced radionuclide solubility when added to cement-equilibrated water (no cement present). Furthermore, elevated concentrations of radionuclides were determined in some cement bleed water obtained during the preparation of cement blocks for the intact leaching experiments. This had previously been observed in Young et al. (2013), where 19 % of Ni(II), 32 % of U and 26 % of Th reportedly remained in the bleed water of a 9:1 blast furnace slag:OPC grout prepared with a comb-type PCE superplasticiser. However, closer examination of this data shows that the percentages were calculated from the concentration in the bleed water compared to the initial concentration, without taking account of the amount of liquid water consumed during cement/pozzolan hydration. This means that a much greater proportion of the total radionuclide added in each experiment became bound to the cement than the data indicate. Young et al. (2013) did not report the volumes of bleed water, so the actual percentages of unbound radionuclides cannot be re-calculated. It should be noted here that blast furnace slag is not used in the cements in SFR.

NDA (2015) reported both the volume of bleed water and the percentage of the original spike remaining in the bleed water. Radionuclide sorption to grout prepared from 3:1 pulverised fuel ash:OPC was complete regardless of a) the superplasticiser used and b) the amount of bleed water. However, when 9:1 ground granulated blast furnace slag:OPC was used together with the commercial polycarboxylate superplasticisers investigated, measurable radionuclide concentrations remained in the bleed water. In every case, the amount of bleed water was very high – more than 13 g of bleed water from a ~100 g block of grout. This appears to be equivalent to > 55 % of the water used in the grout formulation (water:solid ratio of 0.31, i.e. 23.7 g water, 76.3 g cement/pozzolan). The reported percentage of the radionuclides in the bleed water were lower here than in Young et al. (2013), 0.5–7.6 % of the Ni(II), 0.1–0.2 % of the U, 0.1–1.1 % of the Pu and only one positive measurement of Am(II): 0.6 %. Two polycarboxylate superplasticisers synthesized by the authors resulted in less bleed water (1.5–3.3 g) and, in these cases, the radionuclide concentrations were below the detection limit.

Superplasticisers added during casting did not, however, enhance radionuclide mobilisation or transport once the cement had hardened (see Table 4-9). Glaus et al. (2003) also found that the use of commercially available superplasticisers in the preparation of HCP did not affect the sorption of radionuclides. Furthermore, there was no evidence of degradation of the superplasticisers into products with higher complexing power over ~4 months. The superplasticisers tested included LS, PNS, PMS and a polycarboxylate.

Table 4-9. Summary of the NDA (2015) superplasticiser (SP) experiments with radionuclides (RN).

Experiment	Procedure	Results
Solubility experiment	SP + RN added to cement-equilibrated water	Effect seen for all SP except one preparation that had been dialysed
Through diffusion experiments	Grout cast with 0.5 % SP and cured, 6 month diffusion experiments using RN in solution phase	No diffusion seen
Intact leaching experiments	Grout cast with 0.5 % SP and RN, cured then leached for a maximum of 36 days	RN present in the bleed water when SP were used (which were thought to carry into the curing water to an extent), but no significant effect in the leach tests
Crushed leaching experiments	Grout cast with 0.5 % SP and RN, cured then crushed. Half of the samples irradiated 1.04 MGy @ 0.85 kGy/h. Leached max 24 h	RN did not leach significanty with reference to the blank

4.3.10 PhreeqC calculations

Thermodynamic calculations were not performed as experimental data were available.

4.3.11 Recommendations for WAC 4.0

Experimental evidence suggests that superplasticisers used in the production of waste stabilisation matrices may affect radionuclide sorption. However, the only direct evidence that this can occur when superplasticisers are added to cement as it is cast, as opposed to cement that has already hardened, is from bleed water. The evidence was obtained using grout that differed significantly in its preparation and composition from the materials used in SFR waste stabilisation. First, the radionuclides and superplasticisers were both added to water that was then mixed with cement powder to initiate cement hydration. This differs from the situation of cement or concrete being cast with water and superplasticiser and then the slurry being poured over waste materials that are contaminated with radionuclides. Secondly, the effect was seen when using a grout composed of 9:1 high blast furnace slag:OPC, which is not relevant to any cement used in SFR. Finally, a large amount of bleed water was produced, which is not the case during waste stabilisation.

The amount of superplasticiser used in industry is optimised with regard to the best effect with as little as possible wastage. Essentially, the amount of superplasticiser that does not bind to the cement is minimised. Excessive bleed water is also undesirable as a cement or concrete recipe should be reliable and give a product of specific properties. To ensure that this is the case, SKB stated that it must be demonstrated that minimal bleeding occurs (Hedström 2019a) as a part of the acceptance criteria introduced for the use of superplasticisers in waste matrices.

Hedström (2019a) defined waste acceptance criteria for PVMA (polyvinylmaleic acid), PNS and PCE. The WAC were calculated assuming that the mass fraction of superplasticiser used that is in the pore water was the maximum amount identified in selected studies, and that the superplasticiser material in the pore water consists purely of a single type of molecular unit, with a high capacity for complexation as follows (Hedström 2019a, b):

- PNS: 0.8 % of the superplasticiser material in the pore water, assumed to be a PNS trimer (647 g/mol), with three sulfonate groups.

- PCE: 7.5 % of the superplasticiser material in the pore water, assumed to be a PC trimer (725 g/mol to account for the mass of two PEG sidechains that are hydrolysed to give the three carboxylate groups).

- PVMA: 7.5 % of the superplasticiser material remains in the pore water (by analogy with PCE), assumed to be a PC trimer (259 g/mol).

These were then judged against the 1 mM concentration limit for tricarboxylic acids given in WAC 3.0 (Section 1.1, Table 5-5). Based on the literature discussed in Section 4.3.3, the structures assumed by Hedström (2019a, b) are pessimistic:

- Monomers and dimers of PNS are the dominant materials remaining in the pore water of cements prepared with PNS.

- PCE monomers (acrylate/methacrylate/methacrylate-PEG) and dimers (dimers of acrylate or methacrylate with or without a PEG sidechain) are the dominant materials identified as remaining in the pore water of cements prepared with PCE. PEG has also been identified.

- The charge density of a PVMA is greater than a PCE because there are two carboxylate groups in maleic acid that are not esterified with long PEG sidechains. Therefore, PVMA is likely to interact more strongly with cement minerals than PCE, and less would be present in the pore water. As the mass of the side groups increases, the charge density would decrease, but the molecular mass of each "complexing unit" would increase, again lowering the molar concentration of each unit considered.

The concentration limits calculated were equivalent to 2.1 g/L of PCE superplasticiser (Hedström 2019b), 1.2 g/L PNS and 0.7 g/L PVMA (Hedström 2019a). These concentrations of the superplasticiser in solution would certainly affect radionuclide sorption, but the material that is expected to remain in solution is not likely to do so. Although future degradation products of superplasticisers may differ

from the initial material in the pore water, smaller molecules that are similar to the initial material in the porewater are most likely to be released from the cement.

Polycarboxylates have been investigated in this report (see Section 4.2) and the available information led to the conclusion that di- and tricarboxylates will not affect radionuclide sorption under SFR conditions. This is due to both hydrolysis of the radionuclide ions at pH 12.5 and the interaction of polycarboxylates with Ca^{2+}. The structures of acrylate, methacrylate and even maleic acid dimers result in chelate ring sizes of > 6 members, thus their complexes will be less stable than those of oxalate and citrate. Therefore, the concentration limits derived for PCE and PVMA are also conservative from the perspective of the expected effect of polycarboxylates on radionuclide sorption.

The main risk from using superplasticisers is associated with exceeding the binding capacity of the cement for superplasticisers. If this were to occur, oligomeric or polymeric material could remain in pore water and affect radionuclide sorption. Therefore, it is recommended that PCE and PVMA superplasticisers are used at a concentration below or within the suggested concentration range (as a % of dry cement) on the product technical datasheet and, as before, that the formation of bleed water is shown to be minimal.

The PCE and PVMA limits calculated by Hedström (2019b) as a % of dry cement were 0.15 % for pure PCE (equivalent to 0.41 % for the product Glenium 51) and 0.05 % for pure PVMA in cement stabilisation/grout matrices. For concrete grout, the limits were lower at 0.05 % for pure PCE (equivalent to 0.14 % for the product Glenium 51) and 0.02 % for pure PVMA. The manufacturer suggests a dosage of 0.5−1.5 kg Glenium 51 per 100 kg cement or other binder material. Therefore, the manufacturer's suggestion is, at least in this case, higher than the limits defined in Hedström (2019b). The technical data sheet also states that the dosage must be determined in laboratory experiments.

The effect of sulfonates on radionuclide speciation has not been examined in this report but it is known that sulfate is a strong complexing group (Table 2-3). In the absence of further information, the limits suggested by Hedström (2019a) are therefore recommended for PNS as conservative values. These limits were equivalent to 1−3 % of the dry cement for the PNS product Sikament 210.

For PMS, the compounds that have been identified in solution were related to methylol amine, which is not expected to be a strong complexing agent. The multiple amine groups present in PMS may make PMS more important than PNS for Ni(II). However, due to the relatively limited amount of information for PMS, it is recommended that it is handled in the same way as PNS, and is assumed to be a trimer with tridentate complexing ability. The mass of the repeat unit in PMS is similar to PNS (219 (PNS) and 230 (PMS) g/mol based on the structures in Table 4-8), as is the frequency of the sulfonate group. Therefore, the same concentration limit can be applied.

The concentration limits derived in Hedström (2019a) for PNS are recommended here for PNS and PMS.

4.4 Plasticisers

4.4.1 Origin

Plasticisers are present in many plastic and rubber wastes disposed of in SFR. They are used to modify the properties of the plastic and rubber polymers materials. For example, PVC is a rigid polymer and non-polymeric plasticiser molecules are added as a significant proportion of the total mass to make it more flexible (Baston et al. 2017, Dawson 2013a). Rubber also contains additives, including phthalate ester plasticisers (Filby et al. 2016).

4.4.2 Structure

Common plasticisers include phthalic acid and its esters (Figure 4-15).
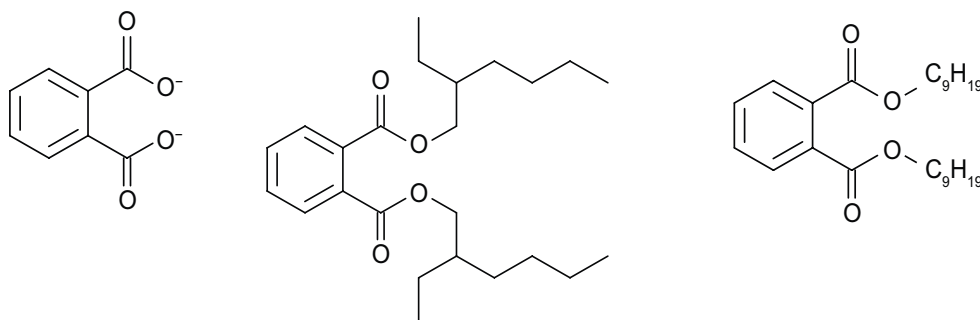
Figure 4-15. *Chemical structure of phthalate and two of the phthalic acid esters, diethylhexyl phthalate and diisononyl phthalate.*

4.4.3 Degradation characteristics and reactions

Based on the chemistry of esters, phthalic acid esters are expected to undergo alkaline hydrolysis of the ester groups to produce phthalate and two aliphatic alcohols.

Baston et al. (2017) investigated the degradation products of commercial PVC film and three phthalic acid ester plasticisers that were gamma irradiated at different temperatures in saturated $Ca(OH)_2$ solution. As expected, the phthalic acid esters underwent de-esterification to phthalate and alcohols. However, gas chromatography-mass spectrometry (GC-MS) analysis identified phenols as the main dissolved organic species arising from alkaline irradiation of a commercial PVC material. As the phenols did not arise from the polymer chain or the plasticisers, they were thought be derived from other additives in the PVC, potentially triphenyl phosphate.

Baston et al. (2017) identified a small amount of phthalate in the aqueous phase of the PVC irradiation experiments and identified it as coming from the plasticiser. The concentrations were < 0.5 % of the total dissolved organic carbon (DOC) concentration. Benzene was also observed in volatile organic carbon (VOC) analysis, which could be a degradation product of phthalate.

4.4.4 Solubility

The solubility of phthalate esters depends on the length of the alkyl chain.

Potassium hydrogen phthalate has a solubility of 0.4 M at 29 °C (ECHA 2017). According to the NCBI (2004a), phthalate has reported solubilities in water of 0.042 M at 25 °C, 0.04 M (temperature not given) and 0.006 M at 20 °C. Baston et al. (2017) dissolved 0.03 M phthalic acid in water and confirmed that it remained in solution after the pH was adjusted to pH 12.5 and 13.1. The solubility at 10–15 °C, as expected in SFR, may be slightly lower than this.

4.4.5 Coordination and denticity

Phthalate is a bidentate dicarboxylate, which forms a seven-membered chelate ring.

4.4.6 Presence in SFR

Since plasticisers are present in the plastics and rubber waste, they will be inside the waste packages.

4.4.7 Occurrence in future waste

Plastic and rubber wastes are likely to be present in future wastes, thus plasticisers are likely to be present.

4.4.8 Form following the resaturation of SFR

The relatively low solubility of plasticisers in water will limit the transport of plasticisers out from the plastic or rubber source.

4.4.9 Literature review of effect on radionuclide speciation and sorption

Baston et al. (2017) found that PVC degradation products, formed during gamma irradiation at alkaline pH, influenced the sorption of Pu and U(VI) to cement. However, the authors of the study were not able to identify the organic species responsible. They also conducted experiments with phthalate. The solubility of plutonium and nickel were not affected by phthalate, but phthalate appeared to affect U(VI) solubility, particularly in Portland cement porewater. However, when the data were examined further in a modelling exercise, it was apparent that part of the effect was due to differences in the inorganic chemistry of the experiments. The effect of phthalate on U(VI) sorption to Portland cement was then investigated and found to be negligible.

Thakur et al. (2011) derived stability constants for trivalent actinides and phthalate from potentiometric titrations and solvent extraction experiments. The stability constants were relatively low (see PHA in Table 4-5).

Neither the long chain alkanes seen to diffuse out of rubber nor the *N*-methyl-aniline ($C_6H_5NH(CH_3)$) degradation product (Dawson 2013c) are expected to be able to complex radionuclides. Phthalates present in the rubber were not observed to diffuse out experimentally.

Modelling studies have suggested that Ni(II), Eu(III) and Am(III) (Garcia et al. 2018) are not complexed by phthalate under alkaline conditions, even though phthalate is an important complexing agent under near neutral conditions.

4.4.10 PhreeqC calculations

The calculations of Garcia et al. (2018) and Baston et al. (2017) and the low stability constants derived by Thakur et al. (2011) show that relevant radionuclides are not predicted to be complexed by phthalate at alkaline pH. Further calculations were not judged to be necessary here.

4.4.11 Recommendations for WAC 4.0

Plasticisers are important components of PVC and rubber disposed of in SFR. However, the concentration of dissolved phthalate in SFR will be limited by its solubility, and phthalate is not expected to form complexes with radionuclides under the high pH conditions of SFR (Garcia et al. 2018) or affect radionuclide sorption (Baston et al. 2017). Organic molecules associated with rubber additives including plasticisers are therefore judged to be of low concern for SFR and WAC are not required.

4.5 Plastics and Rubber

4.5.1 Origin

A variety of plastic is expected to be present in the waste due to the use of plastic products on the active side of nuclear facilities, and during decommissioning.

The main plastic and rubber polymers identified in SFR wastes were identified in the recent survey of products with potential for complexation used by the waste producers[5]:

- Polyethylene
- Polypropylene
- Polyvinyl chloride (PVC)
- Polyester
- Polyamide
- Rubber (including latex)
- Nitrile

---

[5] Inventering av produkter med komplexbildare hos avfallsproducenter. SKBdoc 1904743 ver 1.0, Svensk Kärnbränslehantering AB. (In Swedish.) Internal document.

4.5.2 Structure

An overview of the chemical structures of plastics and rubber was given in Table 2-8, and the formation and degradation of condensation and addition polymers was introduced in Section 2.3.

Important condensation polymers are polyesters and polyamides and the structure of PET, a common polyester, and Nylon 6,6, a common polyamide, are shown in Figure 4-16. PET is formed through the reaction of 1,4-benzendicarboxylate and ethane-1,2-diol (ethylene glycol). Aliphatic polyesters have a similar structure to this but are based on, for example, adipic or succinic acid with a diol.

Nylon is a generic name for synthetic, aliphatic polyamides and Nylon 6,6 and Nylon 6 are the most important commercial products (Gauthier 1995). In the nomenclature Nylon x,y, x and y indicate the length of the carbon chains in the diamine and dicarboxylate reactants, respectively. Therefore, Nylon 6,6 is formed by reaction of hexamethylenediamine (HMDA) and adipic acid. Nylon 6 (Figure 4-17) is formed by a ring-opening of caprolactam into an aminocaproic acid intermediate which is then polymerised.

According to Vagholkar (2016), Nylon 6,10, Nylon 6,12, Nylon 11, Nylon 12 and Nylon MXD6 (an aromatic Nylon) are also used in everyday life. All of these possess fairly long carbon chains between the functional groups. Nylon 4,6 is a less common Nylon used in engines and has a four-carbon chain in the diamine.

Although the term polyamide is often considered synonymous with Nylon, there are some polyamides that are not Nylons. These can contain the shorter chain ethylenediamine or even the triamine diethylenetriamine. They are used in inks, varnishes and coatings (Gauthier 1995). Certain polyamides are found in anti-corrosion paints (Section 4.6.1), but apart from those, it is assumed that polyamides relevant to SFR wastes are Nylons and that neither ethylenediamine nor triamines are components of the polyamides.

Nitrile rubber used in disposable gloves is formed through a reaction of nitrile and butadiene. The structure of nitrile rubber is shown in Figure 4-18.
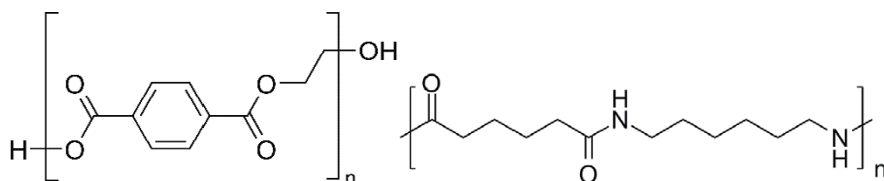
Figure 4-16. *Chemical structures of PET and Nylon 6,6.*
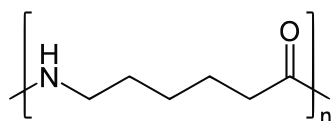
Figure 4-17. *Chemical structure of Nylon 6.*
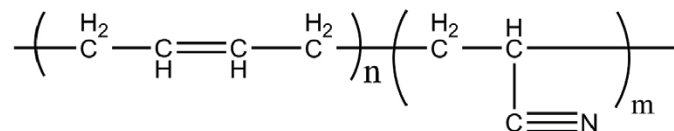
Figure 4-18. *Chemical structure of nitrile rubber.*

4.5.3 Degradation characteristics and reactions

Condensation polymers

For condensation polymers, the functional groups in the polymer backbone generally provide a point of chemical attack (Section 2.3), introducing the possibility of hydrolysis of the polymeric chain (Van Loon and Hummel 1995). Hydrolysis is essentially the reverse of the condensation reaction used to form the polymer. Therefore, hydrolysis of polyamides produces dicarboxylic acids and diamines, while alkaline degradation of polyesters produces dicarboxylic acids and diols.

Alkaline hydrolysis of polyester is a well-known process and expected to occur quite rapidly. Alkaline hydrolysis of PET will produce of 1,4-benzendicarboxylate and ethane-1,2-diol (ethylene glycol). Polyamides are more resistant to alkaline hydrolysis and Van Loon and Hummel (1995) identified that they are not attacked by strong alkali. However, Van Loon and Hummel (1995) also discussed alkaline hydrolysis of polyamides in some detail. Since the polyamides known to be deposited in SFR are present in cloths, for example, it seems likely that they will be less resistant to hydrolysis than bulk plastic Nylon. Also, the high pH conditions of SFR combined with the long timescales of interest make hydrolysis difficult to exclude as a possibility. Alkaline hydrolysis of Nylon 6,6 would produce HMDA and adipic acid.

Nylon 6 is formed by a ring-opening polymerisation, thus alkaline hydrolysis is expected to result in the formation of a long chain amino acid.

Addition polymers

Addition polymers lack functional groups in their polymeric backbone, which makes them chemically stable. However, addition polymers can degrade in terms of changes to functional groups bonded to the backbone (where present), thermal degradation (not discussed, not relevant in SFR) and/or irradiation. In the case of PVC, degradation of the chloride groups can lead to the formation of HCl, which in turn can catalyse an un-zipping mechanism of the polymer chain (Dawson and Magalhaes 2012). However, HCl will not persist in an alkaline environment. Irradiation leads to the formation of free radicals and, in an oxic environment, particularly reactive peroxy-based radicals form. These can result in oxidative chain scission of otherwise unreactive polymer chains such as polyethylene (Dawson and Magalhaes 2012). Irradiation can also lead to crosslinking within the polymer.

Degradation reactions relevant to the alkaline environment of SFR have been studied by Dawson (2013a, b, c) and give an insight into both alkaline degradation (although oxygen was not excluded in their aqueous experiments) and radiolysis under portlandite-buffered conditions. The experimental chemical degradation time was not given, but the longest irradiation in each set of experiments was 128 days.

Dawson (2013b) carried out experiments to investigate the radiolytic (gamma) degradation of polyethylene in saturated $Ca(OH)_2$ solution with a maximum absorbed dose of 10 MGy. GC–MS analysis of the solution phase identified negligibly low concentrations of a potential complexing agent, benzene dicarboxylic acid, and long chain alkanes. Unidentified and identified GC–MS peaks were then summed to estimate the total concentration of organic substances present and these data were at least 20 % of the total organic carbon (TOC) concentrations determined by UV analysis. The difference was explained by the presence of smaller molecules with 5 or fewer carbon atoms that were not detected by GC–MS. Using the TOC concentration determined by UV analysis, instead of GC–MS, together with data for the saturated $Ca(OH)_2$ solution, the upper limit for aqueous organic degradation products can be estimated to be 60 g/tonne polyethylene. This is a negligibly low yield.

Dawson (2013a) carried out equivalent experiments using PVC, using both saturated $Ca(OH)_2$ solution and water (pH 7). It was found that approximately double the concentration of organic compounds was released into water than the $Ca(OH)_2$ solution at an equivalent radiation dose. This suggests that neutralisation of HCl in the $Ca(OH)_2$ solution reduces the concurrent catalytic HCl degradation mechanism. A number of radiolytic degradation products were identified using GC–MS of the aqueous phase and volatile organic carbon analysis of the gaseous phase (dry experiments). These were the types of compounds expected from the literature, hydrocarbons, carboxylic acids, ketones and to a lesser extent alcohols and aldehydes. However, the sum of the concentration of these molecules from GC–MS was ~1 % of the DOC concentration. Dawson (2013b) suggested that the majority of the aqueous degrada-

tion products may be smaller than C_{5-6} and thus would not be detected by GC–MS. Using the TOC concentration determined by UV analysis, instead of GC–MS, the mass of degradation products formed with a 10 MGy absorbed dose at pH 12.4 would be ~600 g/tonne PVC. This is a negligibly low yield of radiolytic degradation products.

Dawson (2013c) carried out equivalent experiments using neoprene (rubber) in both saturated $Ca(OH)_2$ solution and water (pH 7). In this case the pH of the experiments in water did not decrease. Despite neoprene being a polychloroprene, acid generation was not induced. However, lower concentrations of organic degradation products were detected in the solution at alkaline pH than in the experiments in water. In general, low concentrations of organic compounds were detected in solution, despite neoprene containing additives such as plasticisers. The data indicated that organic compounds produced by radiolysis in the highest absorbed dose experiments undergo further radiolysis. The compound identified with the highest mass concentration was N-methyl-aniline, ($C_6H_5NH(CH_3)$), which was thought to come from the degradation of an additive. The maximum mass of degradation products produced, measured by UV analysis of the TOC, corresponds to 200 g/tonne, again a negligibly low degradation product yield.

The information available from Dawson (2013a, b, c) suggests that radiolytic degradation of the addition polymers polyethylene, PVC or rubber will not lead to significant concentrations of dissolved complexing agents in SFR. It is therefore reasonable to assume that this will also be the case for addition polymers in general.

Work commissioned by SKB is currently underway investigating the degradation and impact of polyacrylate nitrile filter aids on radionuclide sorption (Section 4.7). This will also inform the understanding of nitrile rubber under SFR conditions.

4.5.4   Solubility

Small carboxylic acids, alcohols, amines and amino acids are expected to be soluble in water.

Larger molecular degradation products of plastics have a lower charge density and so become increasingly less water soluble with size. The risk for formation of non-aqueous liquid phases (NAPL) was the driving force behind Dawson (2013a, b, c). However, NAPL were not observed in the experiments and only theoretical maximum values could be estimated, which were very low.

4.5.5   Coordination and denticity

Degradation products from common condensation polymers, such as dicarboxylates and diamines are expected to have a maximum denticity of two. PET is 1,4-benzendicarboxylate, an isomer of phthalate. As discussed in Section 4.4.9, phthalate is not expected to form complexes with radionuclides at alkaline pH. 1,4-benzendicarboxylate is expected to form less stable complexes than phthalate, due to possible steric effects introduced by the position of the carboxylate groups and the larger chelate ring.

In the case of amino acids forming from the degradation of Nylon 6, the chelate effect would also be low due to the large chelate ring size. Amino acids may exhibit monodentate bonding with actinides as the interaction with N is energetically low in the absence of the chelate effect. Bidentate bonding with Ni(II) may occur since the interaction of the amine group with Ni(II) is more favourable.

Diols are not of concern as complexing agents in SFR, due to their low ability to complex radionuclides.

4.5.6   Presence in SFR

Plastics and rubber are present within waste packages.

4.5.7   Occurrence in future waste

Plastics and rubber are expected in future waste. The forecast amount of plastic and rubber in SFR (SKB 2019a) shows that the majority will be disposed of in the BLA vaults. Despite this, 1BMA already contains a large amount of plastic and rubber and is expected to contain 153 tonnes at closure.

4.5.8 Form following the resaturation of SFR

Plastics are solid polymers but the smaller plasticisers and degradation products are expected to have a range of solubilities.

4.5.9 Literature review of effect on radionuclide speciation and sorption

As discussed in Section 4.5.3, addition polymers are not expected to degrade extensively and any degradation that takes place is not expected to lead to the formation of complexing agents.

The risks associated with the degradation of condensation polymers (polyamides and polyesters) into complexing agents have been addressed recently as a part of the drive to replace cellulose materials with alternatives. Källström (2018) evaluated the suitability of a cleaning cloth composed of PET and Nylon 6,6 for disposal in SFR wastes. Concentration limits for these plastics were based on analogy with dicarboxylates and the associated concentration limit of 10^{-2} M in WAC 3.0 (Section 1.1, Table 5-5).

Baston et al. (2017) prepared samples of PVC in saturated Ca(OH)$_2$ solution and irradiated them using a Co-60 source and a dose rate of 100 Gy hr^{-1} at ambient temperature. The total absorbed doses were 0.25, 0.50, 0.75 or 1 MGy. They found that the degradation products influenced the sorption of Pu and U(VI) to cement. However, the authors of the study were not able to identify the organic species responsible and they concluded that the effect was small in comparison to the effect of cellulose degradation products.

The speciation of Ni(II) polyamine complexes at high pH has not been investigated, but amines were identified as potentially important under relevant conditions by Van Loon and Hummel (1995). As discussed in Section 2.1.3, the ability for diamines to act as bidentate complexing agents depends on the length of the carbon chain between the amine groups. The review of Blackman (2005) suggests that bidentate bonding would not be expected for diamines with a 6-carbon chain between the amine groups, such as HMDA.

4.5.10 PhreeqC calculations

Diamines that contain no other functional groups may be important complexing agents for Ni(II) at high pH. They are, however, not important for actinides, as nitrogen groups alone cannot displace water in the hydration shell of actinides (Katz et al. 1986). Therefore, in this section, the focus is on the interactions of diamines and Ni(II). First, the speciation of Ni(II) in the presence of ethylenediamine was calculated. Ethylenediamine forms 5-membered chelate rings thus Ni(II)-en complexes are expected to be the most stable Ni(II)-diamine complexes. Stability constants are also available for Ni(II)-en complexes in the literature. There is, however, no evidence at the moment that it is present in SFR in significant amounts.

Then, stability constants were estimated for HMDA and applied in calculations investigating the influence of HMDA on Ni(II) speciation. As diamines do not form complexes with calcium to any large extent (see Section 2.1.3, Table 2-3), the effect of Ca^{2+} on Ni(II)-diamine complex formation is assumed to be negligible. This is supported by calculations in Van Loon and Hummel (1995) that show that Ca^{2+} does not affect Ni(II)-NH$_3$ complex formation over the pH range pH 11–13. The results are shown in Figure 24 of Van Loon and Hummel (1995).

Ni ethylenediamine (en)

The log stability constant of the Ni(en)$^{2+}$ complex has been reported to be 7.51 at 25 °C and $I = 0.1$ M (Tanaka and Tabata 2009) and 7.52 at 20 °C and $I \to 0$ M (Paoletti 1984). Since ethylenediamine is uncharged, the stability constants of Ni(II)-en species are less sensitive to the ionic strength than those of Ni(II) complexes with anionic complexing agents. The log stability constant under standard conditions (25 °C and $I = 0$ M) was therefore assumed to be 7.5. The log stability constants of Ni(en)$_2$$^{2+}$ and Ni(en)$_3$$^{2+}$ are 13.84 and 18.3 (20 °C and $I \to 0$ M), respectively (Paoletti 1984). These species and log stability constants were used together with the Thermochimie_v10a database in PhreeqC calculations. pH titrations were calculated in a solution containing 10^{-8} M Ni(II) and 10^{-3} M en ([NaCl$_{init.}$] = 0.2 M),

first with just the 1:1 species included, then the 1:1 and 1:2 species and finally, with all three species. No account was taken of the protonation of en (pKa = 9.89, Tanaka and Tabata 2009) as the focus of this report is pH ~12.5.

Increasing number of en ligands has a much greater effect on the stability constant of the Ni-en complex than seen with carboxylate complexing agents (see Section 2.1.3).

The results in Figure 4-19 show that the bis and tris complexes are important at high pH, whereas the 1:1 complex alone would only result in a small proportion of the Ni to be present as an en complex at pH 12.5. En is predicted to be able to form stable complexes with Ni(II) at pH 12.5 that dominate Ni(II) speciation.
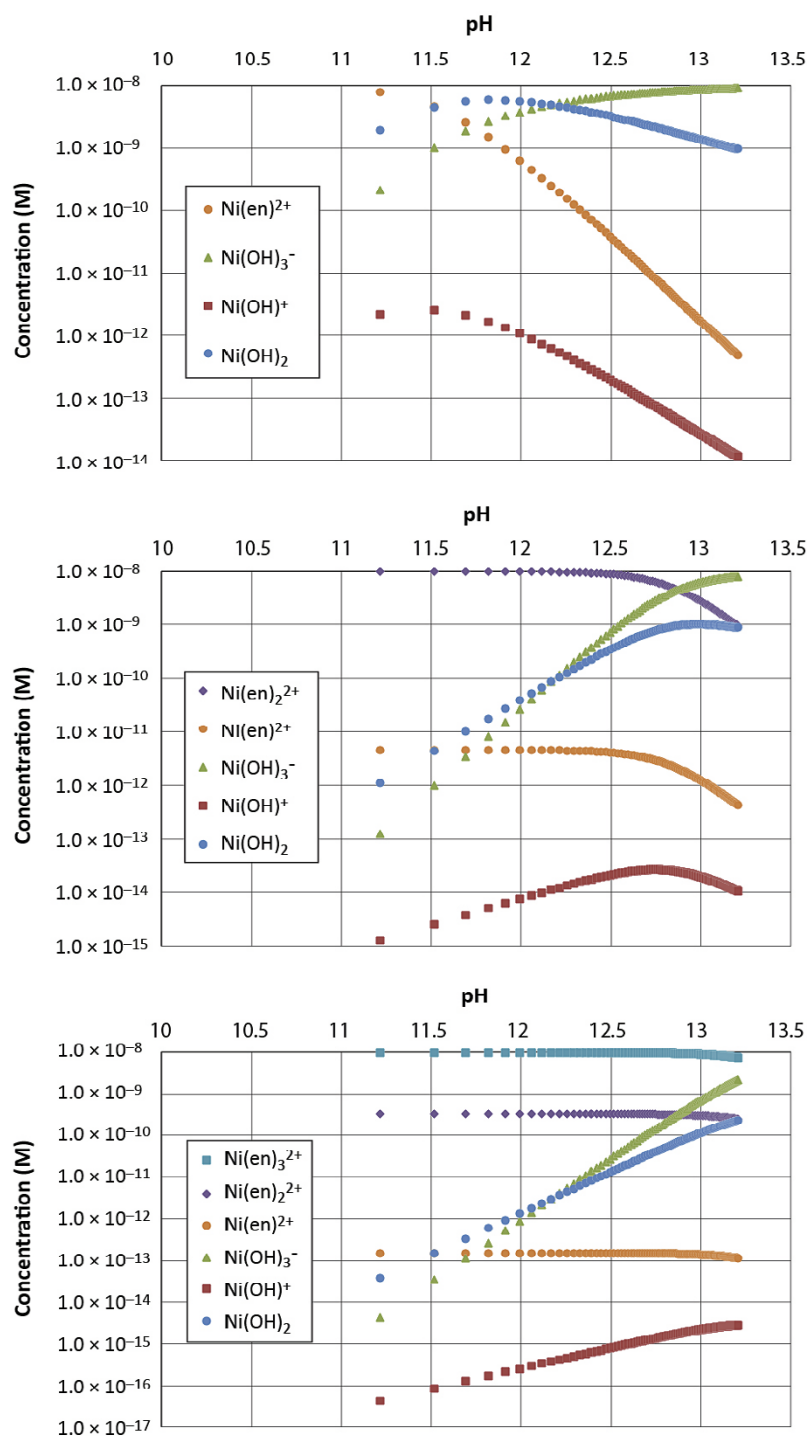
Figure 4-19. *pH titration with 10^{-8} M Ni(II) and 10^{-3} M ethylenediamine, including a) the Ni(en)$^{2+}$ species only, b) the Ni(en)$^{2+}$ and Ni(en)$_2^{2+}$ species, and c) the Ni(en)$^{2+}$, Ni(en)$_2^{2+}$ and Ni(en)$_3^{2+}$ species. Ionic strength > 0.2 M.*

Calculations were carried out titrating en into a solution representative of the experimental conditions of Bruno et al. (2018) (Figure 4-20). The Thermochimie database and the stability constants for Ni-en species given above were used. The calculations predicted that Ni(II)-en complexes dominate from an en concentration of 3×10^{-4} M. Changing the Ni(II) hydroxide thermodynamic data to that suggested by Bruno et al. (2018) and described in Section 2.2.1, would to increase the predicted effect of en on Ni(II) speciation further.

Ni hexamethylenediamine

HMDA is a hydrolysis product of the common polyamide Nylon. HMDA could in theory form 9-membered chelate rings with transition metals but evidence from Blackman (2005) suggests that hypodentate monodentate bonding is more likely. Here, it is assumed that HDMA exhibits the same stability constants with Ni(II) as ammonia (see Table 4-10). This is reasonable since the general trend in complexing strength is ammonia = methylamine > dimethylamine > trimethylamine (Van Loon and Hummel 1995), as derived in Rorabacher and Melendez-Cepeda (1971).

Table 4-10 shows that each additional NH_3 ligand contributes a progressively lower additional stability to the complex. This, and the fact that the concentration of a complex is dependent on the concentration of the ligand to the power of the number of ligands (Equation 2, Section 2.1), makes the formation of $Ni(NH_3)_5^{2+}$ and $Ni(NH_3)_6^{2+}$ generally unfavourable. These two species are not included in Thermochimie.

Table 4-10. Stability constants for $Ni(NH_3)_x^{2+}$ species included in Thermochimie.

	log$K$	Additional stability
$Ni(NH_3)^{2+}$	2.61	2.61
$Ni(NH_3)_2^{2+}$	4.76	2.15
$Ni(NH_3)_3^{2+}$	6.79	2.03
$Ni(NH_3)_4^{2+}$	8.34	1.55
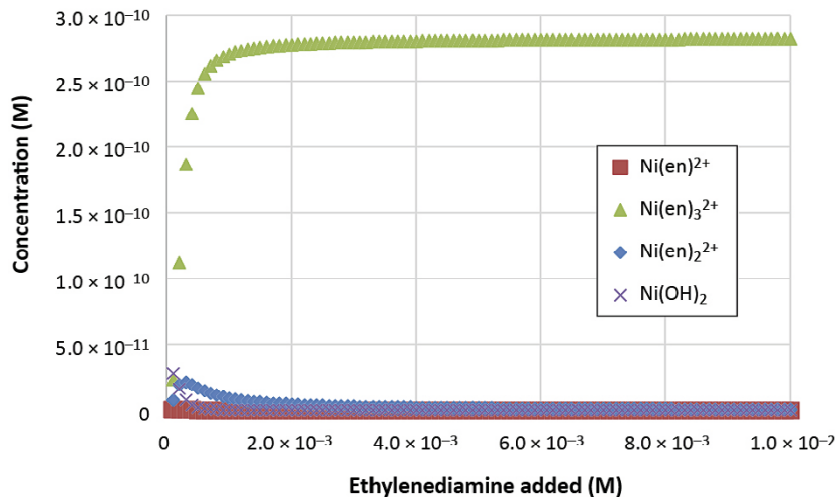
Figure 4-20. PhreeqC calculation to examine the speciation of Ni(II) in the presence of ethylenediamine under the experimental conditions of Bruno et al. (2018), using the thermodynamic data in Thermochimie. 25 °C, 0.5 M NaCl, in equilibrium with 25 g/L HCP (0.0525 mol Ca(OH)$_2$), calculated pH = 12.6.

A fabricated ligand "Amm" was defined in order to examine the influence of an amine on Ni(II) speciation without including the complex inorganic redox reactions involved in nitrogen chemistry. Ni-Amm species were assigned the Thermochimie stability constants for the equivalent Ni-NH$_3$ complexes.

The results of a pH titration into a solution containing 10^{-8} M Ni(II) and 10^{-3} M "Amm" ([NaCl$_{init.}$] = 0.2 M), using the Thermochimie database and data for Amm, are shown in Figure 4-21. In this case, the Ni-Amm complexes are predicted to comprise 10^{-6} % of the Ni(II) species at pH 12.5.

Calculations were then carried out to predict the effect of HMDA on Ni(II) speciation, using the fabricated ligand "Amm", in a solution representative of the experimental conditions of Bruno et al. (2018). First, the data for Ni(II) hydroxide complexes were taken directly from Thermochimie_v10a. Then, the relevant data were replaced with the data from Bruno et al. (2018), shown in Table 4-2.
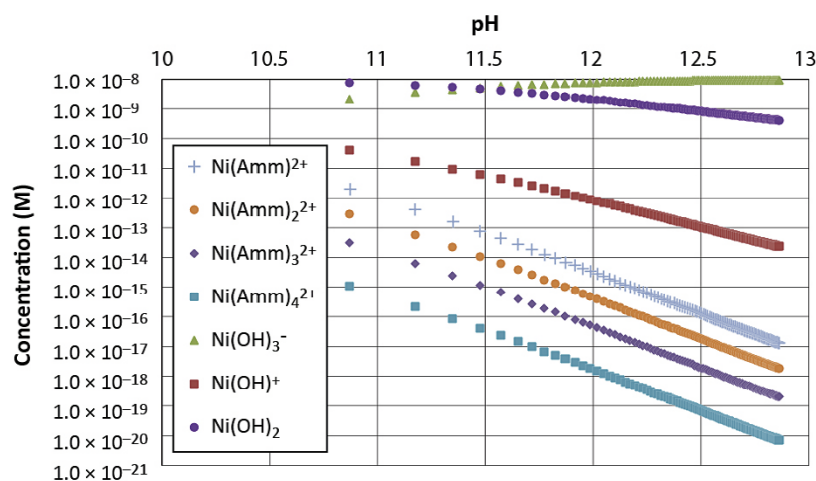
Figure 4-21. *pH titration with Ni(II) 10^{-8} M and Amm (10^{-3} M), a fabricated NH$_3$ ligand, to avoid redox reactions of NH$_3$ (I = 0.2–0.3 M).*

With the Thermochimie data, $\sim$0.1 % of the 2.8×10^{-10} M Ni(II) is predicted to be complexed by Amm when Amm is present at a concentration of 0.1 M (Figure 4-22 upper panel). Although bidentate HDMA bonding is not expected, there is a degree of uncertainty in the assumption of monodentate bonding. Since a bidentate Ni(II)HDMA$_2^{2+}$ complex would form as a function of $1/[\text{HDMA}]^2$ whereas NiAmm$_4^{2+}$ is dependent on $1/[\text{Amm}]^4$, bidentate bonding would increase the formation of the complex. Applying the log$K$ value for Ni(NH$_3$)$_4^{2+}$ to bidentate NiHDMA$_2^{2+}$ resulted in the calculated formation of bidentate NiHDMA$_2^{2+}$ as $\sim$10 % of the Ni(II) species with 0.1 M HDMA.

With the Ni(II) hydroxide data of Bruno et al. (2018), the percentage of Ni(II) predicted to be complexed by Amm when Amm is present at a concentration of 0.1 M increases to 37 % (Figure 4-22 lower panel). In the ISA experiments and modelling of Bruno et al. (2018), more than 50 % of Ni(II) in the solution phase was predicted to be complexed by ISA when a sorption reduction effect of 3–6 times was observed. Therefore 37 % complexed would be expected to result in a small reduction in sorption here.
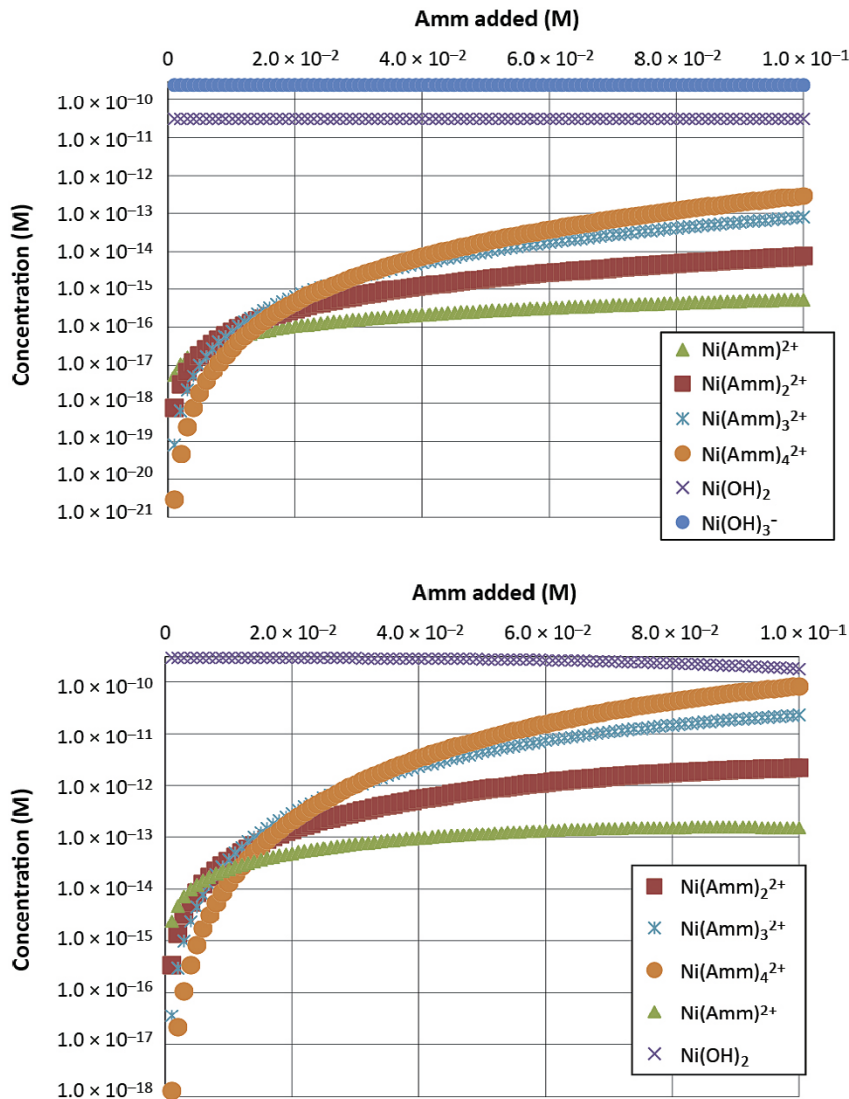
Figure 4-22. *PhreeqC calculation to examine the speciation of Ni(II) in the presence of "Amm" an artificial NH$_3$ ligand, under the experimental conditions of Bruno et al. (2018). The thermodynamic data in Thermochimie were used in the upper panel and the Ni(II) hydroxide data proposed by Bruno et al. (2018) in the lower panel. The conditions were 25 °C, 0.5 M NaCl, in equilibrium with 25 g/L HCP (0.0525 M Ca(OH)$_2$), calculated pH = 12.6.*

4.5.11 Recommendations for WAC 4.0

Addition polymers

Addition polymers are judged to be acceptable for disposal in SFR in any amount from the perspective of radionuclide sorption.

Condensation polymers

PET

As discussed in Section 4.5.3, PET is expected to undergo alkaline hydrolysis to form 1,4-benzene dicarboxylate and ethane-1,2-diol. The isomer of 1,4-benzenedicarboxylate, 1,2-benzenedicarboxylate, is phthalate and, as discussed in Section 4.4.9, phthalate cannot compete with radionuclide hydrolysis at alkaline pH. Diols are not of concern as complexing agents in SFR, due to a low ability to complex radionuclides.

Since the degradation products of PET are not expected to form stable complexes with radionuclides under SFR conditions, there is no need to limit the disposal of PET from the perspective of radionuclide sorption.

Aliphatic polyesters

Aliphatic condensation polymer dicarboxylate degradation products are expected to form less stable complexes than oxalate (Carbonaro et al. 2011). Since oxalate is not able to form complexes with radionuclides significantly under SFR conditions (see Section 4.1.11), these degradation products are not of concern.

Nylon 6,6 and Nylon 6

Nylon 6,6 degrades to HMDA (116.2 g/mol) and adipic acid (146.1 g/mol). Adipic acid has bidentate capacity but forms large 9-membered chelate rings. As a result of this, the stability constants for adipic acid with Ni(II) and Eu(II) are two log units lower than the corresponding complexes with oxalate (Figure 2-2). These dicarboxylates are not of concern in SFR (see Section 4.1.11).

Ni(II)-HMDA complexes are expected to involve monodentate bonding, as diamines of this size do not generally act as bidentate ligands (Blackman 2005). The calculations carried out using the Thermochimie database suggest that 0.1 M HMDA can be tolerated without affecting Ni(II) speciation and therefore sorption significantly. This concentration could be tolerated even if bidentate coordination should occur. The Ni(II) hydroxide chemistry proposed by Bruno et al. (2018) reduces competition from the formation of Ni hydroxide solutions species. Using the Ni(II) hydroxide stability constants from Bruno et al. (2018) resulted in ~40 % of Ni(II) being present as a monodentate HMDA species with 0.1 M HMDA. 40 % complexation is expected to result in a small reduction in the sorption of Ni(II). The concentration limit recommended here is therefore 0.1 M HMDA. This limit allows for either the Ni(II) hydroxide stability constants from Bruno et al. (2018) to be correct or for HDMA to bond as a bidentate ligand, but not both.

Nylon 6,6 has a unit mass of 226 g/mol, thus degradation of 226 g of Nylon 6,6 produces one mole of HDMA. Complete degradation of 1 kg of Nylon 6,6 therefore produces 4.4 mol HMDA. This value is used with the available pore volume in every waste package to calculate the maximum mass of Nylon 6,6 allowed.

Nylon 6 is expected to degrade to aminocaproic acid, an amino acid that would form a 9-membered chelate ring. The amino acid glycine and ethylenediamine form 5-membered chelate rings and have similar first log stability constants with Ni(II) of 5.78 and 5.87 (Tanaka and Tabata 2009), respectively. The diamine and amino acid of interest for Nylon 6,6, and Nylon 6 would form 9-membered chelate rings. Therefore, since HMDA is judged to have a low effect, it is inferred that this amino acid will also have a low effect. Therefore, the same limit of 0.1 M can be applied to aminocaproic acid from Nylon 6. The comparison with ethylenediamine is not perfect as the interaction of the amino acid with Ca^{2+} is expected to be greater. It is however, a reasonable and conservative approach.

Other polyamides

No common Nylons appear to be based on molecules capable of forming 5- or 6-membered chelate rings and so the limit for Nylon 6,6 is reasonable for all commercial Nylons/polyamides. If polyamides are identified in the waste streams that can degrade to triamines with multidentate complexing ability, a specific limit should be evaluated for the polyamides.

4.6 Anti-corrosion paint

4.6.1 Origin

Zinc anti-corrosion paints may be present on metal components within the waste packages, but they are primarily are used on the outside of steel waste packages in SFR. The most common types of zinc anti-corrosion paints are based on either organosilicates or cured epoxy resins. The organosilicate products do not contain any components that are of concern as complexing agents.

Epoxy products are supplied in two components, a base and a hardener. The base contains the uncured epoxy resin and zinc powder. A common epoxy for this purpose is formed by reaction of epichloro-hydrin with bisphenol A (Figure 4-23). The product of the reaction in Figure 4-23, bisphenol A diglycidyl ether, is reacted with further bisphenol A to make oligomers or "prepolymers" (Figure 4-24). The ring-opening polymerisation involved is an addition reaction, although the products contain ether functional groups in the polymeric backbone.
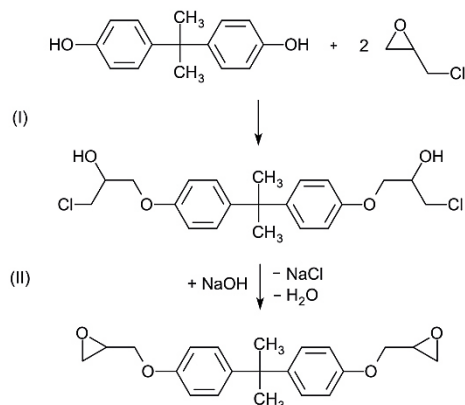
Figure 4-23. *Reaction of epichlorohydrin with bisphenol A. Reproduced from Wikipedia (2020), with permission.*
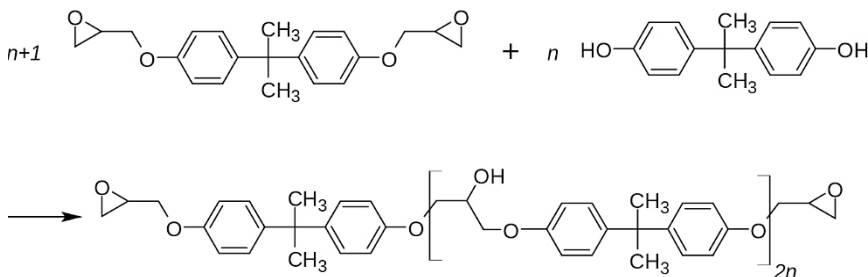
Figure 4-24. *Prepolymerisation of bisphenol A diglycidyl ether with further bisphenol A. Reproduced from Wikipedia (2020), with permission.*

The hardener contains a polyfunctional curing agent with amine, acid, acid anhydride, phenol, alcohol or thiol functional groups. Each molecule of curing agent can react with a number of terminal epoxide groups in the resin, opening the epoxide rings, and forming a highly crosslinked product (e.g. Figure 4-25). Amines must have a reactive hydrogen to act as a curing agent, which excludes tertiary amines from this function. However, tertiary amines are used to accelerate the reaction and can catalyse homopolymerisation of epoxy (Wikipedia 2020). In some cases, epoxy resins are cured in reactions with themselves (homopolymerisation).

According to Wu et al. (2006), the stoichiometric ratio of curing agent to epoxy is usually calculated assuming full reaction for both epoxy groups and amine groups. The reaction between epoxy and primary amines is faster than the reaction with secondary amines.

An example of an epoxy-based anti-corrosion paint is Sigmazinc 109 from PPG Coatings, a "two-component, high solids polyamide adduct cured zinc rich epoxy primer" (Sigma 2005). The base and hardener are mixed in a ratio of 4:1. The base contains the uncured bisphenol-A-(epichlorhydrin) epoxy resin and zinc powder (PPG 2019a). The epoxy is not of concern regarding complexation (see Figure 4-24). The ingredients listed on the safety data sheet (PPG 2019b) for the hardener are presented in Table 4-11, together with a comment on the structure or function of the chemical.

Table 4-11. Ingredients listed on the safety data sheet for Sigmazinc 109 hardener (PPG 2019b), together with a comment on the structure or expected function of the chemical.

Ingredient	CAS number	% by weight	Comment
Xylene	1330-20-7	25 – < 50	Benzene ring with two methyl groups
Fatty acids, C18-unsatd., dimers, oligomeric reaction products with polyethylenepolyamines	68082-29-1	20 – < 25	Oligmers formed from amine and acid are polyamides. As fatty acids are C_{18} monocarboxylic acids, the oligmers have relatively high molecular mass. Fatty acids and partially reacted polyethylene-polyamines may act as **curing agents**
Ethylbenzene	100-41-4	5 – < 10	Benzene ring with ethyl group
2-methylpropan-1-ol	78-83-1	5 – < 10	An alcohol
1-methoxy-2-propanol	107-98-2	3 – < 5	An ether with an alcohol group
3,6-diazaoctanethylenediamine: triethylenetetraamine in its linear form	112-24-3	1–3	Linear triethylenetetraamine is a tetraamine with two primary and two secondary amine groups (Figure 4-26) – present as a curing agent
Toluene	108-88-3	0.1 – < 0.3	
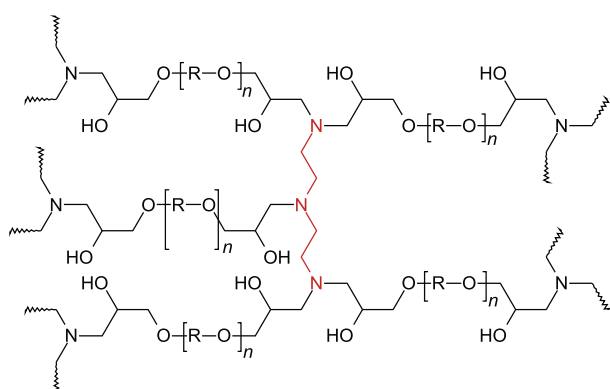
Figure 4-25. *Structure of a generic epoxy resin cured with a triamine (shown in red). Reproduced from Wikipedia (2020), with permission.*

The main ingredient in the hardener is fatty acids, C_{18}-unsaturated, dimers, oligomeric reaction products with fatty acids and polyethylenepolyamines. Oligomeric reaction products with fatty acids and polyethylenepolyamines are polyamides. Unreacted fatty acids and/or any unreacted amine groups in the polyamides are expected to act as curing agents when mixed with the base. Unreacted triethyl-tetramine (TETA) is also listed as an ingredient, at a small percentage of the mass of the product, and this is expected to act as a curing agent. Fatty acids themselves are not of concern as complexing agents, as they have a single carboxylate group on a long aliphatic chain. TETA, however, can potentially act as a tetradentate complexing agent, and so is of concern if a) if it remains unreacted when the product is used or b) is present as a polyamide, as amides degrade to amines under alkaline conditions.

Hedström (2020) analysed the potential dissolved concentrations of polyamines in SFR resulting from the use of four hardeners that contain TETA: Sigmazinc 109, Teknozinc 90 SE A, Inerta 165 A and Sigmacover 280, and four that contain the triamine tris(dimethylaminomethyl)phenol (TDP): Interzinc 315, Inerta primer 5 A, Sigmashield 420, Sigmacover 280. When the ingredient "fatty acids, C18-unsatd., dimers, oligomeric reaction products with polyethylenepolyamines" was present in a product, for example Sigmazinc 109 (Table 4-11), the polyethylenepolyamine was assumed to be TETA. As the product and the reactions that take place during hardening. Hedström (2020) assumed that all TETA present in the fatty acid ingredient becomes free dissolved TETA in SFR. TETA used as a curing agent was assumed to react with epoxy to form tertiary amines and thus would not undergo alkaline degradation nor dissolve. TDP is a tertiary polyamine and therefore expected to act as an accelerator. It is expected to be present in the paint in an unreacted form.

Each product is used slightly differently, for example the thickness of the paint varies, and they have different compositions. The thick layer of Inerta 165A used contributes to it containing the most potentially available TETA of 0.345 moles/mould. Inerta primer 5 A and Sigmashield 420 contained the most TDP, 0.053 moles/mould.

Interzinc 315 also contains a small amount of diamine (ethylenediamine, 0.5 % by mass), but this is expected to act as a curing agent. Inerta 165A contains large amounts of trimethylhexane-1,6-diamine, which is also expected to act as a curing agent. These diamines were not assessed by Hedström (2020) as they are expected to react to form tertiary amines and were present in products that contained TETA or TDP.

Hedström (2020) calculated concentrations of TETA and TDP in the pore or void volume around a single package in different parts of SFR. All of the products that contain TDP were approved for use, as the calculated concentrations were less than the proposed concentration limit of 10^{-3} M TDP. None of the products containing TETA-based polyamides, which are susceptible to alkaline degradation back into TETA, were approved for use, as the calculated TETA concentrations exceeded the concentration limit assigned of 10^{-5} M. Teknozinc 90 SE A, however, only contains TETA as a curing agent, thus this was approved for use.

Additionally, F499/SVART containing the esters dimethylglutarate (2.5–10 %) and dimethylsuccinate 1–2.5 % (assumed to be weight-%) is used on B.04 waste packages (Hedström 2019c).

4.6.2 Structures

The main polyamines of concern in anti-corrosion paints are TETA, TDP and trimethylhexane-1,6-diamine.

TETA is produced by reaction of ethylenediamine or ethanolamine and ammonia, followed by separation from the resulting mix of many products with varying number of ethyl and amine groups. Two isomers of TETA are shown in Figure 4-26. However, the linear isomer, 3,6-diazaoctanethylene-diamine, is often specified in paints. TDP is shown in Figure 4-27 and a trimethylhexane-1,6-diamine in Figure 4-28. The hydrolysis products of the esters dimethylglutarate and dimethylsuccinate used in F499/SVART are glutarate and succinate, and the structures of these were shown in Table 2-4.
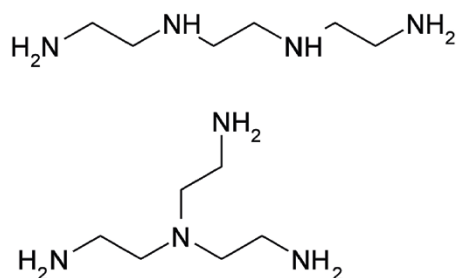
Figure 4-26. *Linear and branched TETA (146.2 g/mol).*
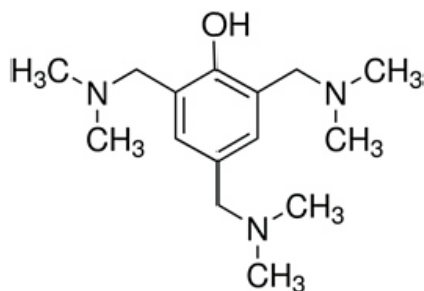
Figure 4-27. *Chemical structure of TDP (265.4 g/mol).*
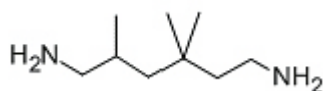
Figure 4-28. *Structure of trimethylhexane-1,6-diamine (158.3 g/mol).*

4.6.3 Degradation characteristics and reactions

Amines in the hardener may be present in the finished anti-corrosion finishing as:

a) Polyamides formed via a condensation reaction between the polyamines and fatty acids.

b) Tertiary amines formed by ring-opening reactions with epoxy groups in the epoxy resins.

c) Molecules bound partially as amides to fatty acids and partially as tertiary amines to the epoxy resin.

d) Unreacted tertiary amines that were present as accelerators.

Polyamides are expected to undergo alkaline hydrolysis under the conditions of SFR, which would regenerate the polyamines. Tertiary amines formed during addition, ring-opening reactions are, however, not expected to undergo hydrolysis.

The esters dimethylglutarate and dimethylsuccinate are expected to undergo hydrolysis to the respective dicarboxylic acids.

4.6.4 Solubility

The solubility of the hardened zinc anti-corrosion paint is very low. However, TETA and TDP are highly soluble in water (NCBI 2004b, 2005).

TDP has a solubility of 164 g/L at 25 °C (0.62 M) (NCBI 2005).

Trimethylhexane-1,6-diamine has a solubility of 1 g/L at 23 °C (6 mM) (ECHA 2018).

Succinic acid has a solubility of 83 g/L at 25 °C (0.7 M) (NCBI 2004c), while glutaric acid is even more soluble – 1.6 kg/L at 28 °C (12 M), or 639 g/L at 20 °C (4.8 M) (NCBI 2004d).

4.6.5 Coordination and denticity

Linear TETA is known as trien in complexation chemistry. Trien is a tetradentate complexing agent, bonding via the four amine groups. It is not expected to form complexes with actinides as nitrogen donors cannot displace water in the inner coordination sphere of actinides. However, it forms strong complexes with Ni(II) and other transition metal ions. The chelate rings involve 5 members, inferring high stability.

TDP has three amine groups and a phenol that can potentially be involved in multidentate bonding. Simplified quantum chemistry calculations suggested that the most stable Ni(II)-TDP complexes involve tridentate bonding, via two amine groups and the deprotonated phenol (Hedström 2020). However, Romashkina et al. (2011) examined the crystal structures of six metals, including Cu(II) and Eu(III), with the chloride and nitrate forms of TDP. They found that the complexing agent interacted via the deprotonated phenol group only, thus multidentate bonding was not observed. Bidentate bonding has, however, been observed for the aminophenolato complexing agent shown in Figure 4-29 with Cu(II) and Zn(II) (Connac et al. 1997). With Cu(II), two ligands coordinated with the Cu(II) centre in a square planar arrangement and coordinated by the phenol and a neighbouring amino group.

Trimethylhexane-1,6-diamine could form bidentate complexes with Ni(II), but the large 9-membered chelate rings involved suggest that monodentate bonding is more likely (Blackman 2005).

As shown in Table 2-4, succinate and glutarate are bidentate complexing agents that form 7- and 8-membered chelate rings, respectively.
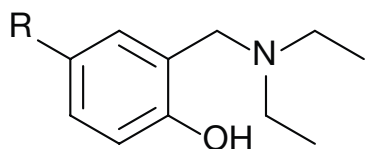
Figure 4-29. *Aminophenolato complexing agents, where R = H or CH₃.*

4.6.6 Presence in SFR

Zinc rust paints have been used on the outside of many steel waste packages in SFR. They have also been used to paint some components of the scrap metal in the waste.

4.6.7 Occurrence in future waste

Anti-corrosion paints are expected to be used on waste packages in the future.

4.6.8 Form following the resaturation of SFR

Anti-corrosion paints will be present as solid phases. The degradation products are assumed to be in the dissolved phase.

4.6.9 Literature review of effect on radionuclide speciation and sorption

A log stability constant of 14 is given for the 1:1 complex of Ni(II) with TETA (trien) at 20 °C and $I = 0.1$ M (Tanaka and Tabata 2009). Trimethylhexane-1,6-diamine would be expected to have a similar stability constant with Ni(II) as HMDA, which can be estimated to be similar to that of NH_3 (Section 4.5.10).

Hedström (2020) identified using simplified quantum chemical calculations that the free energy of Ni(II) complexation by tridentate TDP is associated with approximately half the free energy of complexation by TETA. The free energy of complexation is negatively proportional to the log stability constant (Gibbs free energy isotherm equation), thus the log stability is proportional to the energy released during complexation. Therefore, the log stability constant for Ni(II)-TETA of 14 was used to estimate a log stability constant of ~ 7 for the Ni(II)-TDP complex.

According to spectroscopic data, metal-TDP involves mondentate bonding via the phenol group (Romashkina et al. 2011), which would suggest a much weaker interaction. Based on the observations of Connac et al. (1997), bidentate 1:2 Ni(II)-TDP complexes could form with complexation via one amine group and the phenol group on each molecule. There is therefore a great deal of uncertainty in the denticity of TDP and the strength of metal-TDP complexes.

4.6.10 PhreeqC calculations

PhreeqC calculations here are intended to complement those presented earlier in this report. Section 4.2.10 identified that oxalate, and therefore glutarate and succinate, will not control radionuclide speciation at pH 12.5, due to preferential formation of hydroxide complexes. Section 4.5.10 showed that Ni(II)-en complexes dominated Ni(II) speciation at pH 12.5 from an en concentration of $\sim 10^{-4}$ M. HMDA was predicted to have a much weaker effect. Here, the effect of TETA and TDP are investigated.

The effect of Ca^{2+} on the formation of Ni(II) complexes with amines is, as before, assumed to be negligible since Ca^{2+} has a negligible interaction with amines.

Ni(II) complexes with TETA

The $NiTETA^{2+}$ complex with a log stability constant of 14 (20 °C and $I = 0.1$ M) was used together with the Thermochimie database in PhreeqC calculations. The uncertainty associated with using this value without correction to standard conditions is judged to be acceptable for the purpose of this report. The effect of ionic strength on the $NiTETA^{2+}$ stability constant is expected to be limited, as seen for Ni-ethylenediamine complexes (Section 4.5.10). The first calculations involved the titration of low concentrations of TETA into a solution representative of the experimental conditions of Bruno et al. (2018), containing 2.8×10^{-10} M Ni(II). Figure 4-30 suggests that $NiTETA^{2+}$ forms as the dominant Ni(II) species from a TETA concentration of around 3×10^{-7} M. If the Ni(II) hydroxide chemistry proposed by Bruno et al. (2018) was applied, this would reduce this concentration further.
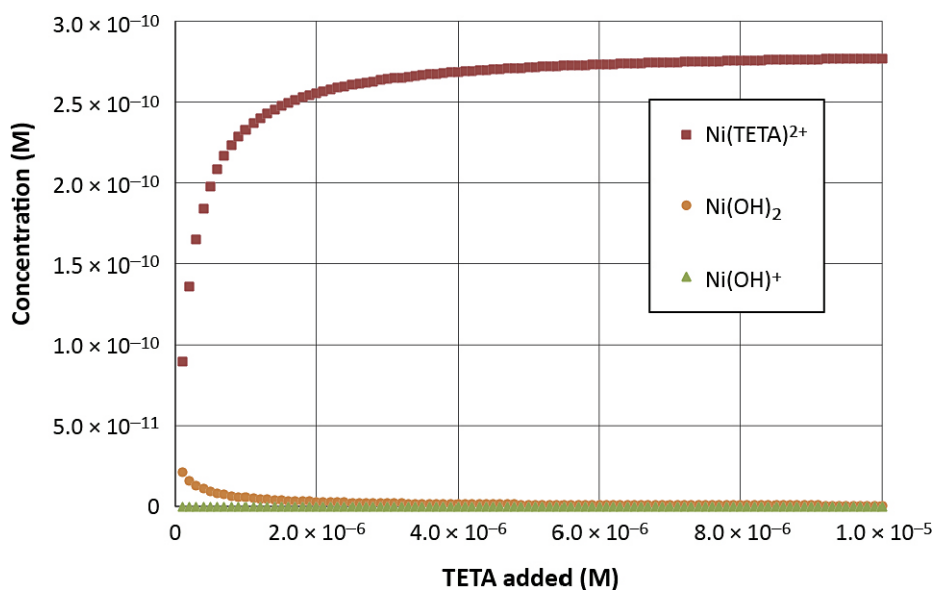
***Figure 4-30.** PhreeqC calculation to examine the speciation of Ni(II) in the presence of TETA into a solution representative of the experimental conditions of Bruno et al. (2018), containing 2.8×10^{-10} M Ni(II). The thermodynamic data in Thermochimie were used and a log stability constant of 14 was assigned to NiTETA^{2+}. The conditions were: 25 °C, 0.5 M NaCl, in equilibrium with 25 g/L HCP (0.0525 mol Ca(OH)$_2$), calculated pH = 12.6.*

Ni(II) with Tris(dimethylaminomethyl)phenol (TDP)

According to spectroscopic data, metal-TDP complexes involve mondentate bonding via the phenol group. However experiments with a related compound indicate bidentate 1:2 metal(II)-TDP complexes could form with complexation via one amine group and the phenol group on each molecule. As the phenol group is a weaker complexing agent than a carboxylic acid, the bidentate complex would be expected to be less stable than the equivalent glycine complex. The log stability constant for the 1:1 Ni(II)-glycine complex is 5.78 at 25 °C and $I = 0.1$ M (Tanaka and Tabata 2009). Therefore, the log stability constant of 7 estimated from the calculations of Hedström (2020), where tridentate coordination was identified, appears to be conservative.

The influence of TDP was investigated by defining a 1:1 Ni complex with the conservative log stability constant (K_1) of 7. Since this log stability constant is associated with tridentate bonding, a second log stability constant (K_2) of 5.84 was defined for the coordination of a second TDP to the Ni(II) centre. This gives an overall log stability constant for the 1:2 complex of 12.8. The log stability constants follow the trend for Ni(II) with ethylenediamine where the log stability constant for Ni(en)$^{2+}$ is 7.5 (Tanaka and Tabata 2009, Paoletti 1984) and Ni(en)$_2{}^{2+}$ 13.84 (Paoletti 1984), i.e:

$$\log K_2 = \log K_1 - 1.16$$

where K_1 and K_2 are the stability constants for the consecutive reactions with the first and second complexing agent, respectively. The trend for en is judged to be conservative as coordination of a second en confers much more stability than, for example, coordination of a second carboxylate (e.g. Table 2-6). The 1:3 complex was judged irrelevant, since the first stability constant used is associated with tridentate bonding and the complexing agent is bulky.

These stability constants were then used in calculation of a titration TDP into a solution representative of the experimental conditions of Bruno et al. (2018). The Ni(II) hydroxide chemistry in Thermochimie was applied. The results in Figure 4-31 suggest that, if the 1:1 complex is the only species that forms, only ~4 % of Ni(II) would be present as NiTDP^{2+} at a TDP concentration of 0.1 M. However, if the 1:2 complex forms, NTDP$_2{}^{2+}$ is predicted to dominate Ni(II) speciation under these conditions from a TDP concentration of 5×10^{-4} M. The Ni(II) hydroxide chemistry proposed by Bruno et al. (2018) would result in TDP dominating Ni(II) speciation at lower concentrations, but the uncertainties associated with this case are sufficiently high that this was not calculated here.
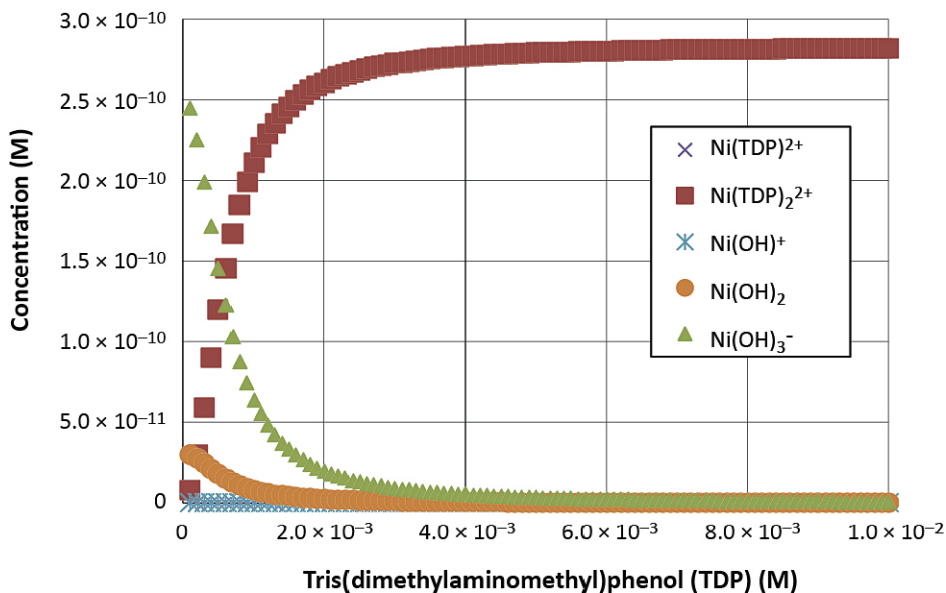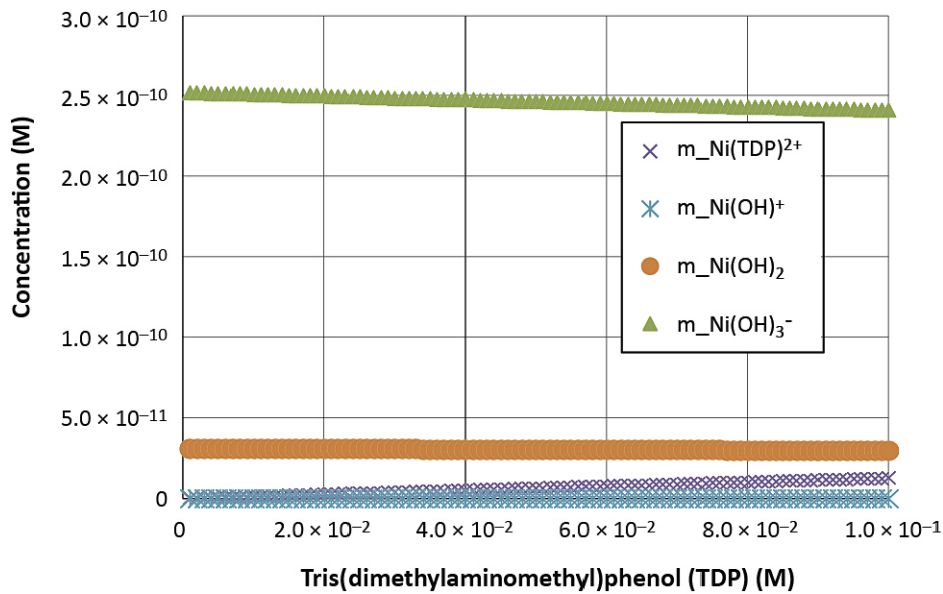
Figure 4-31. *PhreeqC calculation to examine the speciation of Ni(II) in the presence of tris(dimethylaminomethyl)phenol (TDP) under the experimental conditions of Bruno et al. (2018), (a) including a single Ni(II) species (NiTDP^{2+}) and (b) also including the bis complex NiTDP$_2$$^{2+}$. The Ni-hydroxide thermodynamic data in Thermochimie was used. 25 °C, 0.1 M NaCl, in equilibrium with 25 g/L HCP (0.0525 mol Ca(OH)$_2$), calculated pH = 12.6.*

4.6.11 Recommendations for WAC 4.0

TETA

TETA that reacts as a curing agent to form tertiary amines with epoxy groups is not expected to be released, as tertiary amines are very resistant to alkaline hydrolysis. However, TETA present in the mixed ingredient containing fatty acids will be present as amides and therefore vulnerable to alkaline hydrolysis. The PhreeqC calculations indicate that TETA will control Ni(II) speciation from very low TETA concentrations.

Hedström (2020) applied a concentration limit of 10^{-5} M TETA arising from the mixed fatty acid ingredient in the void or pore space around the waste packages in each defined part of SFR. None of the products that contain (or may contain) TETA in this fraction were judged to be acceptable for disposal, as they exceeded this limit. One product (Teknozinc 90 SE A) contained TETA as a single ingredient only. This TETA curing agent is expected to react with epoxy and form an unreactive tertiary amine. No concentration limit was applied to TETA curing agents and Teknozinc 90 SE A was judged to be acceptable for use.

The data in the current report suggest that the 10^{-5} M limit is too high for TETA arising from the mixed fatty acid ingredient. It is therefore recommended that products containing TETA in the mixed fatty acid ingredient are forbidden in SFR.

The very low concentration calculated for TETA complexes to dominate Ni(II) speciation also raises questions over whether products containing free TETA as a curing agent should be allowed. The information from Wu et al. (2005) suggests that all TETA molecules will react to form at least one tertiary amine with the epoxy. The ratio of the reagents is expected to be optimised for full reaction of all amine groups. The faster reaction of primary amines with epoxy encourages the reaction of all TETA molecules with epoxy. There are only two primary amines in the TETA molecule, while four secondary amines are available for reaction. The secondary amines comprise the two secondary amines initially present in TETA and the two secondary amines created by the reaction of the primary amines. Therefore, reactions between epoxy and at least some of the secondary amines in each TETA molecule can be expected. It is judged to be unlikely that > 1 % of the TETA will fail to form at least one tertiary amine group by reacting with epoxy. It is therefore reasonable to apply a concentration limit of 10^{-5} M TETA, calculated assuming that all TETA in the free curing agent is released into the void or pore volume surrounding the waste package. In reality, the dissolved concentration would be much lower than calculated because the TETA will be mainly present as tertiary amines.

Tris(dimethylaminomethyl)phenol (TDP)

Hedström (2020) assigned a concentration limit of 10^{-3} M TDP in the pore or void volume surrounding each waste package in SFR. Hedström (2020) found that the products investigated that contain TDP resulted in maximum concentrations in the pore or void volume of $< 5 \times 10^{-4}$ M, when used according to their product information sheets.

The evidence available for judging the stability of the Ni(II) species that form with TDP does not produce a consistent picture. To be reasonably conservative while not introducing any practical difficulty in using anti-corrosion paints, the current limit can be maintained.

Trimethylhexane-1,6-diamine

Products that contain trimethylhexane-1,6-diamine as a curing agent are of limited concern because it is expected to react with epoxy. Even if trimethylhexane-1,6-diamine were to be present in the fatty acid fraction of a product, it is unlikely to affect radionuclide sorption as its solubility in water (6 mM) is lower than the concentration at which it may affect Ni(II) sorption (0.1 M based on HMDA, see Section 4.5.11).

General comments

Any new products that contain polyamines should be assessed using the procedure in Hedström (2020) and the background information in this report as a starting point. Any new information that becomes available should also be considered.

4.7 Filter aids

4.7.1 Origin

Filter aids are used to reduce the clogging of filters and thus improve filtration. They are finely divided solid materials and the most common products are based on inorganic perlite and diatomaceous earth. However, organic filter aids based on polyacrylonitrile (PAN) fibres with a chemical formula of $[C_3H_3N]_n$ are also used at Forsmark and Oskarshamn nuclear power plants and Clab. UP2 and UP2W are examples of this type of product.

4.7.2 Structure

Polyacrylonitrile consists of a carbon polymer chain with nitrile (CN) functional groups (Figure 4-32).

4.7.3 Degradation characteristics and reactions

PAN undergoes alkaline degradation, with the nitrile groups slowly hydrolysed to amides and carboxylic acids (e.g. Litmanovich and Platé 2000). This reaction is shown in Figure 4-33. Amides may go on to hydrolyse to an amine and carboxylate.

Depolymerisation or other reactions generating low molecular units also take place, for example Duro et al. (2012) found that soluble UP2 degradation products were a mixture of carboxylic acids, amides, alkenes and ketones. However, only a limited proportion of the degradation products were characterized in the study (8 and 28 % at pH 12.5 and 13.4, respectively).

The rate of alkaline UP2 degradation has been investigated (Dario et al. 2004, Duro et al. 2012, Holgersson et al. 2011). Duro et al. (2012) showed that temperature and pH have a very clear influence on the rate of degradation and the lowest rates of degradation were found at pH 12.5 compared to pH 13.4, and room temperature compared to 60 °C. The initial increase in the DOC concentration due to degradation was most rapid, and this was followed by a slower rate of degradation. The rate of UP2 degradation (25 g/L) at pH 12.5 and room temperature was very slow by about 300 days and the DOC concentration reached about 8 mg/L by 694 days. At pH 13.4 and room temperature, the DOC concentration was about 30 mg/L by 694 days. The study by Holgersson et al. (2011) determined higher DOC concentrations over time with a similar UP2 concentration (24 g/L) and the DOC concentration reached ~45 mg/L at pH 12.5 and ~150 mg/L at pH 13.4 after about 3.3 years. The experimental data were however too few to determine how the rate changes over time and whether degradation had reached a plateau.

Tasdigh (2015) also found that the degradation rate of UP2 was faster at higher pH. Over 6 months and at 32 °C, the TOC concentration in solution reached 900 mg/L at pH 12.5 and 5 100 mg/L at pH 13.5. It is noted that acetate filters were used in the study, potentially contributing to the measured organic content.
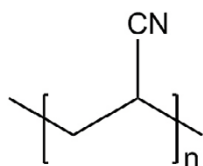
Figure 4-32. *Chemical structure of polyacrylonitrile.*
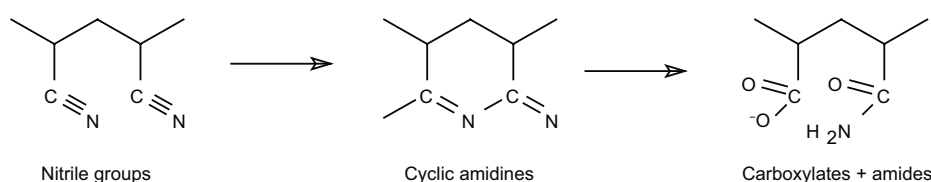
Figure 4-33. *Degradation sequence proposed by Litmanovich and Platé (2000). Reproduced from Duro et al. (2012).*

4.7.4 Solubility

PAN filter aids are solid but degradation products are expected to be soluble.

4.7.5 Coordination and denticity

The degradation products need to be characterised in more detail before this is possible to state with any confidence.

4.7.6 Presence in SFR

PAN filter aids disposed of in F.17 type waste packages will be conditioned in bitumen and disposed of in 1–2BMA. Those used at Oskarshamn are dewatered and disposed of in concrete tanks (waste type O.07, deposited in 1–2BTF), while those used at Clab are cement-solidified in concrete moulds (waste type C.02, deposited in the Silo).

4.7.7 Occurrence in future waste

PAN filter aids are expected to be present in future wastes since they are an integral part of the filtration systems at Forsmark, Oskarshamn and Clab.

4.7.8 Form following the resaturation of SFR

The filter aids will be present as solid polymers but the smaller degradation products are expected to be dissolved in the pore water of the waste packages.

4.7.9 Literature review of effect on radionuclide speciation and sorption

Dario et al. (2004) investigated the effect of UP2 degradation products on the sorption of ^{152}Eu to cement. The data presented in Dario et al. were also presented in Duro et al. (2012), together with the results of additional experiments. The experiments used an initial UP2 fibre concentration of 25 g L^{-1}, which is broadly similar to the concentration expected in 1–2BTF. The degradation products obtained at pH 12.5 (buffered by Ca(OH)$_2$) and room temperature did not affect Eu sorption significantly. The maximum degradation product concentration in this experiment (approximately 8 mg L^{-1} DOC) was equal to the maximum concentration obtained in the associated degradation experiments, when the on-going rate of degradation was very slow. However, a similar concentration of degradation products obtained at pH 13.4 reduced Eu(III) sorption significantly.

Tasdigh (2015) investigated the influence of UP2 degradation products from degradation experiments at pH 12.5 and 32 °C on the solubility of Eu(III) and Ni(II), and found that they had a greater influence on Eu(III).

4.7.10 PhreeqC calculations

The exact chemical structure of PAN degradation products was not known at the time of writing, thus speciation calculations were not performed.

4.7.11 Recommendations for WAC 4.0

Disposal of UP2 in bitumen conditioning appears to be advantageous since the influx of cement leachate will be delayed, reducing the likelihood of PAN filter aid degrading at pH 13. This may therefore decrease both UP2 degradation (Section 2.2.3) and the complexing power of the degradation products (Section 4.7.9). This is the case for F.17 waste packages that are disposed of in 1–2BMA. However, the greatest concentrations of UP2 are in 1–2BTF, and this waste (O.07) is dewatered and disposed of in concrete tanks. PAN filter aids are also potentially of significant concern in the Silo.

The evidence available suggests that the disposal of PAN type filter aids in SFR should be limited by WAC. However, experiments are currently being carried out to allow the risks and WAC to be assessed with confidence (Section 7.2.1 in SKB 2019b). The results are expected to be available within two years of this report and only then can reliable WAC be established for PAN. The number of waste packages containing PAN that may be disposed of in the next two years is significantly lower than the number already disposed of in the relevant vaults. Nevertheless, disposal of these would entail a risk for increased complexing-agent concentrations and possibly reduced sorption.

4.8 Tributyl phosphate

4.8.1 Origin

Tributyl phosphate (TBP) is an important complexing agent in the PUREX solvent extraction processs, used in nuclear fuel manufacture and reprocessing. In the PUREX process, TBP extracts UO_2^{2+} from a 6–7 M nitric acid aqueous phase into a kerosene organic phase through the formation of $U(NO_3)_2 \cdot 2TBP$.

4.8.2 Structure

The structure of TBP is shown in Figure 4-34.

4.8.3 Degradation characteristics and reactions

As TBP has three ester groups, it is prone to hydrolysis. Hydrolysis occurs as a stepwise process and, under acidic conditions, the first step is more rapid than the second or third (Burger 1958) However, the reaction stops at dibutyl phosphate (DBP) under alkaline conditions (Burger 1958), Therefore the expected degradation products in SFR would be DBP and butyl alcohol.

4.8.4 Solubility

The solubility of TBP in water is about 0.4 g/L at 25 °C (Velavendan et al. 2013), which is equivalent to ~1 mM. The solubility of DBP is higher, 18 g/L[6].

4.8.5 Coordination and denticity

TBP and DBP coordinate via a lone pair on the double bonded oxygen (Gopakumar et al. 2016), thus are monodentate complexing agents. The complexation number with U(VI) is low because of the oxygen atoms present in the uranyl oxycation (UO_2^{2+}) and because TBP is a bulky monodentate complexing agent. $UO_2(NO_3)_2 \cdot 2TBP$ is often described as an adduct rather than a complex, hence the notation with a middle dot. This indicates a relatively weak interaction between $UO_2(NO_3)_2$ and the TBP molecules.
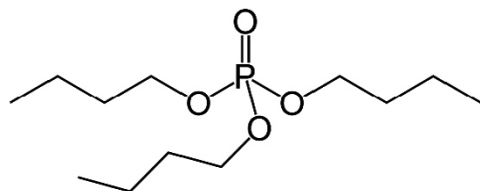
Figure 4-34. *The chemical structure of TBP.*

---

[6] https://pubchem.ncbi.nlm.nih.gov/compound/7881#section=Physical-Description

4.8.6 Presence in SFR

TBP is not present in existing SFR wastes.

4.8.7 Occurrence in future waste

TBP is not expected to be present in future wastes.

4.8.8 Form following the resaturation of SFR

A small amount of TBP would dissolve in the aqueous phase, to a maximum of 1 mM TBP (see Section 4.8.3). If sufficient TBP were present, it could form an NAPL.

4.8.9 Literature review of effect on radionuclide speciation and sorption

Allard et al. (1984) included TBP in experiments investigating the sorption of Cs(I), Sr(II), Th(IV), U(VI), Np(V), Pu(unknown oxidation state) and Am(III) to a range of concretes over time. Different porewater compositions were also used, but these had little impact on the results. The type of concrete also had little impact on the results. TBP was added to a series of experiments with one concrete-porewater combination, at 2 % of the weight of the concrete. It did not affect sorption of any of the radionuclides beyond the experimental uncertainties over the ~100 day equilibrium period.

4.8.10 PhreeqC calculations

Not judged necessary.

4.8.11 Recommendations for WAC 4.0

Based on the results of Allard et al. (1984), the low solubility of TBP in water and the overview of complexation chemistry in Section 2.1, there is no reason to believe that dissolved TBP will affect radionuclide sorption.

The suitability of TBP disposal in SFR should however be evaluated with respect to the formation of a NAPL in the repository.

4.9 Bitumen

4.9.1 Origin

Bitumen is present in SFR as a waste stabilisation matrix for ion exchange resins.

4.9.2 Structure

Bitumen is a mixture of high molecular weight aliphatic and aromatic hydrocarbons, and contains nitrogen, oxygen and sulfur (Allard and Persson 1985).

4.9.3 Degradation characteristics and reactions

The Waste process report for SR-PSU (Section 3.1.3 in SKB 2014) provided a literature review of the degradation of bitumen. Oxalate has been identified as the main degradation product formed during the irradiation of bituminised waste under aerobic conditions, with smaller amounts of formate and (bi) carbonate (Valcke et al. 1999, Kagawa et al. 2000). A review of experimental results concluded that radiolysis-induced gas generation, swelling, hardening and heating were negligible for absorbed doses of less than 0.1 MGy, although the leach resistance decreased (Eschrich 1980). The type of radiation (α, β, γ) was not found to affect the rate of radiolytic gas generation significantly (Eschrich 1980).

Kagawa et al. (2000) examined the chemical and radiolytic (gamma, Co-60 source) degradation of pure bitumen and concluded that oxidation is the dominant chemical degradation pathway for bitumen under circumneutral and alkaline pH conditions. Oxidation led to the formation of leachable organic degradation products that were identified to be mainly acetate and formate. Reducing conditions were found to limit chemical degradation. Radiolytic degradation, which was examined in distilled water rather than at high pH, was minor in comparison to this. The experiments applied a dose rate of ~10.6 kGy/h to total absorbed doses of l and 10 MGy. Valcke et al. (2009) also found that the effect of radiolysis is highly dependent on access to oxygen.

Under the highly alkaline, anoxic environment characteristic of the SFR repository, and at the absorbed doses expected in SFR (< 0.1 MGy), bitumen is generally considered to be chemically stable (Petterson and Elert 2001).

The main degradation products from oxic degradation of bitumen is oxalate (Valcke et al. 1999). Radiolytic degradation of bitumen under high pH conditions has been shown to produce primarily mono- and dicarboxylic acids and carbonates (Van Loon and Kopajtic 1991).

It is less clear what the degradation products are under alkaline, anoxic conditions may be, but they are not expected in any significant concentrations.

4.9.4 Solubility

Bitumen consists of hydrophobic hydrocarbons with very low solubility in water but small organic degradation products are soluble. The solubility of oxalate is limited by the formation of CaOx(s).

4.9.5 Coordination and denticity

No complexing agents of relevance are expected from bitumen.

4.9.6 Presence in SFR

Bitumen is present within the waste packages, as part of the waste form.

4.9.7 Occurrence in future waste

Continued use of bitumen is expected, based on the current waste descriptions.

4.9.8 Form following the resaturation of SFR

Bitumen is a liquid but, at room temperature and below, its viscosity is one of the highest of any substance. It will therefore behave as a solid in SFR for all practical purposes.

4.9.9 Literature review of effect on radionuclide speciation and sorption

As bitumen is expected to be stable under SFR conditions, degradation products are not expected in significant concentrations. Oxalate is discussed in Section 4.2 and calcium oxalate will precipitate at low oxalate concentrations in SFR. Furthermore, the products of α- or γ-induced radiolytic degradation of bitumen were not found to influence plutonium solubility under conditions representative of a cement backfilled repository (Greenfield et al. 1997, JAEA 2007).

4.9.10 PhreeqC calculations

N/A.

4.9.11 Recommendations for WAC 4.0

Based on the literature study and the limited solubility of oxalate, there is no need to limit the use of bitumen in SFR waste packages from the perspective of radionuclide sorption.

4.10 Lignin

4.10.1 Origin

Lignin is a structural material in wood and is present in SFR due to the disposal of wooden furniture and equipment that has been used on the active side of the nuclear facilities.

4.10.2 Structure

Lignin is a class of complex heterogeneous cross-linked phenolic polymers. An example structure is shown in Figure 4-35.

4.10.3 Solubility

Lignin is a solid material with a very low solubility.

4.10.4 Degradation characteristics and reactions

As reviewed by Klapiszewski et al. (2017), the alkaline degradation of lignin has been studied as a means of understanding its structure in experiments carried out under optimised laboratory conditions. The functional groups of the degradation products of lignin in general, and of the alkaline degradation products of lignin specifically, include phenols, alcohols, ketones and ethers (Klapiszewski et al. 2017).

Degradation under oxic conditions involves reactions that lead to the formation of degradation products with carboxylic acid groups (e.g. Baraniak et al. 1997), but this is not relevant for SFR.
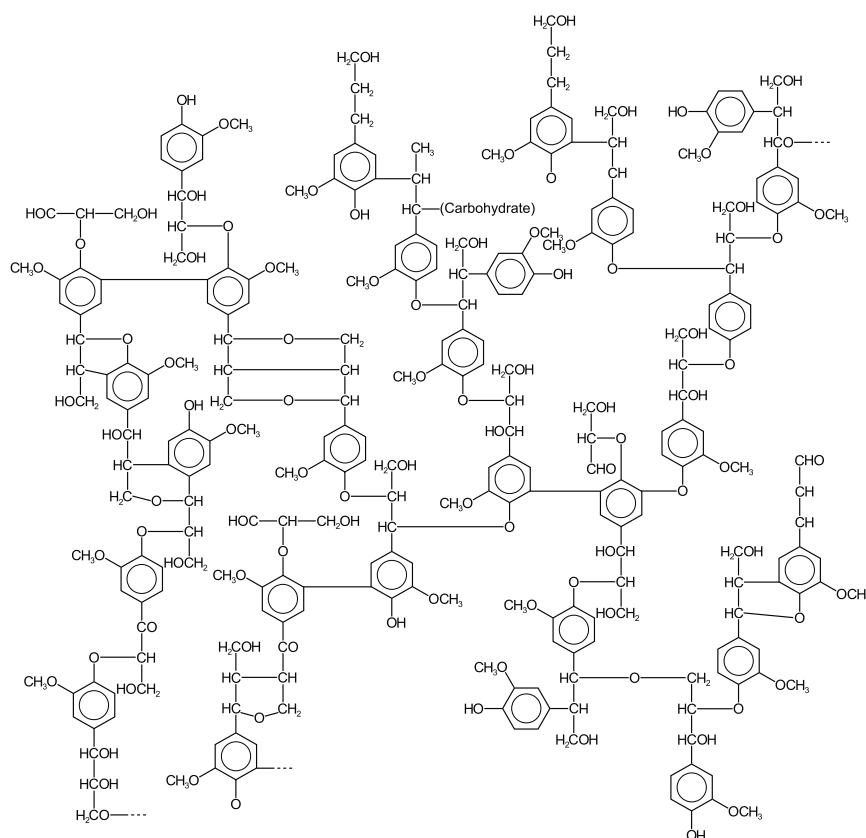
Figure 4-35. Example structure of lignin. Reproduced with permission from Głąb (2007) under Creative Commons Attribution-ShareAlike 3.0 Unported License (https://creativecommons.org/licenses/by-sa/3.0/deed.en).

4.10.5 Coordination and denticity

Degradation products of lignin contain groups that are not associated with a strong complex formation.

4.10.6 Presence in SFR

Wood is deposited in SFR within waste packages.

4.10.7 Occurrence in future waste

Wood will continue to be disposed of in SFR, for example the containers used for waste types R.12 and O.12/O.12:1 can contain a plywood floor construction (SKB 2019a). However, these waste types are disposed of in BLA vaults, which are not credited with the safety function *Good retention*.

4.10.8 Form following the resaturation of SFR

Lignin will be present as a solid polymer although soluble degradation products will slowly be released.

4.10.9 Literature review of effect on radionuclide speciation and sorption

There is no literature available relating to the effect of lignin degradation products on radionuclide sorption.

4.10.10 PhreeqC calculations

Not judged necessary.

4.10.11 Recommendations for WAC 4.0

Based on the stability of lignin under alkaline conditions and the type and diversity of degradation products expected, there is no need to limit the disposal of wood from the perspective of radionuclide sorption. Wood contains cellulose as well as lignin, and the limits applied to the cellulose will indirectly limit the amount of lignin disposed of.

5 Discussion and conclusions

5.1 Summary of the recommended concentration limits

Table 5-1 summarises the concentration limits derived in this report for complexing agents and organic materials in wastes destined for the Silo, 1BMA, and 1–2BTF. The limits are equally relevant for 2BMA, although WAC 4.0 will not apply to 2BMA. The table also shows when the maximum mass of a chemical or material allowed per waste package has been calculated and is presented in Appendix. The limit for TETA in the curing agent of anti-corrosion paint has not been converted into a maximum amount in this report. This concentration must be calculated using the methodology of Hedström (2020) for the different parts of the repository, since the paint is used on the exterior surface of waste packages. This is outside the scope of this report.

No current waste type contains both gluconate and cellulose. Therefore, competition between gluconate and ISA for hydrated cement sorption sites is not of immediate concern. Sorption of gluconate is stronger than sorption of ISA (Glaus et al. 2006, Van Loon and Glaus 1998). Therefore, if a future waste type were to contain gluconate and cellulose, sorption of ISA may be reduced. The effect is expected to be small given the low dissolved concentration limits applied. If both gluconate and ISA were present at their maximum concentrations, calculated by their individual sorption isotherms, the reduced number of sorption sites for ISA would increase the dissolved ISA concentration to $< 2 \times 10^{-4}$ M.

Table 5-1. Summary of the concentration limits recommended in this report.

Type of material/ substance	Name	Origin	Handling in report	Calculation performed?
Cellulose		Waste material	Limit of 10^{-4} M ISA. Cellulose degradation (80 % ISA yield) after 5 000 years (99 % degraded) and sorption accounted for	Yes
Complexing agents	DTPA	May be used at nuclear facilities	Forbidden	No
	Gluconate and other α-hydroxycarboxylates with multiple OH groups	Used at nuclear facilities	10^{-5} M limit once sorption has been accounted for	Yes
	EDTA and other hexadentate aminocarboxylates	Used at nuclear facilities	10^{-4} M limit	Yes
	Iminodisuccinate and other pentadentate aminocarboxylates	Used at nuclear facilities	10^{-3} M limit	Yes
	NTA, MGDA and other tetradentate aminocarboxylates	Used at nuclear facilities	10^{-3} M limit	Yes
	Capryliminodipropionate (CIDP) and other tridentate aminodicarboxylates	Used at nuclear facilities	10^{-2} M limit	Yes
	Capryloamphodipropionate (CADP) and other tridentate carboxylate diamines	Used at nuclear facilities	10^{-4} M limit	Yes
	Glutamate and other bidenate amino acids	Used at nuclear facilities	10^{-2} M limit	Yes
	Other complexing agents	Used at nuclear facilities	1 % of the moles of $Ca(OH)_2$ in HCP	Yes
Superplasticisers	PMS	May be used in waste stabilisation	Based on PNS in Hedström (2019a)	No
	PNS	Used in waste stabilisation	See Hedström (2019a)	No
	PCE	Used in waste stabilisation	Below or within the range suggested by the manufacturer	No

Type of material/ substance	Name	Origin	Handling in report	Calculation performed?
Superplasticisers	Polyvinylmaleinic acid	Used in waste stabilisation	Below or within the range suggested by the manufacturer	No
Plasticisers	Phthalate esters	PVC and rubber	No limit	No
Plastics and rubber	PET polyester	Waste	No limit	No
	Aliphatic polyesters	Waste	No limit	No
	Polyamides	Waste	Diamine limit 10^{-1} M. Assume that 1 kg degrades to 4.4 moles diamine	Yes
	Addition polymers	Waste	No limit	No
Filter aids (PAN)		Waste	No limit now due to lack of information. A limit may be applied in the future	No
Anti-corrosion paint	Containing TETA in the mixed fatty acid ingredient	Waste packages	Forbidden	No
	Containing TETA as a curing agent	Waste packages	10^{-5} M*	Yes, but not within this report
	Containing TDP	Outside of waste packages	10^{-3} M	No, no change from Hedström (2020)
TBP		None	Needs to be evaluated for risk for NAPL	No
Bitumen		Waste conditioning	No limit	No
Lignin		Waste	No limit	No

* This concentration reflects dissolution of all TETA in the curing agent. In reality, < 1 % of the TETA in this fraction is expected to be released. Therefore, the maximum dissolved concentration expected with this limit would be < 10^{-7} M.

In addition to the concentration limits based on radionuclide sorption reduction, a general limit for complexing agents of 1 % of the moles of $Ca(OH)_2$ in HCP is recommended. This is intended to limit the potential impact on cement degradation. In order to limit the number of organic molecules that are included in this, the cement-degrading complexing agents are assumed to comprise:

- Hard complexing agents (i.e. not amines or other soft complexing agents).

- At least the stability of the 1:1 Ca-malonate complex ($\log K = 2.4$). This excludes dicarboxylates produced during Nylon and polyester degradation).

Appendix shows the results of this calculation for oxalate, citrate and CIDP. CIDP was included to compare the mass limits based on radionuclide sorption reduction and cement degradation. It was selected because the CIDP concentration limit based on radionuclide sorption reduction is relatively high. Even in this case, the mass limit based on radionuclide sorption reduction is more restrictive. This gives confidence that the mass limits based on cement degradation only limit the disposal of unreasonably high concentrations of complexing agents.

In Section 2.4, the effect of the alkaline hydrolysis of organic materials on cement integrity was also discussed. The implementation of a limit based on consumption of OH^- through alkaline degradation reactions is outside the scope of this report. It is, however, recommended that SKB considers this further.

5.2　Effect of several complexing agents within a waste package

It is possible that a waste package contains the maximum allowed mass of several different complexing agents. Some combinations of complexing agents and organic materials do not affect an individual radionuclide. For example, the limit for ISA is based on tetravalent actinides while amines do not affect tetravalent actinides at all (Table 5-2). However, the presence of gluconate and ISA, for example, would both affect tetravalent actinides to the greatest extent. More notably, many complexing agents affect Ni(II) speciation to the largest extent.

Table 5-2. Radionuclides influenced by complexing agents with a recommended concentration limit.

Type of material/substance	Complexing agent	Concentration limit [M]	Limit based on
Cellulose	ISA	10^{-4}	Th(IV)
Complexing agents used at nuclear facilities	Gluconate and other α-hydroxycarboxylates with multiple OH groups	10^{-5}	Th(IV)
	EDTA and other hexadentate aminocarboxylates	10^{-4}	Ni(II)
	Iminodisuccinate and other pentadentate aminocarboxylates	10^{-4}	Ni(II)
	NTA, MGDA and other tetradentate aminocarboxylates	10^{-3}	Ni(II)
	Capryliminodipropionate (CIDP) and other tridentate aminocarboxylates	10^{-2}	Ni(II)
Plastics and rubber	Polyamides	10^{-1}	Ni(II)
Anti-corrosion paint	TETA (in the curing agent)	10^{-5} *	Ni(II)
	TDP	10^{-3}	Ni(II)

* This concentration reflects dissolution of all TETA in the curing agent. In reality, < 1 % of the TETA in this fraction is expected to be released. Therefore, the maximum dissolved concentration expected with this limit would be < 10^{-7} M.

PhreeqC calculations were carried out to demonstrate the combined effect of several complexing agents present at the concentration limit suggested in this report. The solution phase used in the calculations contained 10^{-8} M Ni(II) ($[NaCl_{init.}]$ = 0.1 M) in equilibrium with a representative concentration of portlandite for SFR, together with 10^{-3} M NTA, 10^{-4} M EDTA or 10^{-1} M "Amm" as a representation of HMDA, and then all three complexing agents. The results show the nearly additive effect of complexing agents on the percentage of Ni(II) present as an organic complex (Table 5-3). However, the individual concentration limits are conservative so that the total percentage of Ni(II) present as an organic complex remains very low, and below a level expected to affect sorption measurably.

As the combined effect remains low, the recommended limits can be applied without modification even when several complexing agents are present in a single waste package. This is supported by the fact that the uncertainties associated with many of the predicted effects of the complexing agents are often quite large. The combined effect of several complexing agents may well fall within the uncertainty of the effect of one complexing agent. Furthermore, although several complexing agents are often found in waste packages, it is fairly unlikely that they would all be present at their concentration limit.

Table 5-3. Demonstration of the combined effect of NTA, EDTA and "Amm" as a representation of hexmethylenediamine, at their recommended concentration limits on the speciation of Ni(II) (10^{-8} M).

	Ni-NTA complexes [M]	Ni-EDTA complexes [M]	Ni-Amm complexes [M]	% Ni(II) as an organic complex
10^{-3} M NTA only	4.33×10^{-11}			0.43
10^{-4} M EDTA only		6.88×10^{-11}		0.69
10^{-1} M Amm only			5.60×10^{-12}	0.056
10^{-3} M NTA, 10^{-4} M EDTA and 10^{-1} M Amm	4.30×10^{-11}	6.81×10^{-12}	5.43×10^{-12}	1.17

Applying individual concentration limits is also consistent with the selection of sorption reduction factors for the radionuclide transport modelling of the SFR post-closure safety assessment (SKB 2015b). For each group of chemically similar radionuclides, the largest sorption reduction effect from a single complexing agent was applied, based on the concentrations of complexing agents in a defined part of SFR. This was judged to be reasonable because of the uncertainties in the predicted sorption reduction effect. Also, while several complexing agents may be present in a defined part of SFR, one generally has a much greater effect than the others because of being a stronger complexing agent and/or present at a high concentration.

Finally, in the safety assessments for SFR (SR-PSU and SR-PSU(PSAR)), sorption reduction factors were applied to defined parts of SFR, such as 1BMA compartments. In these defined parts of SFR, the concentrations of complexing agents will be lower than in the waste packages due to dilution with water in the void or backfilled volume surrounding the waste packages.

5.3 Specific recommendations for waste packages allocated to SFR vaults

A new waste package that contains an acceptable concentration of complexing agents may in some cases add to an already unacceptable mass of a complexing agent in a defined part of SFR. Therefore, the concentration limits recommended may not be suitable for waste packages allocated to certain parts of SFR. The current estimates of complexing agent concentrations in defined parts of SFR are given in Table 5-4.

The NTA concentration in the Silo, 2BTF and several 1BMA compartments is over or close to the suggested limit of 10^{-3} M. *Therefore, NTA should not be allowed in waste packages allocated to the Silo or 2BTF. Care should be taken to ensure that waste packages allocated to 1BMA that contain NTA are placed in compartments that contain low amounts of NTA.*

The ISA concentration in 1BMA exceeds the concentration limit of 10^{-4} M. *Therefore, cellulose should not be allowed in waste packages allocated to 1BMA.* The recommended cellulose limit is reasonable for waste packages allocated to the other vaults.

Table 5-4. Concentrations [M] of complexing agents in defined parts of SFR (Keith-Roach et al. 2021).

	EDTA	Caprylimino-dipropionate	NTA	Citric acid	Oxalic acid	Gluconate following sorption	ISA following sorption
1BMA Compartment							
1							
2							6.0×10^{-5}
3			1.5×10^{-3}	6.4×10^{-4}	7.7×10^{-5}	8.4×10^{-10}	5.1×10^{-5}
4	3.5×10^{-6}		1.7×10^{-3}			7.0×10^{-10}	1.2×10^{-4}
5			2.7×10^{-4}	1.2×10^{-4}	1.4×10^{-5}	1.6×10^{-10}	2.6×10^{-6}
6	9.5×10^{-6}		2.4×10^{-3}	1.0×10^{-3}	1.2×10^{-4}	1.5×10^{-9}	1.4×10^{-5}
7							7.4×10^{-5}
8	8.1×10^{-7}		3.8×10^{-4}			2.6×10^{-10}	2.5×10^{-4}
9	1.4×10^{-6}		6.4×10^{-4}			3.0×10^{-10}	2.2×10^{-4}
10	6.6×10^{-6}		1.3×10^{-3}	5.6×10^{-4}	6.7×10^{-5}	4.4×10^{-10}	2.4×10^{-4}
11	4.9×10^{-7}		1.7×10^{-4}	1.7×10^{-5}	2.1×10^{-6}	3.0×10^{-10}	4.2×10^{-4}
12	8.0×10^{-7}		1.6×10^{-4}	6.7×10^{-5}	8.1×10^{-6}	4.1×10^{-10}	1.1×10^{-6}
13							
14	1.9×10^{-6}		3.8×10^{-4}	1.6×10^{-4}	2.0×10^{-5}	3.9×10^{-10}	
15	3.8×10^{-7}		7.6×10^{-5}	3.3×10^{-5}	3.9×10^{-6}	8.4×10^{-11}	
Total 1BMA structure	1.5×10^{-6}		5.2×10^{-4}	1.6×10^{-4}	1.9×10^{-5}	3.4×10^{-10}	1.1×10^{-4}
1BMA vault incl. Macadam and shotcrete	6.1×10^{-7}		2.1×10^{-4}	6.5×10^{-5}	7.8×10^{-6}	3.3×10^{-10}	1.0×10^{-4}

	EDTA	Caprylimino-dipropionate	NTA	Citric acid	Oxalic acid	Gluconate following sorption	ISA following sorption
2BMA							
Total 2 BMA structure	1.3×10^{-6}		2.2×10^{-6}			6.4×10^{-13}	1.8×10^{-5}
2BMA vault incl. Macadam and shotcrete	4.4×10^{-7}		7.7×10^{-7}			5.1×10^{-13}	1.4×10^{-5}
Silo							
Silo structure	1.0×10^{-6}		1.1×10^{-3}		1.6×10^{-4}	3.6×10^{-10}	1.7×10^{-5}
Silo vault	5.5×10^{-7}		5.7×10^{-4}		8.6×10^{-5}	3.6×10^{-10}	1.7×10^{-5}
BTF							
1BTF waste block	7.6×10^{-7}	7.4×10^{-5}	1.7×10^{-4}	1.9×10^{-4}			5.7×10^{-7}
1BTF vault	2.7×10^{-7}	2.6×10^{-5}	6.0×10^{-5}	6.6×10^{-5}			5.4×10^{-7}
2BTF waste block	6.1×10^{-6}	2.1×10^{-5}	6.9×10^{-3}	7.0×10^{-3}		9.6×10^{-12}	
2BTF vault	2.2×10^{-6}	7.6×10^{-6}	2.5×10^{-3}	2.5×10^{-3}		9.1×10^{-12}	

The concentrations of EDTA, CIDP and gluconate in all defined parts of SFR are well below their respective recommended limits. The recommended concentration limits can therefore be applied to waste packages allocated to all these vaults.

5.4   Comparison of the recommended limits with WAC 3.0

The concentration limits recommended in this report are compared with those given in WAC 3.0 (Section 1.1) in Table 5-5. The concentration limit for ISA, and therefore mass of cellulose allowed, has not changed. The masses of cellulose allowed in specific waste types are given in Appendix. These limits account for sorption to cement in the packaging material. The limit of 5 g cellulose per kg dry cement in a waste package recommended by Rosdahl (2020) was slightly less restrictive than the limits given here, due to their assumption that the maximum ISA concentration is reached when 85 % of the cellulose has degraded.

The concentration limits recommended for complexing agents used at the nuclear facilities are generally less restrictive than the limits in WAC 3.0. This is the result of the detailed examination of the effect of each complexing agent in this report. High concentrations of hydroxide and Ca^{2+} limit complexation of radionuclides by most carboxylate or aminocarboxylate complexing agents. The effect of citrate and oxalate on radionuclide sorption is judged to be negligible under cementitious conditions and, instead, their effect on cement degradation is taken into account.

The limit recommended for PNS superplasticiser is the same as in Hedström (2019a) and has been extrapolated to apply to PMS superplasticisers. The limit recommended for PCE and PVMA super-plasticisers is less restrictive than the limit given in Hedström (2019b). This is consistent with the con-clusion that di- and tricarboxylates have a negligible effect on radionuclide sorption under cementitious conditions. WAC 4.0 will be the first WAC document that addresses superplasticisers, as they were not included in WAC 3.0.

The potential impact of plastics, rubber and plasticisers has been examined and the conclusions were generally consistent with previous assumptions in the safety analysis (e.g. Keith-Roach et al. 2021). Addition polymers and some condensation polymers are innocuous in the context of radionuclide complexation. They are either stable under alkaline conditions or degrade to smaller organic molecules with a relatively low ability to affect radionuclide sorption. The exception to this is polyamides, as previously identified in Källström (2018). The recommended limit for polyamides is less restrictive than proposed by Källström (2018). WAC 4.0 will be the first WAC document that addresses poly-amides, as they were not included in WAC 3.0.

The impact of PAN-type filter aids on radionuclide sorption is difficult to define at present. SKB-funded experiments are being carried out and the results of these will inform the concentration limits defined in the future. Before that time, disposal of C.02 and O.07 waste packages that contain PAN could increase complexing-agent concentrations in the Silo and 1–2BTF vaults, respectively. F.17 waste packages in 1–2BMA are of less concern as the waste is stabilised in bitumen.

Although the use of anti-corrosion paint was not addressed in WAC 3.0, concentration limits were selected in Hedström (2020) and the acceptability of eight commercial products assessed. Following the review in this report, the recommended concentration limit for TDP has not changed and the four TDP-containing products assessed by Hedström (2020) are still acceptable for use. The review of TETA identified the importance of its interactions with Ni(II). This resulted in a change in the recommendations for TETA containing products. As shown in Table 5-5, it is now recommended that products containing TETA in the mixed fatty acid fraction (i.e. as amides) are forbidden. Products containing free TETA as a curing agent should only be allowed if the release of all TETA into the void or pore volume surrounding the waste package would result in a concentration $< 10^{-5}$ M. This concentration was selected based on the underlying assumption that < 1 % is expected to be released, i.e. the maximum dissolved concentration expected would be $< 10^{-7}$ M. Where appropriate, products that contain TETA as a curing agent need to be re-assessed using this limit. This analysis is out of the scope of this report. WAC 4.0 will be the first WAC document that addresses polyamines and anti-corrosion paints, as they were not included in WAC 3.0.

TBP was forbidden in WAC 3.0 because of its potential effect on radionuclide sorption. The review in this report suggests that TBP will not be an important complexing agent in SFR. However, TBP needs to be evaluated with regard to the risk for NAPL formation.

Lignin and bitumen were judged to be innocuous in SFR in terms of radionuclide sorption and this is consistent with the previous handling in the safety assessments (e.g. Keith-Roach et al. 2021).

Table 5-5. Comparison of the recommended dissolved concentration limits with WAC 3.0[a].

Type of material or substance	Name	Dissolved concentration limit in WAC 3.0	Recommended dissolved concentration limit	Comment on limit
Cellulose		10^{-4} M ISA	10^{-4} M ISA	No change
Complexing agents	DTPA	Forbidden	Forbidden	No change
	Gluconate and other α-hydroxycarboxylates with multiple OH groups	Forbidden	10^{-5} M	Less restrictive
	EDTA and other hexadentate aminocarboxylates	Forbidden	10^{-4} M	Less restrictive
	Iminodisuccinate and other pentadentate aminocarboxylates	Forbidden	10^{-3} M	Less restrictive
	NTA, MGDA and other tetradentate aminocarboxylates	Forbidden	10^{-3} M	Less restrictive
	Capryliminodipropionate (CIDP) and other tridentate aminodicarboxylates	Forbidden	10^{-2} M	Less restrictive
	Capryloamphodipropionate (CADP) and other tridentate carboxylate diamines	Forbidden	10^{-4} M	Less restrictive
	Glutamate and other bidenate amino acids	Unclear	10^{-2} M	Less restrictive
	Citrate	10^{-3} M	1 % of the moles of $Ca(OH)_2$ in HCP	Less restrictive
	Oxalate	10^{-2} M	1 % of the moles of $Ca(OH)_2$ in HCP	Less restrictive

Type of material or substance	Name	Dissolved concentration limit in WAC 3.0	Recommended dissolved concentration limit	Comment on limit
Super-plasticisers	PMS	Not given	Based on PNS in Hedström (2019a)	New
	PNS	Not given	See Hedström (2019a)	No change from Hedström (2019a)
	PCE	Not given	Below or within the range suggested by the manufacturer	Less restrictive than Hedström (2019a)
	Polyvinylmaleinic acid	Not given	Below or within the range suggested by the manufacturer	Less restrictive than Hedström (2019a)
Plasticisers	Phthalate esters	Not given	No limit	No change
Plastics and rubber	PET polyester	Not given	No limit	No change
	Aliphatic polyesters	Not given	No limit	No change
	Polyamides	Not given	Diamine limit 10^{-1} M. Assume that 1 kg degrades to 4.4 moles diamine	Less restrictive than 10^{-2} M given in Källström (2018)
	Addition polymers	Not given	No limit	No change
Filter aids (PAN)		Not given	No limit now due to lack of information. A limit may be applied in the future	No change
Anti-corrosion paint	Containing TETA in the mixed fatty acid ingredient	Not given	Forbidden	No practical change. All products considered exceeded 10^{-5} M limit applied in Hedström (2020)
	Containing TETA as a curing agent	Not given	10^{-5} M[b]	More restrictive than Hedström (2020)
	Containing TDP	Not given	10^{-3} M	No change from Hedström (2020)
TBP		Forbidden	Needs to be evaluated for risk for NAPL	No change
Bitumen		Not given	No limit	No change
Lignin		Not given	No limit	No change

[a] **Lihnell M, Södergren K, 2018.** Acceptanskriterier för avfall i SFR1. SKBdoc 1336074 ver 3.0, Svensk Kärnbränslehantering AB. (In Swedish.) Internal document.

[b] This concentration reflects dissolution of all TETA in the curing agent. In reality, < 1 % of the TETA in this fraction is expected to be released. Therefore, the maximum dissolved concentration expected with this limit would be < 10^{-7} M.

5.5 Limitations of this study

The main limitations of this study are the limited amount of experimental data for the effect of complexing agents and degradation products on Ni(II) sorption. Ni(II) has been identified as a particularly important radionuclide in the context of complexing agents, because it forms less stable hydrolysis products than actinides and because it interacts with both soft and hard complexing agents. The lack of experimental data makes the analysis dependent on stability constant data. Bruno et al. (2018) highlighted uncertainties in the Ni(II) hydroxide chemistry, which is a fundamental part of understanding the impact of complexing agents at high pH.

The effect of ISA and gluconate sorption on the surface properties of cement has not been considered explicitly. For example, certain anionic sorption sites may become saturated and the surface charge can be affected (e.g. Pointeau et al. 2006, Tasi 2018).

The effect of complexing agents in the bentonite of the Silo has not been considered. The pH buffering effect of bentonite can result in conditions that favour complex formation. However, the effect of complexing agents within bentonite is poorly defined and experiments would be required to address this properly.

The influence of iron on complexing agents could be very significant. Since iron chemistry is complex, a specific study would be required to investigate this in detail.

The consumption of OH^- during alkaline degradation of organic materials and resultant influence on the integrity of cement has not been included in the recommended limits.

References

SKB's (Svensk Kärnbränslehantering AB) publications can be found at www.skb.com/publications. SKBdoc documents will be submitted upon request to document@skb.se.

Allard B, Persson G, 1985. Organic complexing agents in low- and medium-level radioactive waste. Nagra NTB 85-19, Nagra, Switzerland.

Allard B, Eliasson L, Höglund S, Andersson K, 1984. Sorption of Cs, I and actinides in concrete systems. SKB/KBS TR 84-15, Svensk Kärnbränslehantering AB.

Allard B, Dario M, Borén H, Torstenfelt B, Puigdomenech I, Johansson C, 2002. Karboxylatjonbytarmassans egenskaper. SKB R-02-40, Svensk Kärnbränslehantering AB. (In Swedish.)

Allscher T, Klüfers P, Mayer P, 2008. Carbohydrate-Metal Complexes: Structural Chemistry of Stable Solution Species. In Fraser-Reid B, Tatsuta K, Thiem J (eds). Glycoscience. Berlin Heidelberg: Springer-Verlag, 1077–1139.

Alonso M M, Puertas F, 2015. Adsorption of PCE and PNS superplasticisers on cubic and orthorhombic C_3A. Effect of sulfate. Construction and Building Materials 78, 324–332.

Altun Y, Köseoğlu F, 2005. Stability of copper(II), nickel(II) and zinc(II) binary and ternary complexes of histidine, histamine and glycine in aqueous solution. Journal of Solution Chemistry 34, 213–231.

American Elements, 2020. Nickel oxalate dihydrate. Available at: https://www.americanelements.com/nickel-ii-oxalate-dihydrate-6018-94-6 [26 November 2020].

Andersson M, Ervanne H, Glaus M A, Holgersson S, Karttunen P, Laine H, Lothenbach B, Puigdomenech I, Schwyn B, Snellman M, Ueda H, Vuorio M, Wieland E, Yamamoto T, 2008. Development of methodology for evaluation of long-term safety aspects of organic cement paste components. Posiva Working Report 2008-28, Posiva Oy, Finland.

Baes C F Jr, Mesmer R E, 1976. The hydrolysis of cations. New York: Wiley.

Baraniak L, Schmidt M, Bernhard G, Nitsche H, 1997. Complex formation of hexavalent uranium with lignin degradation products. In Nietsche H (ed). Annual report 1996: Institute of Radiochemistry. FZR-180, Forschungszentrum Rossendorf, Germany, 28–29.

Baston G M N, Brownsword M, Cowper M M, Manning M C, Pilkington N J, Williams S J, 2002. The influence of gamma irradiation on the alkaline degradation of cellulose and the effects on plutonium solubility. AEA Technology Report AEAT/ERRA-0346, Atomic Energy Authority, UK.

Baston G, Cowper M, Davies P, Dawson J, Farahani B, Heath T, Schofield J, Smith V, Watson S, Wilson J, 2017. The impacts of PVC additives and their degradation products on radionuclide behaviour. Radioactive Waste Management Contractor Report no. AmecFW/0006604/4, Radioactive Waste Management, UK.

Blackman A G, 2005. Overcoming the chelate effect: hypodentate coordination of common multidentate amine ligands. Comptes Rendus Chimie 8, 107–119.

Boult K, McCrohon R, Williams S J, 1998. Further experiments on the effects of Sikament 10 and Sikament N on plutonium solubility. RWMD(97)P95, AEA Technology, UK.

Bradbury M H, Van Loon L R, 1997. Cementitious near-field sorption data bases for performance assessment of a L/ILW repository in a Palfris marl host rock. CEM-94: Update 1, June 1997. PSI Bericht 98-01, Paul Scherrer Institut, Switzerland.

Britannica, 2020. Chelate. Available at: https://www.britannica.com/science/chelate [13 August 2020].

Bruno J, Gonzaléz-Siso M R, Duro L, Gaona X, Altmaier M, 2018. Key master variables affecting the mobility of Ni, Pu, Tc and U in the near field of the SFR repository. Main experimental findings and PA implications of the PhD thesis. SKB TR-18-01, Svensk Kärnbränslehantering AB.

Burger L L, 1958. The chemistry of tributyl phosphate, a review. Report HW-40910, U.S. Atomic Energy Commission, Oak Ridge, Tennessee.

Campos I, Perez D, Colàs E, Duro L, Grivé M, Fuller A J, 2018. Track-changes and track-error document: From version 9b0 to version 10a Thermochimie. Technical Report TCIII-2018-01E, ThermoChimie.

Carbonaro R F, Atalay Y, Di Toro D M, 2011. Linear free energy relationships for metal-ligand complexation: bidentate binding to negatively-charged oxygen donor atoms. Geochimica rt Cosmochimica Acta 75, 2499–2511.

Cartwright A J, May C C, Worsfold P J, Keith-Roach M J, 2007. Characterisation of thorium–ethylenediaminetetraacetic acid and thorium–nitrilotriacetic acid species by electrospray ionisation-mass spectrometry. Analytica Chimica Acta 590, 125–131.

Chang C A, Chen Y H, Chen H Y, Shieh F K , 1998. Capillary electrophoresis, potentiometric and laser excited luminescence studies of lanthanide(III) complexes of 1,7-dicarboxymethyl-1,4,7,10-tetraazacyclododecane (DO2A). Journal of the Chemical Society, Dalton Transactions, 3243–3248.

Choppin G R, 1983. Solution chemistry of the actinides. Radiochimica Acta 32, 43–53.

Colàs A E, 2014. Complexation of Th(IV) and U(VI) by polyhydroxy and polyamino carboxylic acids. PhD thesis. Universitat Politècnica de Catalunya, Spain.

Connac F, Habaddi N, Lucchese Y, Dartiguenave M, Lamande L, Sanchez M, Simard M, Beauchamp A L, 1997. Zinc(II) and copper(II) complexes of monoanionic chelating phenolato ligands containing an amine donor. Crystal and molecular structure of the $(Et_3NH)[ZnCl_2L]$ and CuL_2 compounds with L = 2-[(diethylamino)methyl]-4-methylphenolate. Inorganica Chimica Acta 256, 107–114.

Dario M, Molera M, Allard B, 2004. Effect of organic ligands on the sorption of europium on TiO_2 and cement at high pH. SKB TR-04-04, Svensk Kärnbränslehantering AB.

Dawson J, 2013a. The potential for non-aqueous phase liquid production from irradiated PVC and Vinylesterstyrene (VES). AMEC/PPE-1008/001 Issue 02, AMEC, UK.

Dawson J, 2013b. NAPL generation from the radiolysis of polyethylene and chlorosulphonated polyethylene elastomer (Hypalon®). AMEC/PPE/2834/002, AMEC, UK.

Dawson J, 2013c. The potential for non-aqueous phase liquid production from irradiated neoprene and ion-exchange resin. AMEC/PPE-000283 Issue 01, AMEC, UK.

Dawson J, Magalhaes S, 2012. The potential for non-aqueous phase liquid production in irradiated polymers. Serco report SA/ENV/0997, Serco, UK.

De Windt L, Bertron A, Larreur-Cayol S, Escadeillas G, 2015. Interactions between hydrated cement paste and organic acids: Thermodynamic data and speciation modeling. Cement and Concrete Research 69, 25–36.

Duro L, Grivé M, Gaona X, Bruno J, Andersson T, Borén H, Dario M, Allard B, Hagberg J, Källström K, 2012. Study of the effect of the fibre mass UP2 degradation products on radionuclide mobilisation. SKB R-12-15, Svensk Kärnbränslehantering AB.

ECHA, 2017. Potassium hydrogen phthalate. EC number 212-889-4. European Chemicals Agency. Available at: https://echa.europa.eu/sv/registration-dossier/-/registered-dossier/18786/4/9 [13 August 2020].

ECHA, 2018. 2,2,4(or 2,4,4)-trimethylhexane-1,6-diamine. EC number 247-063-2. European Chemicals Agency. Available at: https://www.echa.europa.eu/fi/web/guest/registration-dossier/-/registered-dossier/21905/4/9 [13 August 2020].

Engkvist I, Albinsson Y, Johansson Engkvist W, 1996. The long-term stability of cement – Leaching tests. SKB TR 96-09, Svensk Kärnbränslehantering AB.

Eschrich H, 1980. Properties and long-term behaviour of bitumen and radioactive waste–bitumen mixtures. SKBF/KBS TR 80-14, Svensk Kärnbränsleförsörjning AB.

Felipe-Sotelo M, Hinchliff J, Field L P, Milodowski A E, Holt J D, Taylor S E, Read D, 2016. The solubility of nickel and its migration through the cementitious backfill of a geological disposal facility for nuclear waste. Journal of Hazardous Materials 314, 211–219.

Filby A, Deissmann G, Wiegers R, 2016. LILW degradation processes and products. OPERA-PU-IBR512, COVRA, Netherlands.

García D, Grivé M, Duro L, Brassinnes S, de Pablo J, 2018. The potential role of the degradation products of cement superplasticisers on the mobility of radionuclides. Applied Geochemistry 98, 1–9.

Gauthier M M, 1995. Engineered materials handbook, Desk edition. Russell Township, OH: ASM International.

Giraudeau C, d'Espinose de Lacaillerie J-B, Souguir Z, Nonat A, Flatt R J, 2009. Surface and intercalation chemistry of polycarboxylate copolymers in cementitious systems. Journal of the American Ceramics Society 92, 2471–2488.

Glaus M A, Van Loon L R, 2008. Degradation of cellulose under alkaline conditions: New insights from a 12 year degradation study. Environmental Science & Technology 42, 2906–2911.

Glaus M A, Van Loon L R, Achatz S, Chodura A, Fischer K, 1999. Degradation of cellulosic materials under the alkaline conditions of a cementitious repository for low and intermediate level radioactive waste. Part I: Identification of degradation products. Analytica Chimica Acta 398, 111–122.

Glaus M A, Laube A, Van Loon L R, 2003. A generic procedure for the assessment of the effect of concrete admixtures on the sorption of radionuclides on cement: Concept and selected results. In Oversby V M, Werme L O (eds). Scientific basis for nuclear waste management XXVII: symposium held in Kalmar, Sweden, 15–19 June 2003. Warrendale, PA: Materials Research Society. (Materials Research Society Symposium Proceedings 807), 101–107.

Glaus M A, Laube A, Van Loon L R, 2006. Solid-liquid distribution of selected concrete admixtures in hardened cement pastes. Waste Management 26, 741–751.

Głąb K, 2007. Molecular structure Lignin. Available at: https://commons.wikimedia.org/wiki/File:Lignin_structure.svg [15 February 2021]

Gopakumar G, Sreenivasulu B, Suresh A, Brahmmananda Rao C V S, Sivaraman N, Joseph M Anoop A, 2016. Complexation behavior of the tri-n-butyl phosphate ligand with Pu(IV) and Zr(IV): A computational study. The Journal of Physical Chemistry A, 4201–4210.

Greenfield B, Spindler M, Woodwark D, 1997. Summary of the effects of organic degradation products on near-field radionuclide chemistry. Nirex Report NSS/R298, Nirex Ltd, UK.

Hedström S, 2019a. Komplexbildande flyttillsatsmedel i kringgjutnings-, solidifierings-och lockgjutningsbruk i kokiller till SFR. SKBdoc 1879757 ver 2.0, Svensk Kärnbränslehantering AB. (In Swedish.)

Hedström S, 2019b. Komplexbildande flyttillsatsmedel i kringgjutningsbetong i kokiller till SFR. SKBdoc 1870598 ver 1.0, Svensk Kärnbränslehantering AB. (In Swedish.)

Hedström S, 2019c. Koncentration av estrar avkomplexbildande dikarboxylsyror från färgen F499 på avfallstyp B.04. SKBdoc 1864008 ver 1.0, Svensk Kärnbränslehantering AB. (In Swedish.)

Hedström S, 2020. Utvärdering av komplexbildande tri- och tetraminer i rostskyddsfärg. SKBdoc 1892917 ver 1.0, Svensk Kärnbränslehantering AB. (In Swedish.)

Herterich U, Volland G, Krauser G, Hansen D, 2003. Determination of concrete admixtures in concrete by NMR spectrometry. Otto-Graf-Journal 14, 101–113.

Holgersson S, Dubois I, Börstell L, 2011. Batch experiments of Cs, Co and Eu sorption onto cement with dissolved fibre mass UP2 in the liquid phase. SKB P-11-24, Svensk Kärnbränslehantering AB.

Holmén J G, Stigsson M, 2001. Modelling of future hydrogeological conditions at SFR. SKB R-01-02, Svensk Kärnbränslehantering AB.

Höglund L O, 2014. The impact of concrete degradation on the BMA barrier functions. SKB R-13-40, Svensk Kärnbränslehantering AB.

JAEA, 2007. Second progress report on research and development for TRU waste disposal in Japan: repository design, safety assessment and means of implementation in the generic phase. JAEA-Review 2007-10, Japan Atomic Energy Agency, Japan.

Kagawa A, Fukumoto M, Kawamura K, 2000. Influence of chemical and radiolytic degradation of bitumen on its performance for disposal. Journal of Nuclear Science and Technology 37, 934–937.

Katz J J, Seaborg G T, Morss L R (eds), 1986. The chemistry of the actinide elements. 2nd ed. London: Chapman and Hall.

Keith-Roach M, Höglund L O, 2018. Review of the long-term risks associated with the use of superplasticisers. Posiva Working Report 2017-52, Posiva Oy, Finland.

Keith-Roach M, Lindgren M, Källström K, 2021. Assessment of complexing agent concentrations for the post-closure safety assessment in PSAR SFR. SKB R-20-04, Svensk Kärnbränslehantering AB.

Klapiszewski Ł, Szalaty T J, Jesionowski T, 2017. Depolymerization and activation of lignin: current state of knowledge and perspectives. doi:10.5772/intechopen.70376. Available at: https://www.intechopen.com/books/lignin-trends-and-applications/depolymerization-and-activation-of-lignin-current-state-of-knowledge-and-perspectives

Kluyver T, Ragan-Kelley B, Pérez F, Granger B E, Bussonnier M, Frederic J, Kelley K, Hamrick J B, Grout J, Corlay S, Ivanov P, Avila D, Abdalla S, Willing C, 2016. Jupyter Notebooks – a publishing format for reproducible computational workflows. In Loizides F, Schmidt B (eds). Positioning and power in academic publishing: players, agents and agendas: proceedings of the 20th Conference on Electronic Publishing (Elpub), Göttingen, Germany, June 2016. Amsterdam: IOS Press, 87–90.

Kołodyńska D, 2013. Application of a new generation of complexing agents in removal of heavy metal ions from different wastes. Environmental Science Pollution Research 20, 5939–5949.

Källström K, 2018. Utlåtande kring införande av microfiberduk ur ett säkerhet efter förslutnings-perspektiv. SKBdoc 1679417 ver 1.0, Svensk Kärnbränslehantering AB. (In Swedish.)

Lagerblad B, Trägårdh J, 1994. Conceptual model for concrete long time degradation in a deep nuclear waste repository. SKB TR 95-21, Svensk Kärnbränslehantering AB.

Litmanovich A D, Platé N A, 2000. Alkaline hydrolysis of polyacrylonitrile. On the reaction mechanism. Macromolecular Chemistry and Physics 201, 2176–2180.

Lumen Learning, 2020. Condensation reactions. Available at: https://courses.lumenlearning.com/introchem/chapter/condensation-reactions/ [13 August 2020].

Manchanda V K, Mohapatra P K, 1990. Complexation of europium(III) and americium(III) with ionizable macrocyclic ligands. Polyhedron 9, 2455–2461.

Martell A E, Smith R M, Motekaitis R J, 1997. Critically selected stability constants of metal complexes database. Version 4.0. National Institute of Standards and Technology (NIST); Texas A & M University. Available at: https://www.nist.gov/srd/nist46

Martell A E, Smith R M, Motekaitis R J, 2003. NIST critically selected stability constants of metal complexes. Version 7.0. Texas A&M University, TX.

NCBI, 2004a. Phthalic Acid, CID=1017. PubChem Database. National Center for Biotechnology Information, Bethesda, MD. Available at: https://pubchem.ncbi.nlm.nih.gov/compound/Phthalic-acid#section=Solubility [13 August 2020].

NCBI, 2004b. Triethylenetetramine, CID=5565. PubChem Database. National Center for Biotechnology Information, Bethesda, MD. Available at: https://pubchem.ncbi.nlm.nih.gov/compound/5565#section=Flash-Point [13 August 2020].

NCBI, 2004c. Succinic acid, CID=1110. PubChem Database. National Center for Biotechnology Information, Bethesda, MD. Available at: https://pubchem.ncbi.nlm.nih.gov/compound/Succinic-acid [13 August 2020].

NCBI, 2004d. Glutaric acid, CID=743. PubChem Database. National Center for Biotechnology Information, Bethesda, MD. Available at: https://pubchem.ncbi.nlm.nih.gov/compound/Glutaric-acid [13 August 2020].

NCBI, 2005. 2,4,6-Tris(dimethylaminomethyl)phenol, CID=7026. PubChem Database. National Center for Biotechnology Information, Bethesda, MD. Available at: https://pubchem.ncbi.nlm.nih.gov/compound/2_4_6-Tris_dimethylaminomethyl_phenol [13 August 2020].

NCBI, 2008. Sodium 2-naphthalenesulfonate, CID=23661868. PubChem Database. National Center for Biotechnology Information, Bethesda, MD. Available at: https://pubchem.ncbi.nlm.nih.gov/compound/Sodium-2-naphthalenesulfonate#section=Solubility [26 June 2020]

NDA, 2015. Solubility studies in the presence of polycarboxylate ether superplaticisers. NDA DRP Lot 2: Integrated Waste Management WP/B2/7, Nuclear Decommissioning Authority, UK.

Ng S, Metwalli E, Müller-Buschbaum P, Plank J, 2013. Occurrence of intercalcation of PCE superplasticisers in calcium aluminate cement under actual application conditions, as evidenced by SAXS analysis. Cement and Concrete Research 54, 191–198.

Onofrei M, Gray M N, Roe L H, 1992. Superplasticizer function and sorption in high-performance cement-based grouts. Atomic Energy of Canada Limited Report AECL-1 0 141/COG-91-293, Atomic Energy of Canada Limited, Canada.

Palmer D A, Bénézeth P, Wesolowski D J, 2004. Solubility of nickel oxide and hydroxide in water. In Nakahara M, Matubayasi N, Ueno M, Yasuoka K, Watanabe K (eds). Proceedings of the 14th International Conference on the Properties of Water and Steam, Kyoto, Japan, 29 August – 3 September 2004. Tokyo: Maruzen, 264–269.

Paoletti P, 1984. Formation of metal complexes with ethylenediamine: A critical survey of equilibrium constants, enthalpy and entropy values. Pure and Applied Chemistry 56, 491–522.

Parkhurst D L, Appelo C A J, 1999. User's guide to PHREEQC (version 2): a computer program for speciation, batch-reaction, one-dimensional transport, and inverse geochemical calculations. Water-Resources Investigations Report 99-4259, U.S. Geological Survey.

Pavasars I, 1999. Characterisation of organic substances in waste materials under alkaline conditions. PhD thesis. Linköping University, Sweden.

Pavasars I, Hagberg J, Borén H, Allard B, 2003. Alkaline degradation of cellulose: Mechanisms and kinetics. Journal of Polymers and the Environment 11, 39–47.

Pettersson M, Elert M, 2001. Characterisation of bitumenised waste in SFR 1. SKB R-01-26, Svensk Kärnbränslehantering AB.

Plank J, Hirsch C, 2007. Impact of zeta potential of early cement hydration phases on superplasticizer adsorption. Cement and Concrete Research 37, 537–542.

Pointeau I, Hainos D, Coreau N, Reiller P E, 2006. Effect of organics on selenite uptake by cementitious materials. Waste Management 26, 733–740.

PPG, 2019a. Säkerhetsdatablad Sigmazinc 109 Base. PPG Coatings SPRL/BVBA. SKBdoc 1886636 ver 1.0, Svensk Kärnbränslehantering AB. (In Swedish.)

PPG, 2019b. Säkerhetsdatablad Sigmazinc 109 Hardener. PPG Coatings SPRL/BVBA. SKBdoc 1885402 ver 1.0, Svensk Kärnbränslehantering AB. (In Swedish.)

Rai D, Kitamura A, 2017. Thermodynamic equilibrium constants for important isosaccharinate reactions: A review. The Journal of Chemical Thermodynamics 114, 135–143.

Rochford J D, 2014. Aqueous speciation of the actinides with organic ligands relevant to nuclear waste. PhD thesis. University of Manchester, UK.

Rojo H, Tits J, Gaona X, Garcia-Gutiérrez M, Missana T, Wieland E, 2013. Thermodynamics of Np (IV) complexes with gluconic acid under alkaline conditions: sorption studies. Radiochimica Acta 101, 133–138.

Romashkina E P, Ilyukhin A B, Strashnova S B, Koval'chukova O V, Palkina K K, Sergienko V S, Zaitsev B E, 2011. Complex compounds of some p, d, and f metals with 2,4,6-tris(N,N-dimethyl-aminomethyl)phenol (HL): Crystal and molecular structure of $H_4L(NO_3)_3 \cdot H_2O$ and $H_4LCl_3 \cdot 3H_2O$. Russian Journal of Inorganic Chemistry 56, 350–356.

Rorabacher D B, Melendez-Cepeda C A, 1971. Steric effects on the kinetics and equilibria of nickel(II)-alkylamine reactions in aqueous solution. Journal of the American Chemical Society 93, 6071–6076.

Rosdahl J, 2020. Bedömning av betongfoder för bitumeningjutet avfall till SFR. SKBdoc 1899355 ver 1.0, Svensk Kärnbränslehantering AB. (In Swedish.)

Ruckstuhl S, Suter M J F, Kohler H-P E, Giger W, 2002. Leaching and primary biodegradation of sulfonated naphthalenes and their formaldehyde condensates from concrete superplasticisers in groundwater affected by tunnel construction. Environmental Science & Technology 36, 3284–3289.

Runde W, 2000. The chemical interactions of actinides in the environment. Los Alamos Science 26, 392–411.

Schaab K M, 1998. Inorganic and bio-inorganic chemistry of lanthanide(III) DTPA-bis-glucosamide complexes. PhD thesis. The Florida State University.

Shahkarami P, Keith-Roach M, 2021. Calculation notebook for new acceptance criteria for organic materials in SFR. SKBdoc 1910845 ver 1.0, Svensk Kärnbränslehantering AB.

Sigma, 2005. Produktdatablad Sigmazinc 109. Sigma Färg AB. SKBdoc 1884733 ver 1.0, Svensk Kärnbränslehantering AB. (In Swedish.)

SKB, 2014. Waste form and packaging process report for the safety assessment SR-PSU. SKB TR-14-03, Svensk Kärnbränslehantering AB.

SKB, 2015a. Safety analysis for SFR. Long-term safety. Main report for the safety assessment SR-PSU. Revised edition. SKB TR-14-01, Svensk Kärnbränslehantering AB.

SKB, 2015b. Radionuclide transport and dose calculations for the safety assessment SR-PSU. Revised edition. SKB TR-14-09, Svensk Kärnbränslehantering AB.

SKB, 2019a. Låg- och medelaktivt avfall i SFR. Referensinventarium för avfall 2016. SKB R-18-07, Svensk Kärnbränslehantering AB. (In Swedish.)

SKB, 2019b. RD&D Programme 2019. Programme for research, development and demonstration of methods for the management and disposal of nuclear waste. SKB TR-19-24, Svensk Kärnbränslehantering AB.

Surya I, Maulina S, Ismail H, 2017. Effects of alkanolamide and epoxidation in natural rubber and epoxidized natural rubbers compounds. IOP Conference Series: Materials Science and Engineering 299, 012061. doi:10.1088/1757-899X/299/1/012061

Sverdrup L E, Kelley A E, Weideborg M, Ødegård K E, Vik E A, 2000. Leakage of chemicals from two grouting agents used in tunnel construction in Norway: Monitoring results from the tunnel Romeriksporten. Environmental Science & Technology 34, 1914–1918.

Tanaka M, Tabata M, 2009. Stability constants of metal(II) complexes with amines and aminocarboxylates with special reference to chelation. Bulletin of the Chemical Society of Japan 82, 1258–1265.

Tasdigh H, 2015. Assessment of the impact of fiber mass UP2 degradation products on nickel(II) and europium (III) sorption onto cement. MSc thesis. KTH Royal Institute of Technology, Sweden.

Tasi A, 2018. Solubility, redox and sorption behavior of plutonium in the presence of α-D-isosaccharinic acid and cement under reducing, alkaline conditions. PhD thesis. Karlsruhe Institute of Technology, Germany.

Thakur P, Conca J L, Choppin G R, 2011. Complexation studies of Cm(III), Am(III), and Eu(III) with linear and cyclic carboxylates and polyaminocarboxylates. Journal of Coordination Chemistry 64, 3214–3236.

Vagholkar P K, 2016. Nylon (Chemistry, properties and uses). International Journal of Scientific Research 5, 349–351.

Valcke E, Sneyers A, van Iseghem P, 1999. The final disposal of bituminised radioactive waste in a deep clay formation: a critical evaluation. In Vanbrabant R, Selucky P (eds). Radwaste bituminization '99: proceeding of the International Workshop on the Safety and Performance Evaluation of Bitumenization Processes for Radioactive Waste, Řež near Prague, 29 June – 2 July 1999. Řež: Nuclear Research Institute, 137.

Valcke E, Rorif F, Smets S, 2009. Ageing of EUROBITUM bituminised radioactive waste: An ATR-FTIR spectroscopy study. Journal of Nuclear Materials 393, 175–185.

Van Loon L R, Glaus M A, 1997. Review of the kinetics of alkaline degradation of cellulose in view of its relevance for safety assessment of radioactive waste repositories. Journal of Environmental Polymer Degradation 5, 97–109.

Van Loon L R, Glaus M A, 1998. Experimental and theoretical studies on alkaline degradation of cellulose and its impact on the sorption of radionuclides. PSI Bericht Nr 98-07, Paul Scherrer Institute, Switzerland. Nagra NTB 97-04, Nagra, Switzerland.

Van Loon L R, Hummel W, 1995. The radiolytic and chemical degradation of organic ion exchange resins under alkaline conditions: effect on radionuclide speciation. PSI-Bericht 95-13, Paul Scherrer Institute, Villigen, Switzerland. Also published as Nagra NTB 95-08, Nagra, Switzerland.

Van Loon L R, Kopajtic Z, 1991. Complexation of Cu^{2+}, Ni^{2+}, and UO_2^{2+} by radiolytic degradation products of bitumen. Radiochimica Acta 54, 193–199.

Van Loon L R, Glaus M A, Laube A, Stallone S, 1999a. Degradation of cellulosic materials under the alkaline conditions of a cementitious repository for low- and intermediate-level radioactive waste. Part II: Degradation kinetics. Journal of Environmental Polymer Degradation 7, 41–51.

Van Loon L R, Glaus M A, Laube A, Stallone S, 1999b. Degradation of cellulosic materials under the alkaline conditions of a cementitious repository for low- and intermediate-level radioactive waste. Part III: Effect of the degradation products on the sorption of radionuclides on feldspar. Radiochimica Acta 86, 221–224.

Velavendan P, Ganesh S, Pandey N K, Geetha R, Ahmed M K, Kamachi Mudali U, Natarajan R, 2013. Studies on solubility of TBP in aqueous solutions of fuel reprocessing. Journal of Radioanalytical and Nuclear Chemistry 295, 1113–1117.

Wang Z-M, van de Burgt L J, Choppin G R, 1999. Spectroscopic study of lanthanide(III) complexes with carboxylic acids. Inorganica Chimica Acta 293, 167–177.

Warwick P, Evans N, Hall T, Vines S, 2003. Complexation of Ni(II) by α-isosaccharinic acid and gluconic acid from pH 7 to pH 13. Radiochimica Acta 91, 233–240.

Warwick P, Evans N, Hall T, Vines S, 2004. Stability constants of uranium(IV)-α-isosaccharinic acid and gluconic acid complexes. Radiochimica Acta 92, 897–902.

Wieland E, Tits J, Spieler P, Dobler J P, 1998. Interaction of Eu(III) and Th(IV) with sulphate-resisting Portland cement. In McKinley I G, McCombie C (eds). Scientific basis for nuclear waste management XXI: symposium held in Davos, Switzerland, 23 September – 3 October 1997. Warrendale, PA: Materials Research Society. (Materials Research Society Symposium Proceedings 506), 573–578.

Wieland E, Tits J, Dobler J P, Spieler P, 2002. The effect of α-isosaccharinic acid on the stability of and Th(IV) uptake by hardened cement paste. Radiochimica Acta 90, 683–688.

Wieland E, Lothenbach B, Glaus M A, Thoenen T, Schwyn B, 2014. Influence of superplasticisers on the long-term properties of cement pastes and possible impact on radionuclide uptake in a cement-based repository for radioactive waste. Applied Geochemistry 49, 126–142.

Wikipedia, 2020. Epoxy. Available at: https://en.wikipedia.org/wiki/Epoxy [13 August 2020].

Winnefeld F, Becker S, Pakusch J, Götz T, 2007. Effects of the molecular architecture of comb-shaped superplasticisers on their performance in cementitious systems. Cement and Concrete Composites 29, 251–262.

Wu L, Hoa S V, Minh-Tan, Ton-That, 2006. Effects of composition of hardener on the curing and aging for an epoxy resin system. Journal of Applied Polymer Science 99, 580–588.

Wyrzykowski D, Chmurzyński L, 2010. Thermodynamics of citrate complexation with Mn^{2+}, Co^{2+}, Ni^{2+} and Zn^{2+} ions. Journal of Thermal Analytical Calorimetry 102, 61–64.

Yamamoto T, Nishida T, Hironaga M, Suzuki S, Ueda H, 2008. Release of superplasticisers and other organic additives from altered cement. NUMO-TR-08-01, Nuclear Waste Management Organization of Japan, Japan.

Young A J, Warwick P, Milodowski A E, Read D, 2013. Behaviour of radionuclides in the presence of superplasticiser. Advances in Cement Research 25, 32–43.

Appendix

Introduction

The maximum mass of complexing agents, cellulose and Nylon that can be disposed of in a package of relevant waste types has been calculated using the Jypiter Notebook interactive computational environment (Kluyver et al. 2016). The calculation notebook is available on SKBdoc (Shahkarami and Keith-Roach 2021).

Relevant waste types were defined as follows:

- For cellulose, waste packages that contain cellulose (based on SKB 2019a).

- For complexing agents used at the nuclear facilities, the waste packages already known to contain complexing agents of any type (e.g. those in Keith-Roach et al. 2021).

- For Nylon, waste packages that contain plastic/rubber (based on SKB 2019a).

The main input data and results are presented below, the full data are available in Shahkarami and Keith-Roach (2021).

Input data

Table A-1. Maximum dissolved concentrations of complexing agents allowed in the waste packages and the relative molecular masses (RMM) of the complexing agents. Note that the RMM given for certain substances (sodium gluconate, CIDP, CADP) are for the sodium salt while the other RMM are for the acid form. This reflects the common forms of these compounds used in cleaning and hygiene products. In the case of CIDP, the single sodium salt is given, although it can also be present as the double sodium salt.

	Maximum dissolved concentration [M]	RMM [g/mol]
ISA	10^{-4}	*
Gluconate (sodium salt)	10^{-5}	218.0
CIDP(sodium salt)	10^{-2}	295.0
NTA	10^{-3}	191.1
EDTA	10^{-4}	292.3
IDS	10^{-3}	249.1
CADP (disodium salt)	10^{-4}	418.2
Glutamic acid	10^{-2}	147.1
Citric acid		192.1
Oxalic acid		90.0
HMDA	10^{-1}	116.0

* The RMM of ISA was not used in the calculations.

Table A-2. Pore and void volume, and mass of hydrated cement in all waste types described in SKB (2019a). These values include the packaging material. Calculations described further in Shahkarami and Keith-Roach (2021).

Waste type	Pore and void volume [m³]	Mass of hydrated cement [kg]
B.04	0.07	248
B.04:D	0.08	199
B.05	0.06	0
B.06	0.05	0
B.07	2.05	2 211
B.12 Halvhöjdscontainer 20 fot	17.38	61
B.12 Helhöjdscontainer 20 fot	35.66	137
B.12:D Skrot	12.90	0
B.12C:D Betong	8.81	3 622
B.12M:D Sekundäravfall	8.79	0
B.12S:D Sand	7.08	0
B.20 Plåtfat	0.05	0
B.20 Container	5.60	0
B.23 Betongkokill	0.33	1 131
B.23 Plåtkokill	0.81	628
B.23:D Enkokill	0.55	964
B.23:D Tvåkokill	0.82	1 354
B.23R:D	0.74	1 227
C.02	0.32	1 322
C.12:D Skrot	12.90	0
C.12C:D Betong	9.11	3 450
C.12M:D Sekundäravfall	10.92	0
C.16:D	0.71	1 693
C.23	0.79	567
C.23:D	0.74	1 227
C.24	0.65	685
E.12	13.07	110
E.12:D	10.00	352
E.23	1.14	226
E.24 Betongkokill	0.84	524
E.24 Plåtkokill	0.78	110
F.05	0.07	0
F.12 Halvhöjdscontainer 20 fot	14.38	0
F.12 Halvhöjdscontainer 10 fot	7.07	0
F.12:D Skrot	12.90	0
F.12C:D Betong	8.25	3 952
F.12M:D Sekundäravfall	8.22	0
F.12S:D Sand	10.92	0
F.15	0.40	2 238
F.17	0.34	0
F.18	0.34	0
F.18:D	0.59	0
F.20 Plåtfat	0.06	0
F.20 Container	4.30	0
F.23 Betongkokill	0.47	625
F.23 Plåtkokill	0.93	214
F.23:D Skrot	0.78	1 283
F.23C:D Betong	0.46	1 331
F.23R:D	0.74	1 227
F.99:01 50	0.91	620
F.99:02 990	0.84	4 566
O.01	0.35	1 212

Waste type	Pore and void volume [m³]	Mass of hydrated cement [kg]
O.02	0.30	1 465
O.07	2.86	2 211
O.12 Halvhöjdscontainer 20 fot	17.23	120
O.12 Helhöjdscontainer 10 fot	16.54	0
O.12 Helhöjdscontainer 20 fot	34.84	0
O.12:D Skrot	12.90	0
O.12C:D Betong	8.40	3 823
O.12M:D Sekundäravfall	8.32	0
O.12S:D Sand	10.92	0
O.16:D	0.71	1 693
O.23	0.49	788
O.23:D Skrot	0.78	1 270
O.23C:D Betong	0.48	1 320
O.23R:D	0.98	315
O.23S:D Sand	0.74	1 227
O.99:01 22	0.54	2 726
O.99:03 620	2.58	10 400
R.01	0.32	1 258
R.02	0.32	1 263
R.10	0.35	1 227
R.12 Halvhöjdscontainer 20 fot	9.07	41
R.12 Helhöjdscontainer 20 fot	22.01	54
R.12:D Skrot	12.90	0
R.12C:D Betong	8.81	3 622
R.12M:D Sekundäravfall	8.79	0
R.12S:D Sand	12.69	0
R.15	0.39	1 633
R.16	0.39	1 643
R.16:D	1.03	1 135
R.23 Betongkokill	0.30	1 006
R.23 Plåtkokill	0.85	628
R.23:D Skrot (Enkokill)	0.55	953
R.23:D Skrot (Tvåkokill)	0.74	1 217
R.23C:D Betong	0.57	1 355
R.23R:D	0.74	1 225
R.24	0.25	1 011
R.29	0.39	1 310
R.99:01 990	1.61	14 701
R.99:02 28	0.23	767
R.99:06 990	0.00	0
S.04	0.07	160
S.09	0.06	180
S.11	0.41	1 312
S.12 Halvhöjdscontainer 20 fot	16.41	96
S.12 Helhöjdscontainer 20 fot	22.01	54
S.12:D	0.14	12
S.13	0.04	91
S.14	0.46	32
S.21:D	0.12	0
S.23:D	0.56	1 232
V.09	0.06	180
V.12	34.08	960
V.12:D	26.60	1 280
V.23	0.84	645
V.23:D Betongkokill	0.38	995

Table A-2. Continued.

Waste type	Pore and void volume [m³]	Mass of hydrated cement [kg]
V.23:D Plåtkokill	0.46	1 014
V.24	0.84	645
Å.12:D Skrot	14.20	0
Å.12C:D Betong	10.28	2 548
Å.12M:D Sekundäravfall	7.08	0
Å.23:D Skrot	0.74	1 222
Å.23C:D Betong	0.60	1 327
Å.23R:D	0.73	1 215

Results

Table A-3. Maximum mass [kg] of cellulose per package of relevant waste types (Shahkarami and Keith-Roach 2021). Note that BLA waste packages are not included in this list as no quantitative restriction on complexing agents applies to the BLA vaults.

Waste type	Cellulose [kg]
B.23 Betongkokill	3.43
B.23 Plåtkokill	1.92
C.23	1.73
C.24	2.09
F.05	0.00
F.15	6.78
F.23 Betongkokill	1.90
F.23 Plåtkokill	0.67
O.01	3.68
O.02	4.44
O.23	2.40
R.23 Betongkokill	3.05
R.23 Plåtkokill	1.92
R.24	3.07
S.11	3.98
S.23:D	3.74
V.23	1.97
V.23:D Betongkokill	3.02
V.23:D Plåtkokill	3.08
V.24	1.97

Table A-4. Maximum mass [g] of complexing agents per package of relevant waste types.

	B.04 (Silo)	B.07 (BTF)	C.02 (Silo)	F.17 (BMA)	O.02 (Silo)	O.07 (BTF)	R.10 (BMA)	R.15 (BMA)	R.16 (Silo)	S.09 (BMA)
Sodium gluconate	3 018	26 914	16 090	0.73	17 827	26 916	14 936	19 883	19 997	2 191
CIDP	212.2	6 046	952.4	989.2	896.4	8 429.6	1 034.9	1 151	1 139.2	189.7
NTA	13.7	391.7	61.7	64.1	58.1	546.2	67.1	74.6	73.8	12.3
EDTA	2.1	59.9	9.4	9.8	8.9	83.5	10.3	11.4	11.3	1.9
IDS	17.9	510.5	80.4	83.5	75.7	711.8	87.4	97.2	96.2	16.0
CADP	3.0	85.7	13.5	14.0	12.7	119.5	14.7	16.3	16.1	2.7
Glutamic acid	105.8	3 014	474.9	493.3	447	4 203.4	516	573.9	568.1	94.6

Table A-5. Maximum mass [g] of citric acid, oxalic acid and CIDP* based on the mass of cement in relevant waste types**, including the packaging material. F.17 does not contain cement and so this approach is not relevant (NR) for F.17.

	B.04 (Silo)	B.07 (BTF)	C.02 (Silo)	F.17 (BMA)	O.02 (Silo)	O.07 (BTF)	R.10 (BMA)	R.15 (BMA)	R.16 (Silo)	S.09 (BMA)
Citrate	958	8 544	5 109	NR	5 660	8 544	4 742	6 313	6 349	696
Oxalate	450	4 007	2 396	NR	2 654	4 007	2 224	2 960	2 977	326
CIDP*	1 473	13 127	7 849	NR	8 696	13 127	7 286	9 699	9 755	1 069

* CIDP is included here to allow comparison of the maximum mass concentration calculated in this way with that based on the dissolved concentration.

** Based on w/c 0.47 (68 % dry cement), 2.96 moles $Ca(OH)_2$ per kg dry cement power, and 1 % of the amount of calcium in the HCP.

Table A-6. Maximum mass of Nylon [kg] per package of relevant waste types. Note that the BLA waste packages are not included in this list as no quantitative restriction on complexing agents applies to the BLA vaults.

Waste Package	Nylon [kg]
B.23 Betongkokill	7.5
B.23 Plåtkokill	18.2
C.23	17.9
C.24	14.7
F.23 Betongkokill	10.7
F.23 Plåtkokill	21.0
O.01	8.0
O.02	6.9
O.07	64.6
O.23	11.1
R.23 Betongkokill	6.9
R.23 Plåtkokill	19.1
R.24	5.7
R.99:02 28	5.1
S.23:D	12.6
V.23	19.0
V.23:D Betongkokill	8.6
V.23:D Plåtkokill	10.4
V.24	19.0